Morgantown Energy Research Center

Morgantown, W.Va.

UGR File #417
TID 27,649
West Virginia Univ.
November 1975

STRUCTURAL RESPONSE GOVERNING HYDRAULIC FRACTURING OPERATIONS IN ROCK MEDIA

by

Sunder H. Advani, WVU
Hota V.S. GangaRao, WVU
L. Zane Shuck, MERC
H.Y. Chang, WVU

United States Energy Research and Development Administration

UGR File #417
TID 27,649
West Virginia Univ.
November 1975

FINAL REPORT

STRUCTURAL RESPONSE GOVERNING HYDRAULIC FRACTURING OPERATIONS IN ROCK MEDIA

Sunder H. Advani, Hota V.S. GangaRao, L. Zane Shuck
and H. Y. Chang

November, 1975

Prepared for ERDA
under Sandia Laboratories Contract No. 63-4997

by

College of Engineering
West Virginia University
Morgantown, West Virginia 26506

TID 27,649
West Virginia Univ.
November 1975

FOREWORD

This report describes analytical and experimental simulations of structural responses associated with hydraulic fracturing operations in rock media. The work was sponsored by Sandia Laboratories, ERDA under Contract No. 63-4997 and was performed in conjunction with staff from the Morgantown Energy Research Center. Mr. H. H. Patterson served as Technical Monitor for Sandia with technical consultation provided by Mr. Richard Hay and Mr. Jack Hinde.

The work presented herein includes (1) a state-of-the-art literature survey of hydraulic fracturing, rock mechanics and fracture mechanics, (2) results of classical elasticity, crack tip and finite element 2D and 3D stress evaluations, (3) experimental studies, and (4) applications relating to determination of critical pressures and orientations in terms of crack geometry, material properties and primitive stresses.

This study was performed by West Virginia University, Morgantown, West Virginia with Dr. Sunder H. Advani serving as Principal Investigator. Dr. Hota V.S. GangaRao and Dr. L. Zane Shuck served as Co-investigators. Experimental contributions to this program were made by Mr. James Heavner, Mr. Tom Keech, and Dr. Rex Haynes under the direction of Dr. L. Zane Shuck.

TABLE OF CONTENTS

Page

FOREWORD ii

1.0 INTRODUCTION 1

1.1 Hydraulic Fracturing Process and Mechanisms..... 3
1.2 Rock Mechanics and Fracture Criteria 8

2.0 ANALYTICAL METHODS AND RESULTS 10

2.1 Exact Elasticity Theory Results 10
2.1.1 Two Dimensional Modeling 13
2.1.2 Three Dimensional Modeling 19

2.2 Finite Element Modeling Results 22
2.2.1 Two Dimensional Modeling 23
2.2.2 Three Dimensional Modeling 39

2.3 Exact Theory and Finite Element Comparisons 42

3.0 EXPERIMENTAL RESULTS 48

3.1 Strain Gage Results 53
3.2 Acoustic Emission Results 56

4.0 DISCUSSION 60

4.1 Fracture Initiation, Extension and Orientation 60
4.2 Effects of Layering and Other Variables 61
4.3 Directional Control of Fractures 62
4.4 Laboratory and Field Experimental Correlations 64

5.0 CONCLUSIONS AND RECOMMENDATIONS 65

REFERENCES 66

APPENDIX A 70

APPENDIX B 72

1.0 INTRODUCTION

Hydrofracturing techniques, introduced by Clark (1) in 1948, have greatly enhanced the recovery of oil and gas reserves. Current applications of this method, in addition to recovery of oil and gas from rock/shale formations, are in the areas of underground coal gasification (UCG), extraction of methane, geothermal energy, solution mining, and radioactive or slurry waste disposal.

Interpretation of the hydrofracturing mechanisms and evaluation of the process parameters involve multi-discipline methodologies. A cross fertilization of several disciplines such as geology, petroleum engineering, solid and fluid mechanics, and instrumentation is involved for obtaining a blueprint characterization of the hydraulic fracturing process. The medium to be fractured generally consists of anisotropic layers of fluid filled rocks subjected to tectonic and overburden stress fields (primitive stresses). Numerous ill-defined variables such as natural fracture systems and material inhomogenities contribute to the structural and constitutive complexities. Characterization of the geological formations is a necessary pre-requisite. The Wagon Wheel Project studies (2), for example, provide typical considerations of local geology, stratigraphy, faulting and site selection. Figure 1 illustrates a representative structural form for this study.

The following sub-sections describe the hydraulic fracturing process with particular emphasis on concepts of rock mechanics and fracture mechanics. A state-of-the-art literature survey is also given.

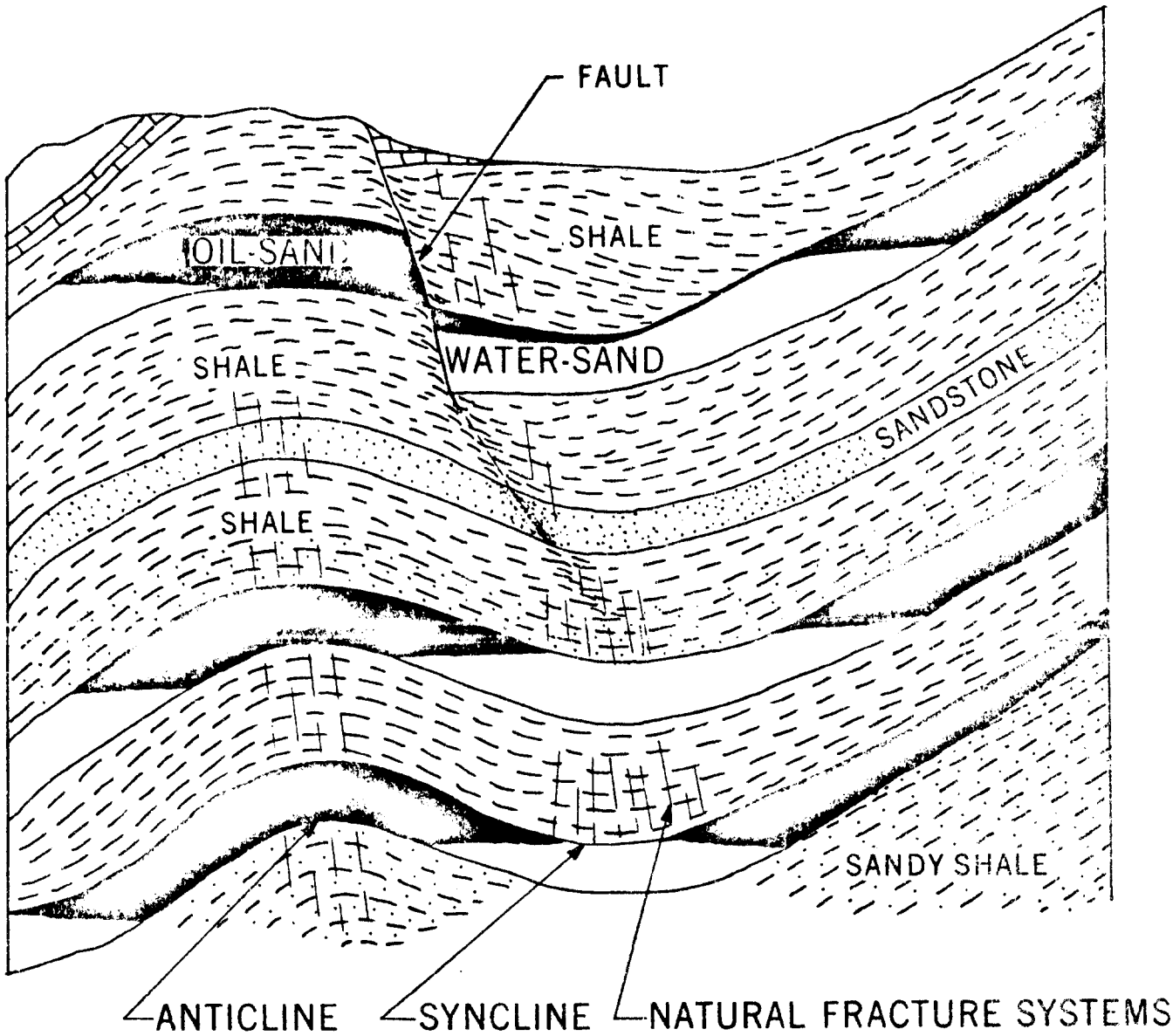

FIGURE 1

STRUCTURAL COMPLEXITY OF OIL BEARING FORMATIONS

1.1 HYDRAULIC FRACTURING PROCESS AND MECHANISMS

The general process of hydraulic fracturing is well documented (3) and salient features of this methodology (4) are reviewed here. A typical well drilling and completion process may involve drilling a hole 6" to 20" in diameter (depending on depth) to the top of an oil/gas bearing formation and placing a steel casing in the hole. Then a cement slurry is forced through the casing until it flows around the outside of the casing back to the surface. The hole is then drilled through the oil/gas bearing formation to some depth. An open well bore completion is illustrated in Figure 2. A fracturing fluid is then injected to build up pressure in the wellbore until the stress and/or energy threshold levels exceed the corresponding values of the formation and fractures propagate from the wellbore. Frequently, the fractures emanate from diametrically opposed locations and leave the wellbore vertically with the crack propagation direction parallel to the larger tectonic stress (Figure 3). Various possible fracture inclinations with the wellbore depend on the stress field, material properties and fluid flow effects (influenced by porosity, permeability and natural fracture systems). (Figure 4)

Following the initial formation breakdown, various injection rates and fluids are used to extend the fractures. At sufficiently high flow rates, sand or other material is added to prop open the fractures to prevent their closing when the well is open at the surface and allowed to backflow. Fracture extension is performed in various stages, rates, and time intervals between stages, and several phases need consideration during hydraulic fracture operations. These basic phases are:

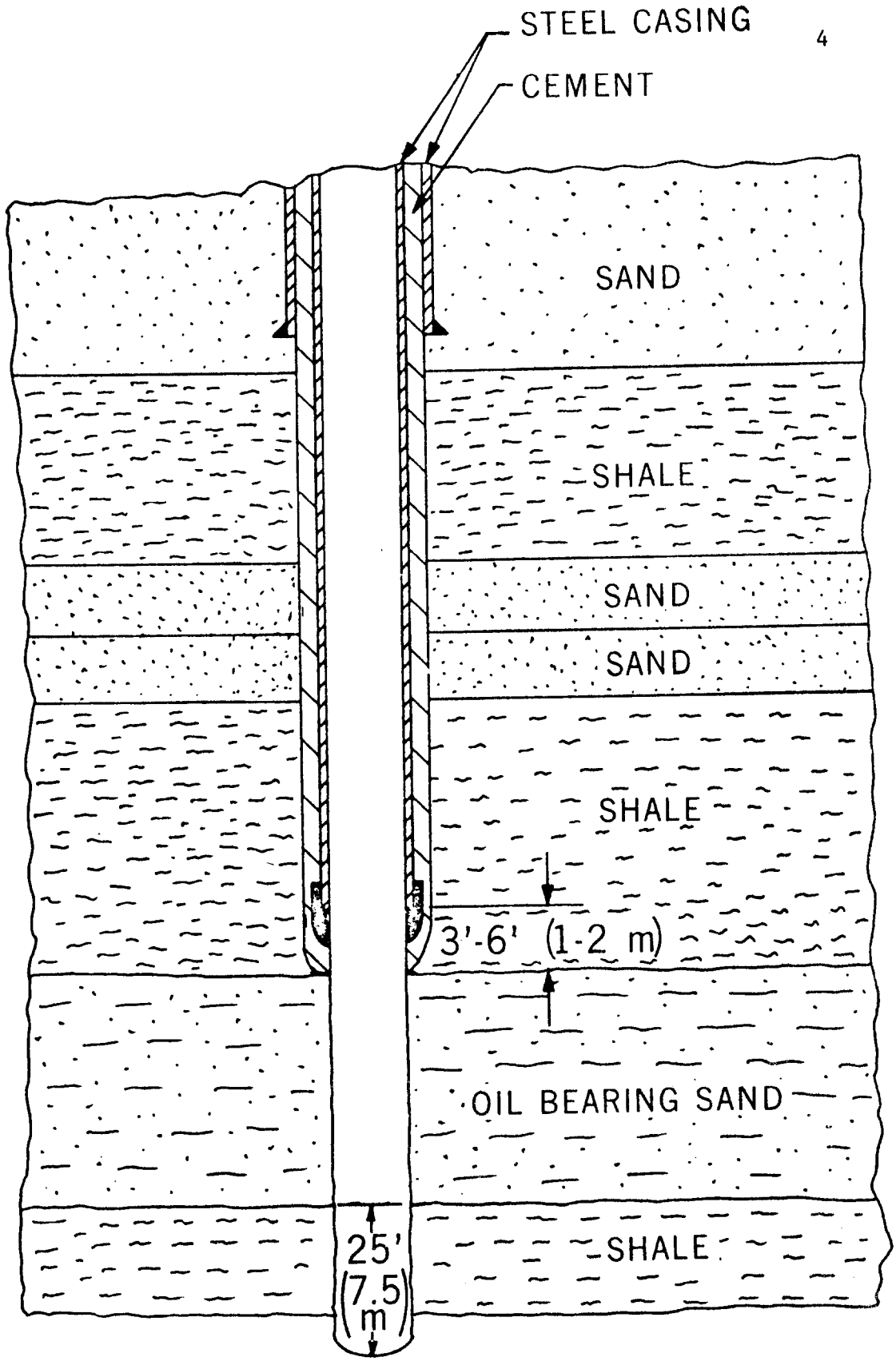

FIGURE 2. TYPICAL " OPEN-HOLE" WELL COMPLETION

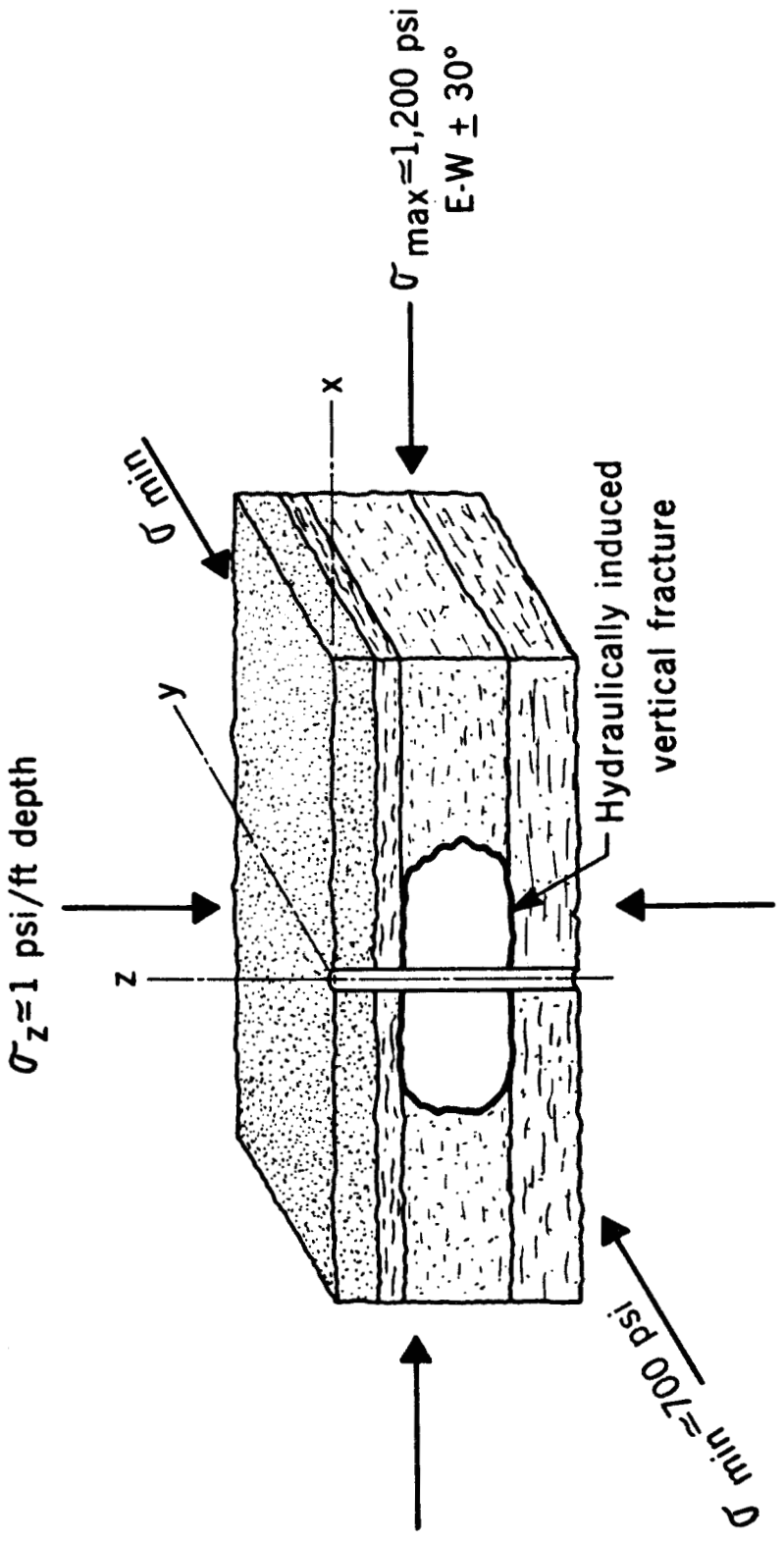

Figure 3. Hydraulically Induced Vertical Fracture in Layered Formation Subjected to Tectonic and Overburden Stresses.

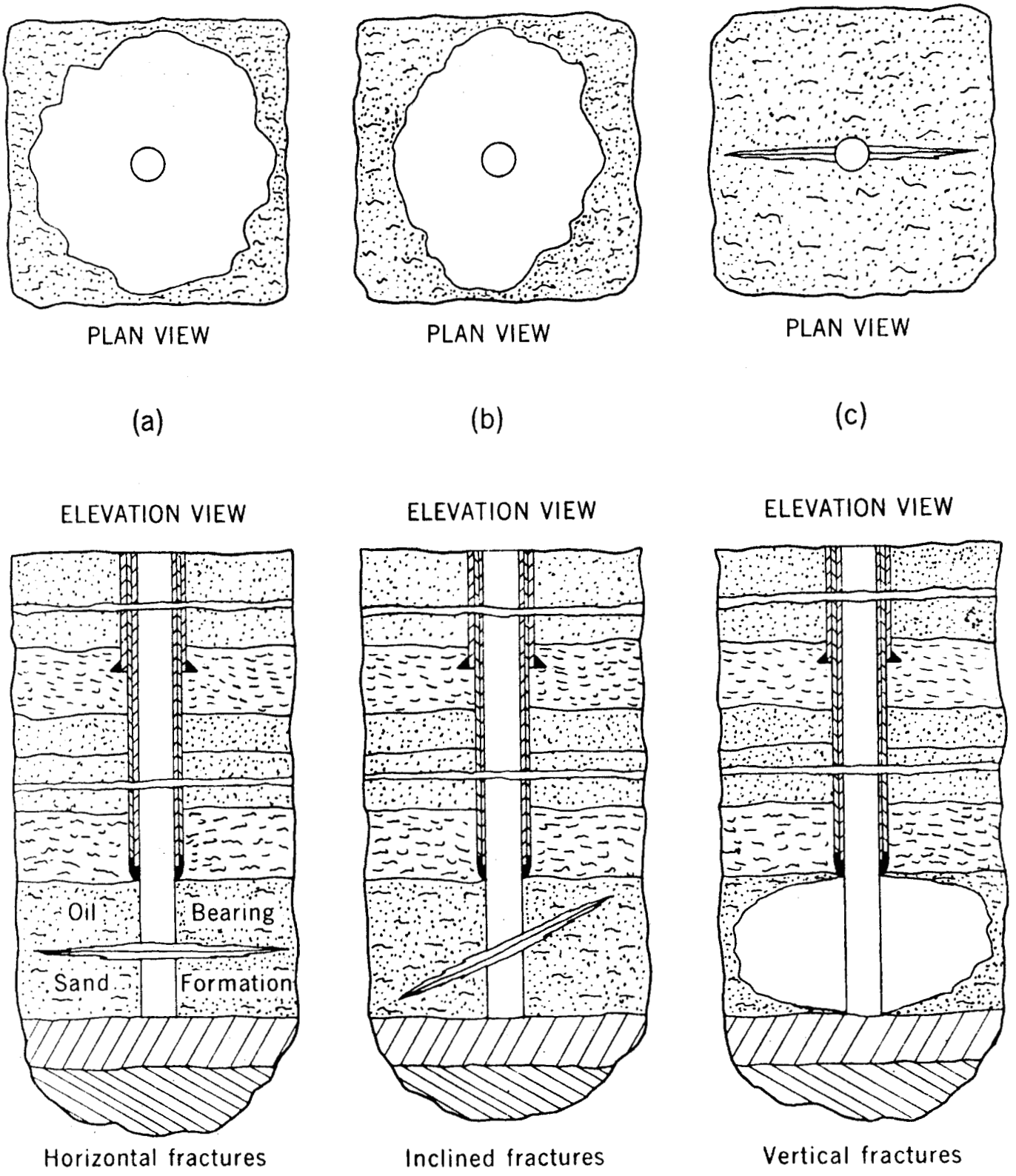

FIGURE 4. TOPOLOGIES OF HYDRAULIC FRACTURE OF GEOLOGICAL FORMATIONS

a. Primitive stress field (tectonic and overburden) in the formation with corresponding fluid pore pressure prior to well drilling.

b. Static state of stress in the formation around the wellbore and vicinity after the well is drilled with negligible fluid-flow effects.

c. Dynamic stress redistribution around the wellbore and field during pressure build-up from injection of fluids.

d. Transient stress distribution at the wellbore and in the formation prior to and during fracture initiation.

e. Transient stress redistribution throughout the reservoir after initial fractures have ceased to propagate and with no further fluid injection.

f. Quasi-static stress distribution after initial fracture and after substantial fluid circulation and formation stress relaxation.

g. Dynamic stress redistribution throughout the field after further pressure build-up through fluid injection in fracture extension stages.

h. Transient local and far field stress redistribution during fracture extension.

i. Repetition of phases f, g, and h.

Most of the research work has been confined to analysis of phases (b) or (f). A comprehensive evaluation of the local (wellbore) and field stresses (away from wellbore) is warranted since fracture initiation and extension are stability problems. The direction of fracture growth, from an energy viewpoint, is a function of the crack length and imposed stress fields. Hence, the fracture may go along a direction from the wellbore for a short distance and assume a different direction further out depending on the prevailing stress conditions and material properties.

The early literature mostly deals with the wellbore analysis of the state of stress (Hubbert and Willis (5), Zhelto and Khristanovich (6), Dunlap (7,8), and Fairhurst (9)). Investigation of tectonic stresses, from hydraulic fracturing data, has been considered by Scheidegger (10) and Kehle (11). More recent papers have dealt with the effects of fluid flow,

fracture initiation and extension (Haimison and Fairhurst (12,13,14), Daneshy (15,16,17,18), Shuck and Advani (4), McClain (19), Wong and Farmer (20), Seth and Gray (21,22) and Lemon and Patel (23).

1.2 ROCK MECHANICS AND FRACTURE CRITERIA

The bibliography in the areas of rock mechanics is vast. However, relatively few attempts have been made to integrate fracture criteria (Griffith/Stress Intensity/Energy Density) with related rock mechanics problems. A review of basic considerations dealing with rock properties and structures can be found in textbooks by Obert and Duvall (24), Dreyer (25), and Jaeger (26). Specialized monographs on the mechanical properties of rock are due to Proto dyakanov and Koifman (27), American Society of Testing Materials (28), Schock, et al (29,30,31). There are numerous investigations of static stress distributions in rock structures with cavities. Classical elasticity and finite element method approaches have been used to obtain stress concentrations (Blake (32), Chugh and Hardy (33) and Barla (34,35).

The earliest rigorous formulation of fracture criteria is due to Griffith (36). Basically Griffith proposed that if a stationary crack ($-a \leq x \leq a$, $y=o$, infinitely long in the Z direction) exists in the interior of an infinite elastic body subjected to an internal pressure $p(x)$ $\left(p(x) = p(-x)\right)$, then the Griffith Criterion for crack extension is that the total energy of the system should be a minimum, i.e., $\partial V/\partial a = 0$ (V being the difference between the strain energy and the surface energy). Irwin (37) and Orowan (38) extended the original Griffith criteria so that it could include plastic energy dissipation occurring in the vicinity of the crack tip. The equations used in linear fracture mechanics can usually be obtained from theory of elasticity considerations by use of complex variable mapping

(two dimensional problems) and potential function methods (three dimensional problems). The local stresses, using this approach, are expressed in terms of the stress intensity factors and local coordinates. The stress intensity factors are also related to the strain energy release rate. In general, three modes of crack tip deformation occur, namely, the crack opening mode (mode I), the crack sliding mode (mode II), and the crack tearing mode (mode III) (39).

In lieu of theoretical solutions to fracture mechanics problems, the finite element modeling technique is a powerful tool for fracture analysis for two and three dimensional problems (40). With variable geometry, material properties, and boundary conditions, the finite element method can provide accurate local and far field stresses by optimizing element arrangement and technique. Stress intensity factors calculated by the finite element method compare favorably with exact elasticity solutions.

2.0 ANALYTICAL METHODS AND RESULTS

A comprehensive review of analytical techniques and exact solutions for two dimensional and three dimensional crack problems can be found in Sih and Liebowitz (39), Sih (41), and the Handbook of Stress Intensity Factors (42). Finite element methods for the calculation of stress intensity factors have been discussed by Hilton and Sih (43), Wilson (44), and Marcal (45). The following subsections detail analytical methods and results for two and three dimensional models representing field hydraulic fracturing operations. Particular attention is paid to the inclusion of fracture criteria for computing critical pressures and fracture orientations in terms of crack lengths and initial orientations. Stress contours along with computed stress intensity factors are also presented.

2.1 EXACT ELASTICITY THEORY RESULTS

Two and three dimensional elasticity theory field solutions, for the reservoir problems defined in Figure 5, have been reported by Shuck and Advani (4).

For two dimensional crack tip modeling, the critical internal pressure necessary to extend a crack of length 2a is governed by the plane strain relation (46)

$$P_{CRITICAL} = \left[\frac{2\gamma E}{\pi a (1-\nu^2)} \right]^{\frac{1}{2}} \qquad (1)$$

where γ is the surface tension (material property), E is the elastic modulus of the material and ν is the Poisson's ratio of the material.

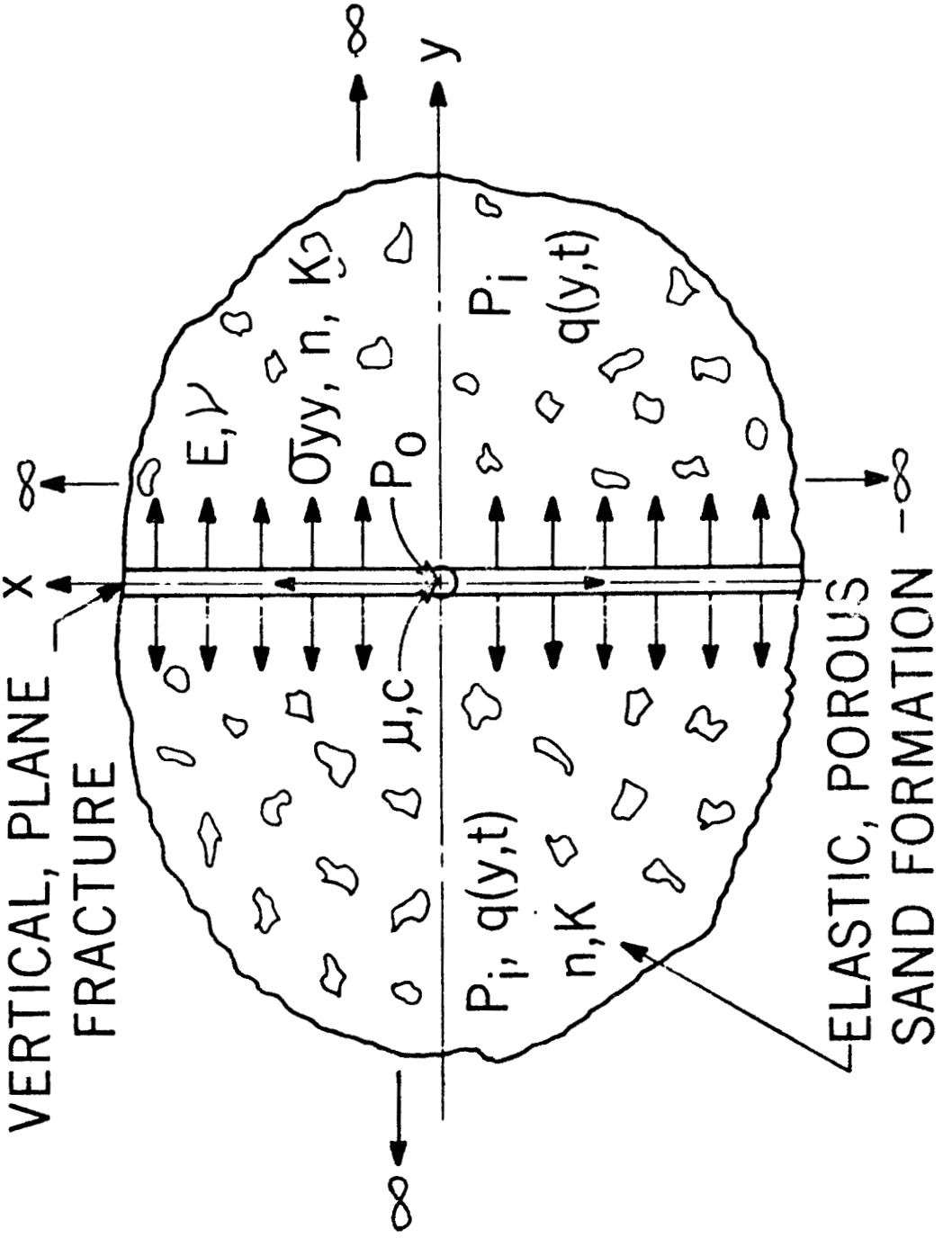

FIGURE 5
ASSUMED RESERVOIR CONDITIONS

For plane stress, the corresponding relation is

$$P_{CRITICAL} = \left[\frac{2\gamma E}{\pi a}\right]^{\frac{1}{2}} \tag{2}$$

The critical pressure for a flat elliptical crack (major axis 2a, minor axis 2b) in a three dimensional medium has been obtained by Kassir and Sih (47) to be given by

$$P_{CRITICAL} = \left[\frac{3\gamma E}{2b(1-\nu^2)} \frac{(1+k'^2)\,E^2(k)}{[2(1+k'^2)E(k) - k'^2 K(k)]}\right]^{\frac{1}{2}} \tag{3}$$

where $k'^2 = 1 - k^2 = b^2/a^2$

and E(k), K(k) are complete elliptic integrals of the first and second kind.

The penny shaped crack (a = b) is a special case of equation (3). The corresponding critical pressure is

$$P_{CRITICAL} = \left[\frac{\pi \gamma E}{2a(1-\nu^2)}\right]^{\frac{1}{2}} \tag{4}$$

In the above equations, the surface energy γ can also be defined in terms of critical stress intensity factors. Considerations of stress intensity factors and the influence of boundary conditions are given with numerical results in the following subsections.

2.1.1 TWO DIMENSIONAL MODELING

The idealized two dimensional model, shown in Figure 6, is subjected to internal pressure p and tectonic stresses σ_1 and σ_2. The crack axis and the initial major tectonic stress σ, axis are assumed to be inclined at an angle β. The total stress intensity factors k_1, k_2 and k_3 due to the combined stress field can be shown to be (39).

$$\begin{aligned} k_1 &= (p + \sigma_1 \sin^2\beta + \sigma_2 \cos^2\beta)\sqrt{a} \\ k_2 &= (\sigma_1 - \sigma_2)\sin\beta\cos\beta\sqrt{a} \\ k_3 &= 0 \end{aligned} \tag{5}$$

The strain energy density is related to the stress intensity factors by (39)

$$S = a_{11}k_1^2 + 2a_{12}k_1k_2 + a_{22}k_2^2 + a_{33}k_3^2 \tag{6}$$

where

$$\begin{aligned} a_{11} &= \frac{(1+\nu)}{8E}(3 - 4\nu - \cos\theta)(1+\cos\theta) \\ a_{12} &= \frac{(1+\nu)}{4E}\sin\theta\,(\cos\theta - (1-2\nu)) \\ a_{22} &= \frac{(1+\nu)}{8E}\left(4(1-\nu)(1-\cos\theta) + (1+\cos\theta)(3\cos\theta - 1)\right) \\ a_{33} &= \frac{(1+\nu)}{2E} \end{aligned}$$

Substitution of equations (5) and (6) yields

$$S = \frac{a(1+\nu)}{8E}\Big\{(p + \sigma_1\sin^2\beta + \sigma_2\cos^2\beta)^2(3-4\nu-\cos\theta)(1+\cos\theta)$$

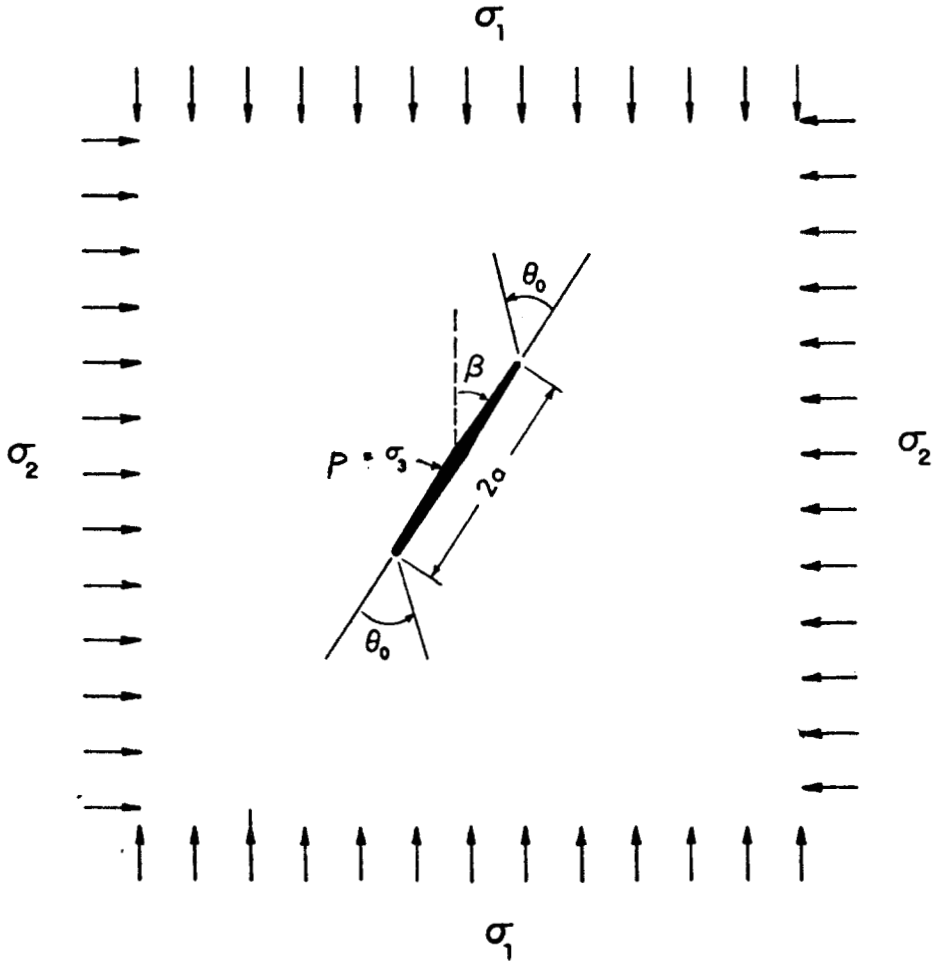

σ_1 = 1200 PSI (Comp)

σ_2 = 700 PSI (Comp)

σ_3 = P

Figure 6. Two Dimensional Model with Inclined Crack and Tectonic Stresses.

$$+ 4\left(p + \sigma_1 \sin^2\beta + \sigma_2 \cos^2\beta\right)\left(\sigma_1 - \sigma_2\right)\sin\beta\cos\beta\sin\theta\left(\cos\theta - 1 + 2\nu\right) \tag{7}$$

$$+ \left(\sigma_1 - \sigma_2\right)^2 \sin^2\beta\cos^2\beta\left(4(1-\nu)(1-\cos\theta) + (1+\cos\theta)(3\cos\theta - 1)\right)\Big\}$$

Equation (7) is the strain energy density relation in terms of the local crack tip angular coordinate, internal pressure, crack length and inclination, tectonic stresses, and material properties.

For crack initiation, we have

$$\frac{dS}{d\theta} = 0 = \frac{a(1+\nu)}{8E}\Big\{\left(p + \sigma_1\sin^2\beta + \sigma_2\cos^2\beta\right)^2\sin\theta\left(2\cos\theta + 4\nu - 2\right)$$

$$+ 4\left(p + \sigma_1\sin^2\beta + \sigma_2\cos^2\beta\right)\sin\beta\cos\beta\left(\sigma_1 - \sigma_2\right)\left(\cos 2\theta - (1-2\nu)\cos\theta\right.$$

$$+ \left(\sigma_1 - \sigma_2\right)^2\sin^2\beta\cos^2\beta\left(2 - 4\nu - 6\cos\theta\right)\sin\theta \tag{8}$$

Equation (8) yields the fracture direction θ for specified p, σ_1, σ_2, and β. For stable crack growth we have

$$\frac{d^2S}{d\theta^2} = \frac{a(1+\nu)}{8E}\Big\{\left(p + \sigma_1\sin^2\beta + \sigma_2\cos^2\beta\right)^2\left(2\cos 2\theta + 4\nu\cos\theta - 2\cos\theta\right)$$

$$+ 4\left(p + \sigma_1\sin^2\beta + \sigma_2\cos^2\beta\right)\sin\beta\cos\beta\left(\sigma_1 - \sigma_2\right)\left(-2\sin 2\theta + (1-2\nu)\sin\theta\right)$$

$$+ \left(\sigma_1 - \sigma_2\right)^2\sin^2\beta\cos^2\beta\left((2-4\nu)\cos\theta - 6\cos 2\theta\right) \geq 0 \tag{9}$$

The above problem formulation, requires determination of the critical internal pressure($P_{critical}$) for specified material constants. (E,ν), inclination β, tectonic stresses σ_1 and σ_2, and critical strain energy density S_c. The critical strain energy density can be computed from the relation

$$S_c = \frac{(1+\nu)(1-2\nu)K_c^2}{2E} \tag{10}$$

where K_c is the critical stress intensity factor determined from experimental tests on sandstone.

The following constants are selected for this problem

K_c = 2000 psi $\sqrt{in}$

$E = 4.25 \times 10^6$ psi

$\nu = 0.22$

$\sigma_1 = -1200$ psi and $\sigma_2 = -700$ psi

The material constants chosen above yield $S_c = .102$ lb/in.

Figure 7 illustrates $P_{critical}$ as a function of β for different values of a (in inches). The critical pressure is obtained by setting $S = S_c$ in equation (7) and using equation (8) to yield θ with condition (9) satisfied. Since S is a quadratic function of p in equation (7), two roots of critical pressure can yield the same value of S_c for fixed θ. However, the root corresponding to an increasing value of S with increasing p is selected from physical considerations. Figure 7 also shows the interactions of mode I and mode II for different values of β. As expected, the tearing mode has the largest significance for values of β close to 45°. Figure 8 reveals the fracture propagation path as a function of β.

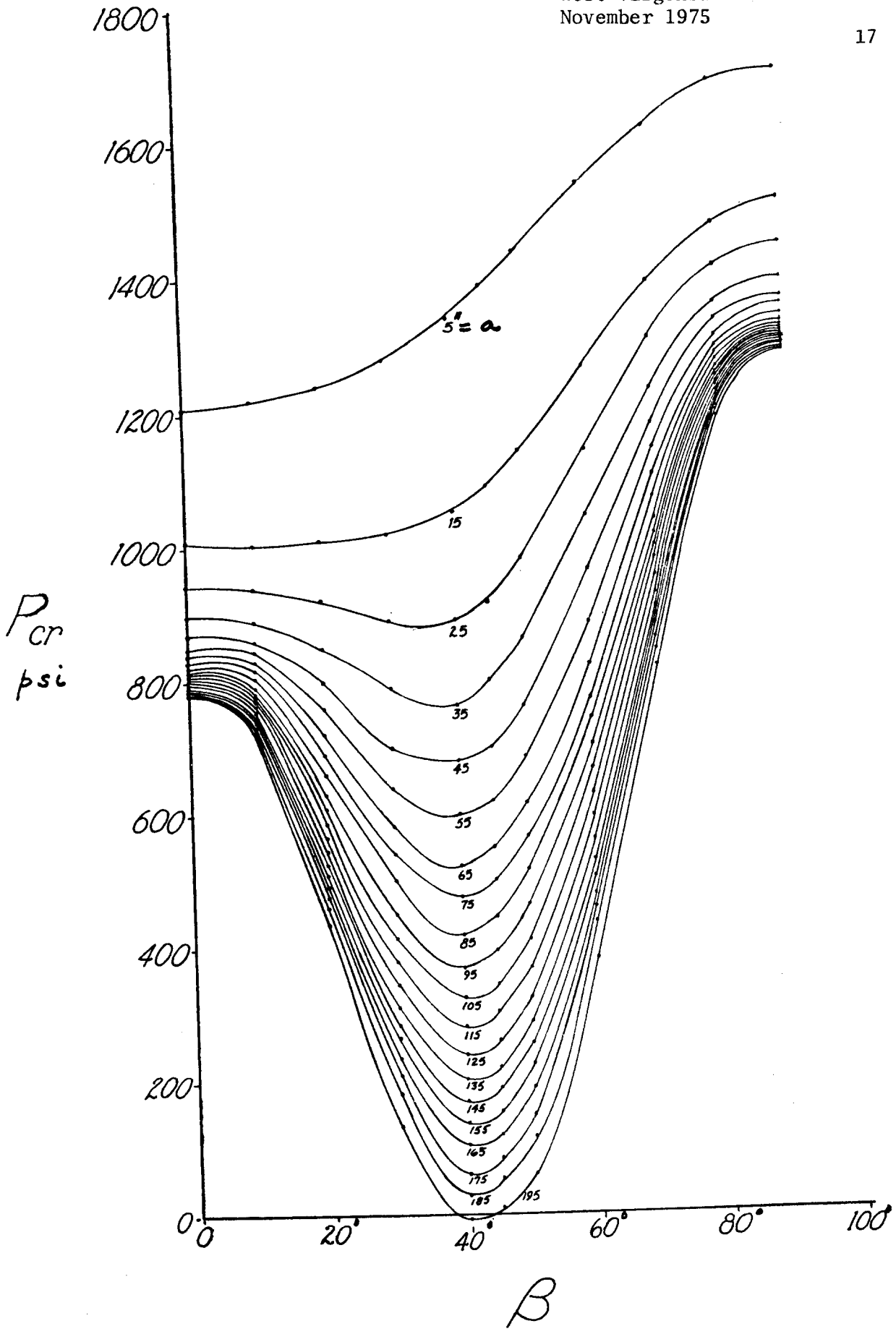

Figure 7. Critical Pressure Versus Inclination β for Two Dimensional Model with Various Crack Half Lengths.

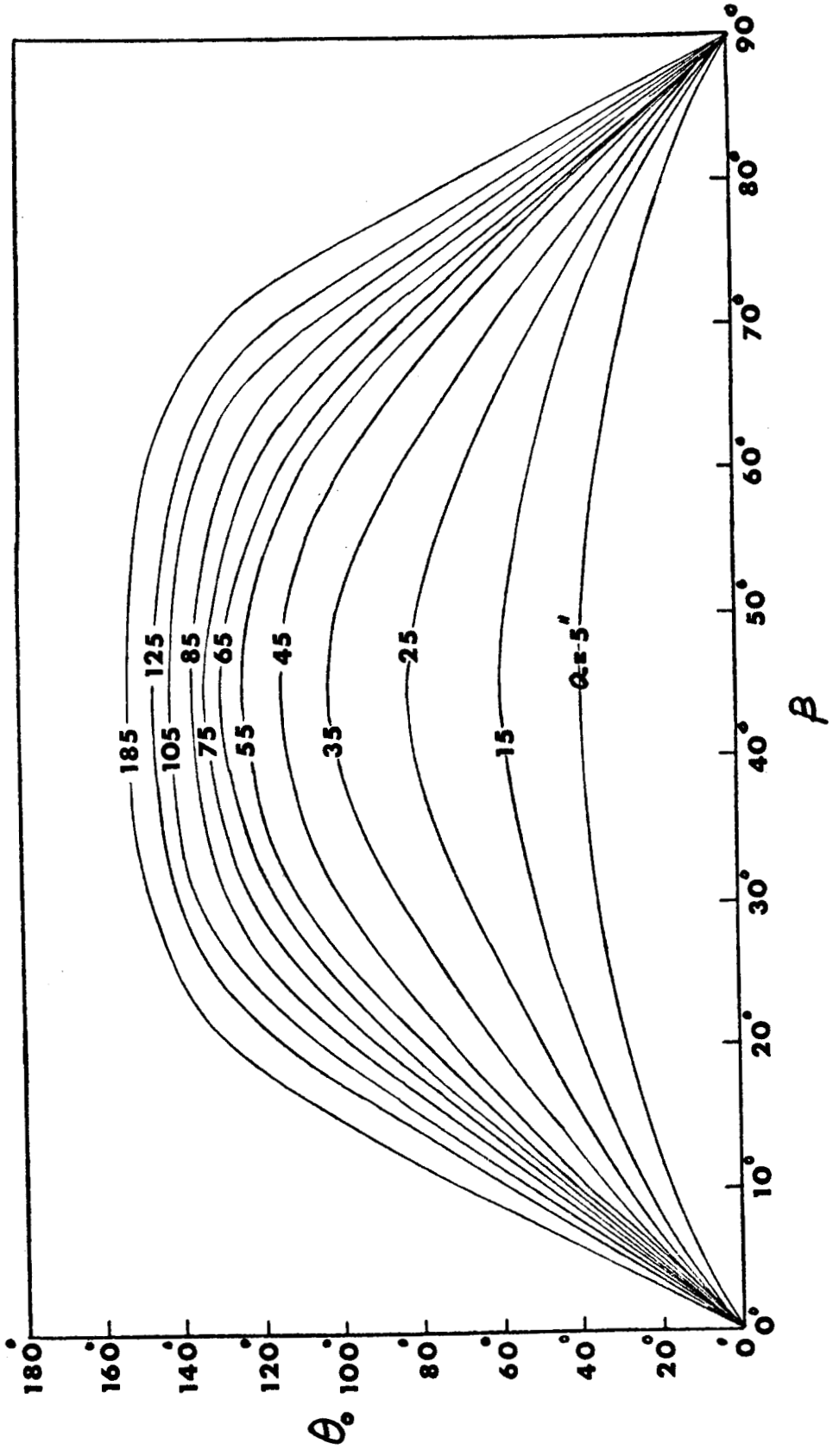

Figure 8. Fracture Extension Orientation versus Initial Crack Inclination for Different Crack Lengths.

The foregoing results for the model can be modified to include any crack pressure distribution. For example, if the pressure distribution in the crack due to fluid flow effects is given by

$$p = p_0 \left(1 - \frac{x^2}{a^2}\right)^{\frac{\gamma}{2}} \qquad \gamma > -1 \tag{11}$$

then the corresponding stress intensity factors in equation(s) will be

$$\begin{aligned} k_1 &= \left(\frac{p_0 \, \Gamma\left(\frac{\gamma+1}{2}\right)}{\Gamma\left(\frac{\gamma}{2}+1\right)} + \sigma_1 \sin^2\beta + \sigma_2 \cos^2\beta\right)\sqrt{a} \\ k_2 &= (\sigma_1 - \sigma_2) \sin\beta \cos\beta \sqrt{a} \\ k_3 &= 0 \end{aligned} \tag{12}$$

where $\Gamma(\gamma)$ is a Gamma Function. The analysis of the problem is therefore identical to before.

The two dimensional modeling analysis discussed here is applicable to a wide variety of hydraulic fracturing conditions such as different pressure profiles, different values of tectonic stresses, and crack configuration. The fundamental ideas can be easily extended to three dimensional modeling.

2.1.2 THREE DIMENSIONAL MODELING

As indicated above, the two dimensional modeling analysis provides basic guidelines for the three dimensional model formulation and solution. Referring to Figure 9, with the crack in the xz plane, the overburden stress σ_z and the tectonic stress σ_1 produce stresses on the surface of the

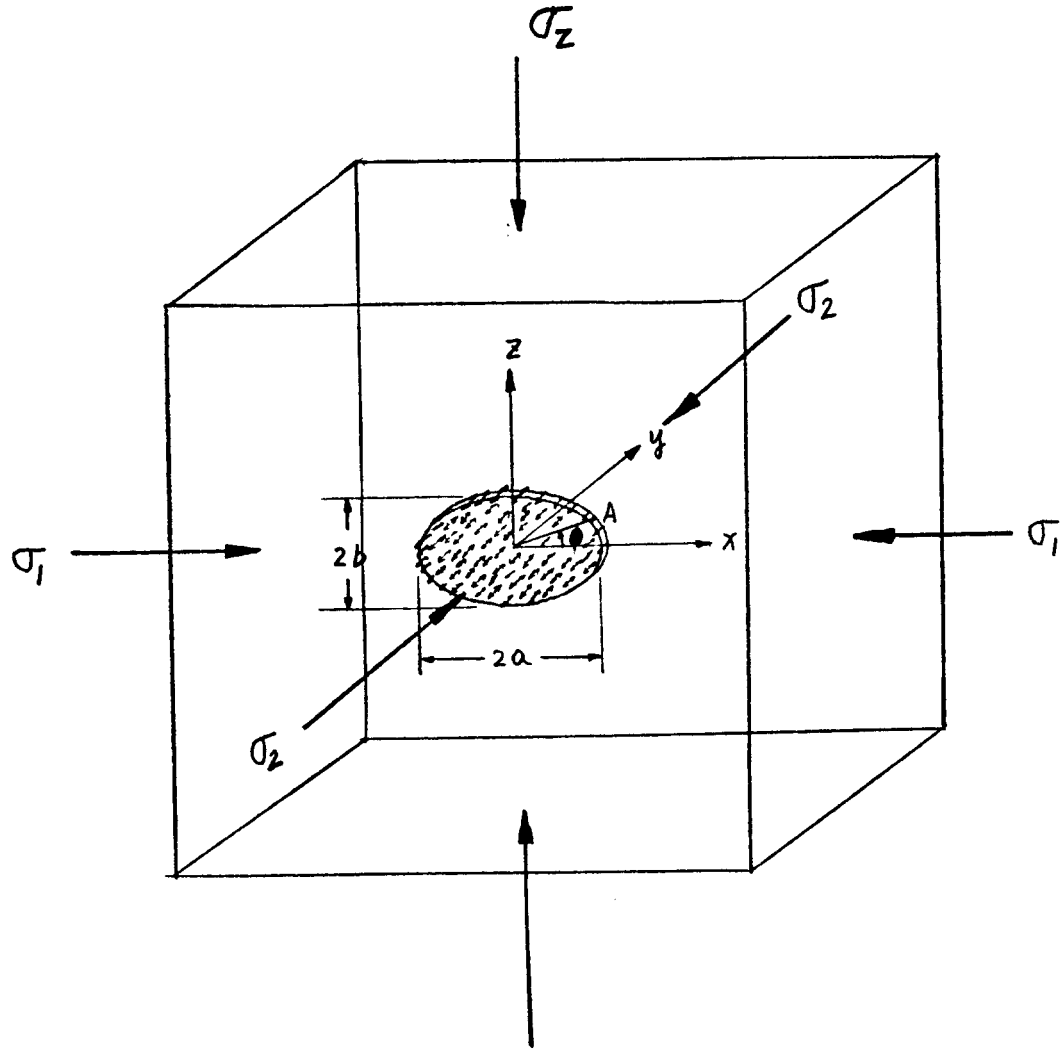

Figure 9. Elliptic Crack Subjected to Triaxial Stresses.

elliptical crack which are negligible compared to those produced by the internal pressure p and the tectonic stress σ_2. For this case ($\sigma_z > \sigma_1 > \sigma_2$) the stress intensity factors at point A on the surface of the elliptical crack are given by

$$k_1 = \frac{(p-\sigma_2)\sqrt{b}}{E(k)}\left\{\sin^2\phi + \frac{b^2}{a^2}\cos^2\phi\right\}^{\frac{1}{4}} \tag{13}$$

$$k_2 = k_3 = 0$$

where ϕ is measured from the x axis in the plane of the crack.

More detailed expressions for an elliptical crack inclined to a three dimensional stress field are given in Appendix A. Investigations of stresses at the surface of a flat ellipsoid and fracture criterion in three dimensions have been conducted by Mirandy and Paul (48,49).

It can be noted from equation (13), that k_1 is maximum at the intersection of the crack boundary with the minor axis b. Crack extension will therefore occur at $\theta = \pi/2$ and the effect of the increased pressure P would be to produce a circular crack ($k_1 = 2\frac{(p-\sigma_2)}{\pi}\sqrt{a}$). However, various considerations such as layered media, natural faults, and fluid flow effects tend to keep the vertical crack propagation in the oil bearing formation. For a/b>5, then the solution for k_1 approaches the plane strain solution for a through crack with length 2b, i.e., $k_1 = \sigma\sqrt{b}$ as $a \to \alpha$.

Table I compares the values of the critical pressures for circular, elliptical, and line (β=0) cracks.

Table I
Comparison of Critical Pressures

Crack Dimension	$(P_{critical} - \sigma_2)$ psi					
	2D line	3D penny	3D elliptical crack			
b inches	crack	crack a=b	a=2b	a=3b	a=5b	a=10b
5	504	792	610	562	530	513
15	291	457	353	324	306	296
25	226	354	273	251	237	229
55	152	239	184	169	160	155
75	130	205	158	145	137	132
125	101	158	122	112	106	103
225	75	118	91	81	79	76
425	55	86	66	61	57	56
625	45	71	55	50	47	46
825	39	61	48	44	41	40
1000	36	56	43	40	38	36

2.2 FINITE ELEMENT MODELING RESULTS

The idealized two and three dimensional models are analyzed by the NASTRAN computer program (50). Triangular and rectangular elements are used in the two dimensional analysis, whereas hexahedral and polyhedra with subtetrahedral (wedge) shapes are used in the three dimensional modeling. The direct stiffness method is used in formulating the stiffness matrix. Two separate and distinct model formulations are used for the crack tip and farfield analysis. For the crack tip analyses,

the displacement compatibility form of boundary conditions is chosen. The stress compatibility formulation is used for the far field solutions.

2.2.1 TWO DIMENSIONAL MODELING

The selected finite element model for the field analysis is illustrated in Figure 10. The same element arrangement is chosen for different crack inclinations. The tectonic stresses are specified with the crack orientation taken into account. Four stress loading cases are considered to compare superposition concepts and effects of boundary conditions. These cases are:

(i) Case I: Plate subjected to tectonic stress σ_1 only.

(ii) Case II: Plate subjected to tectonic stress σ_2 only.

(iii) Case III: Plate subjected to internal pressure p only.

(iv) Case IV: Plate subjected to σ_1, σ_2 and p simultaneously.

Figures 11 through 16 show σ_{max}, σ_{min}, and τ_{max} stress contours for Case III with β=0 and 45°. Corresponding plots for Case IV are revealed in Figures 17 through 22.

Figure 23 illustrates the configuration of the chosen crack tip model. The four cases presented above are analyzed. Detailed results and comparisons with crack tip solutions are presented in Appendix B. Figure 24 gives plots of the maximum principal stress concentration factor for the two dimensional model (Case III).

The stress contour plots are obtained by Wolfe's plotting routine. Symmetry in stress fields (Figures 11 through 22) is not occasionally apparent because of the chosen grid system which is unsymmetric around the two crack tips.

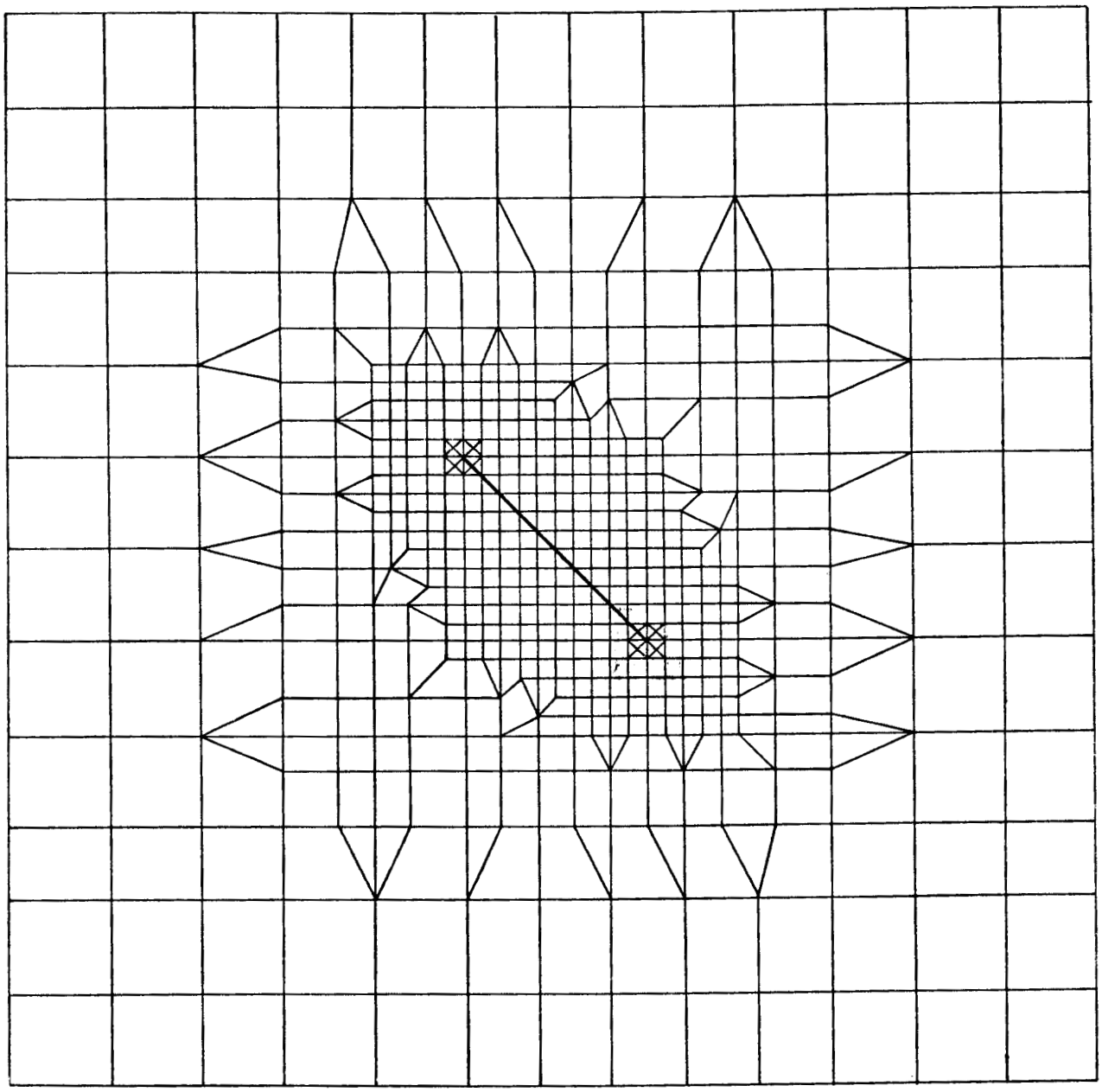

Figure 10. Two Dimensional Finite Element Model Configuration for Field Analysis, Corresponding Crack Tip Configuration is Detailed in Figure 23.

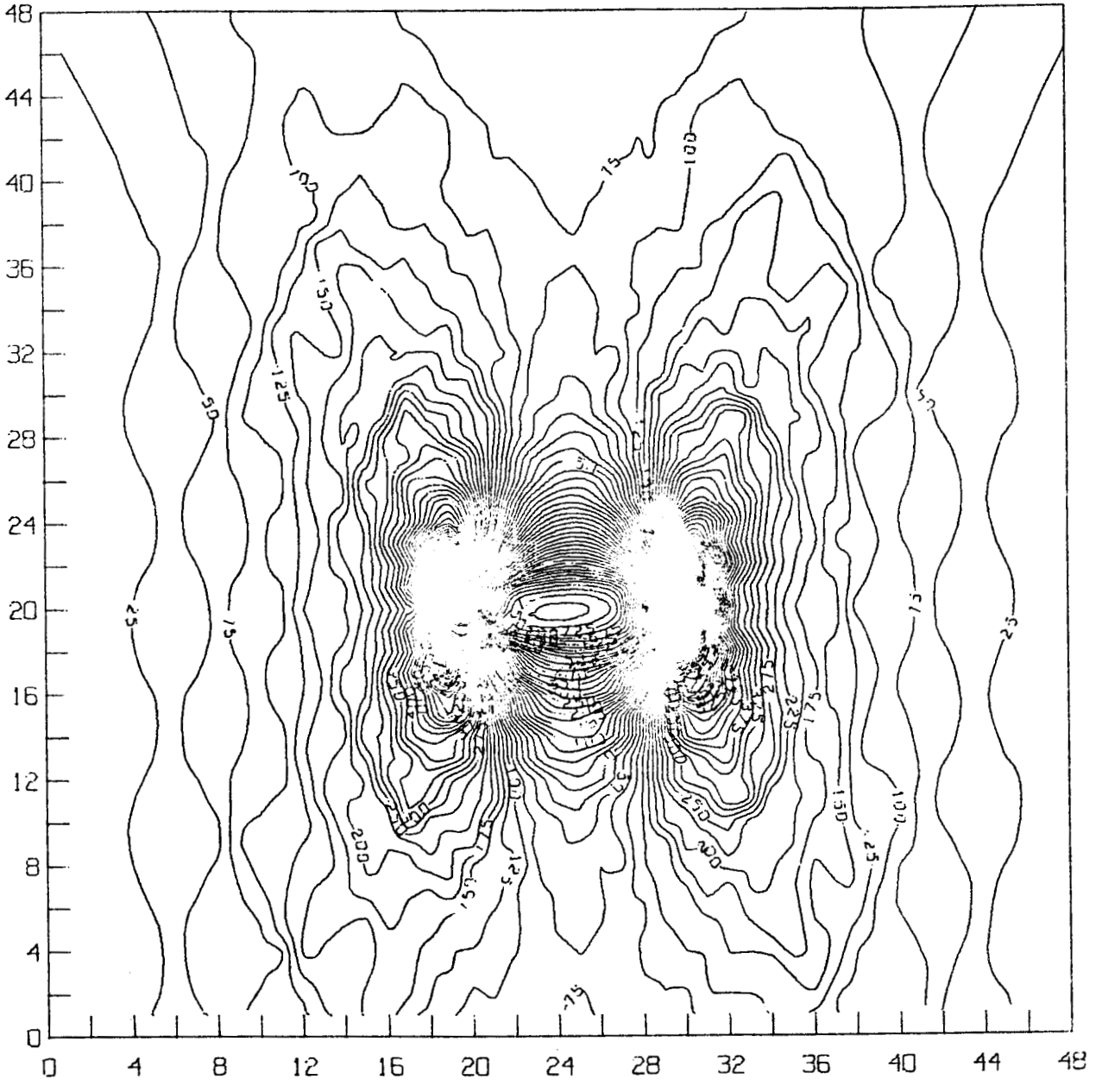

Figure 11. Maximum Normal Stress Contours for Case S_3 and $\beta = 0$
($p = 852$ psi, $a = 55$ in)

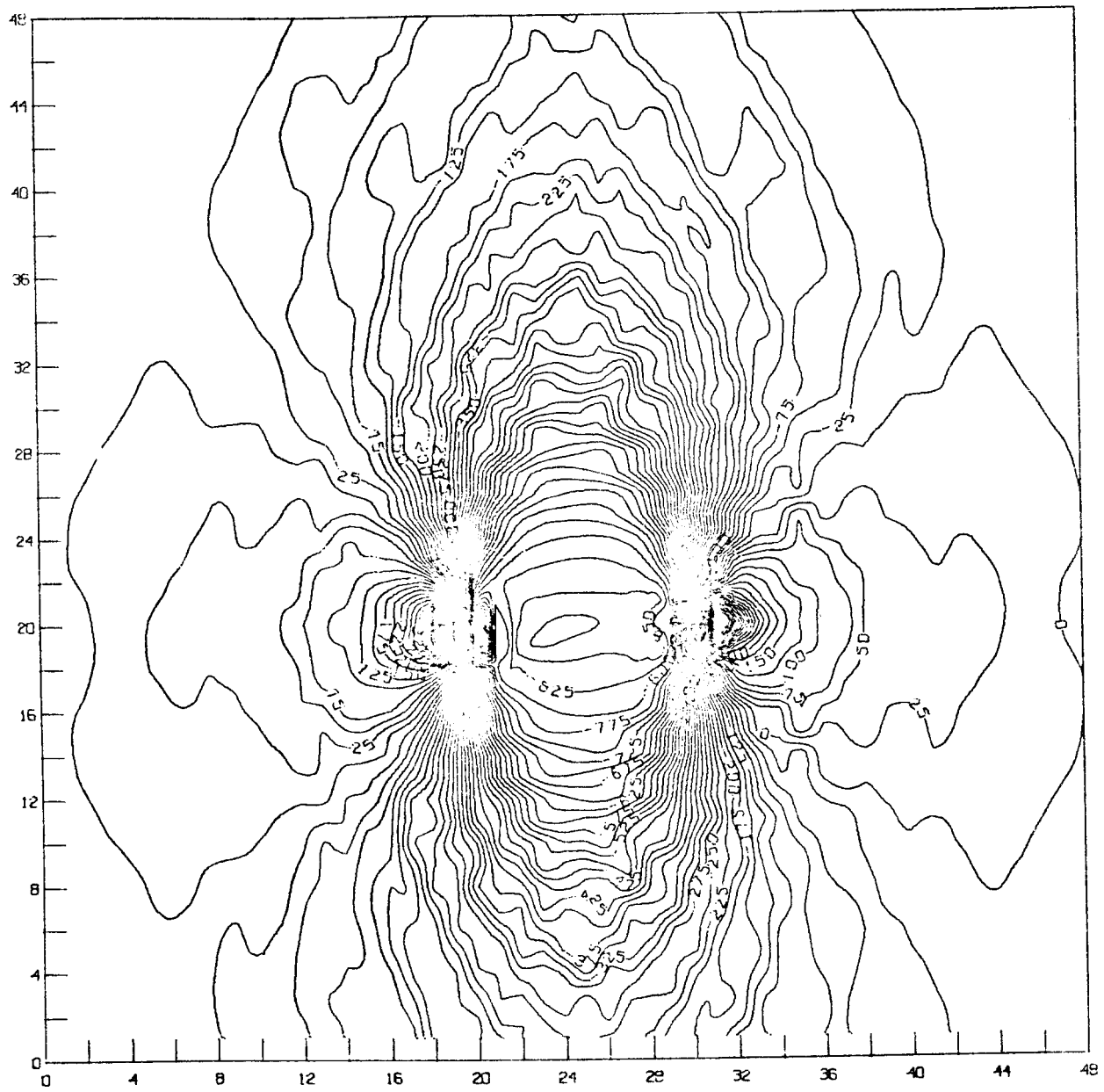

Figure 12. Minimum Normal Stress Contours for Case S_3 and $\beta = 0$
($p = 852$ psi, $a = 55$ in)

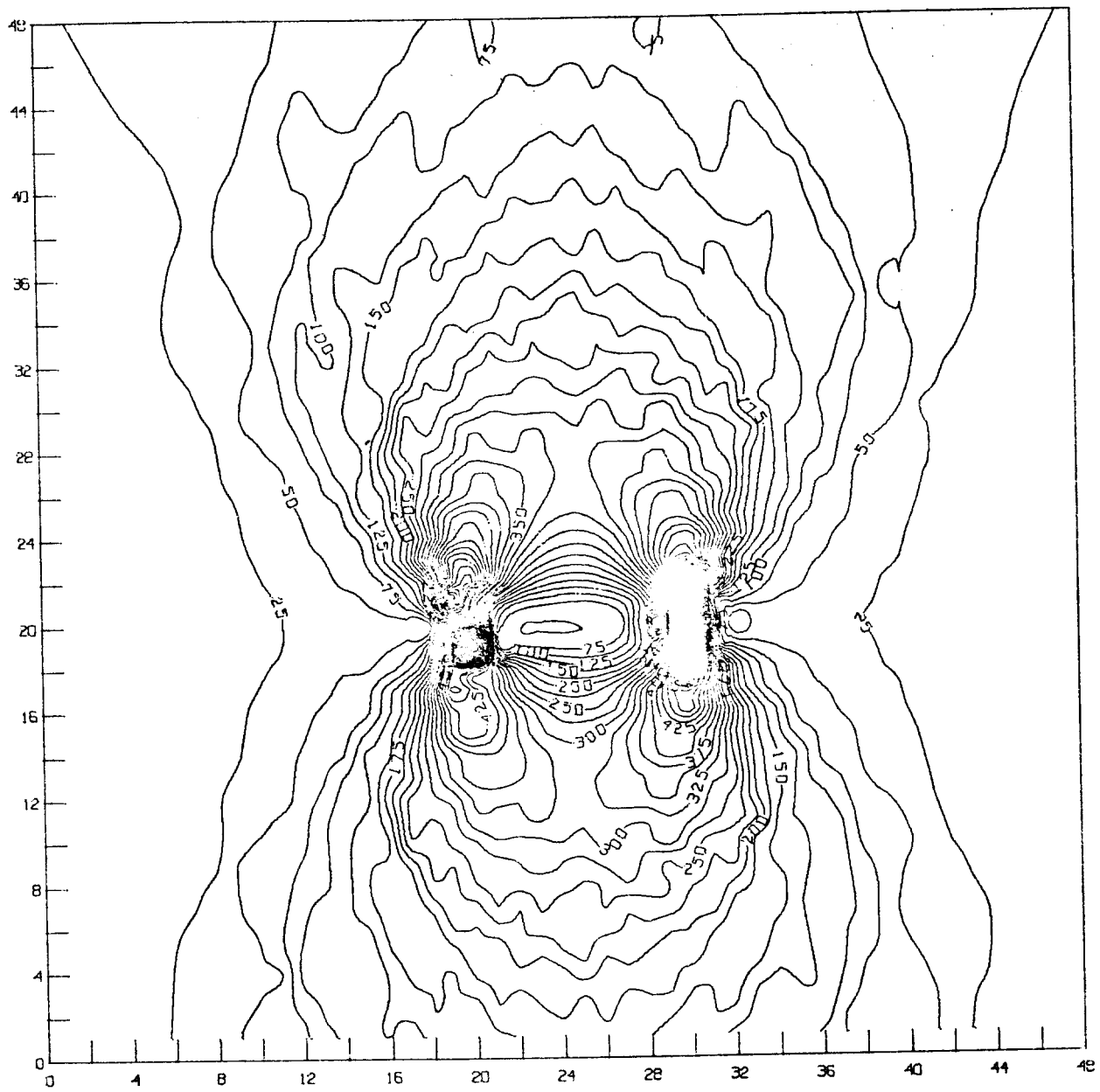

Figure 13. Maximum Shear Stress Contours for Case S_3 and $\beta = 0$
($p = 852$ psi, $a = 55$ in)

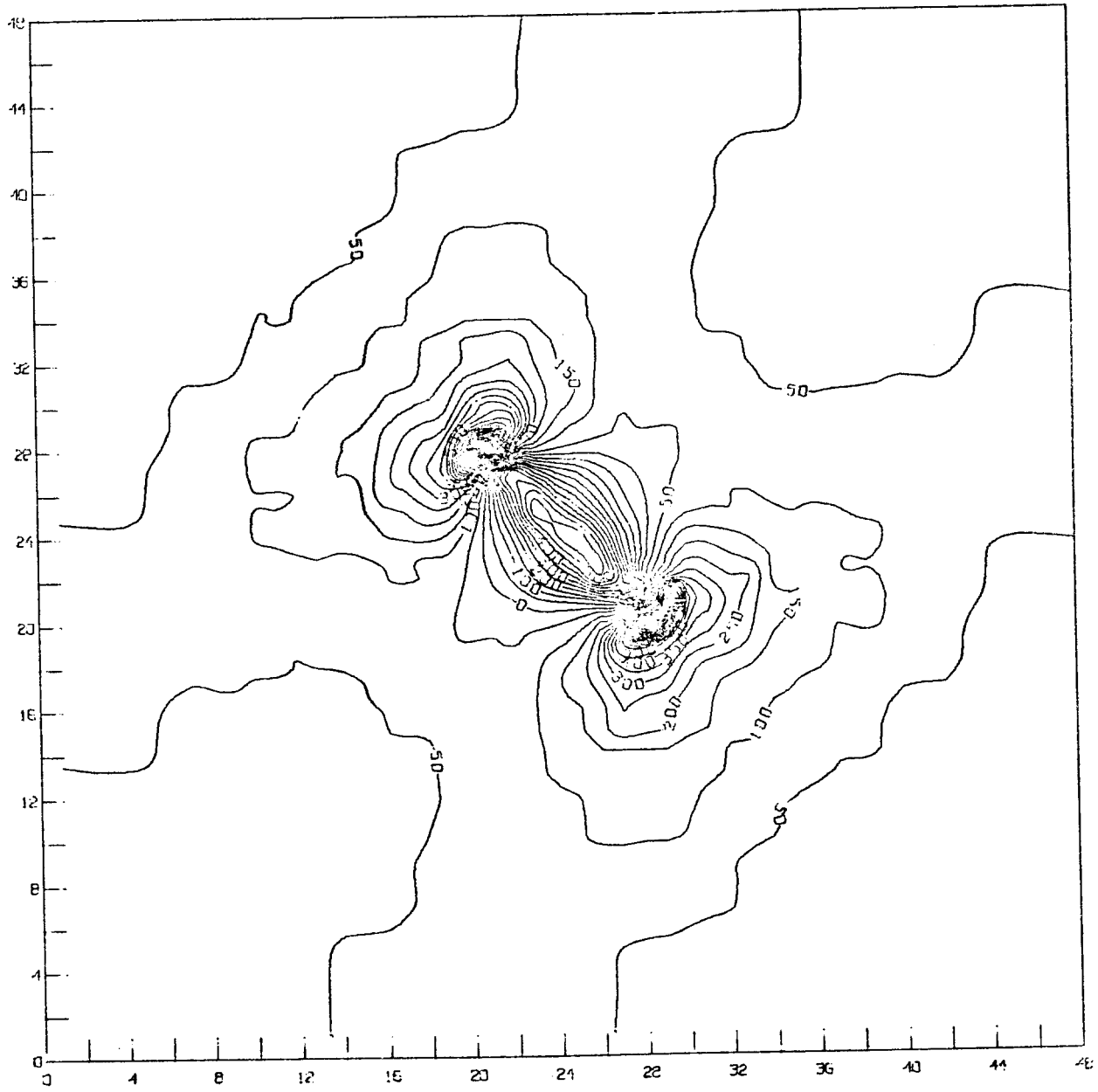

Figure 14. Maximum Normal Stress Contours for Case S_3 and $\beta = 45^o$
(p = 625 psi, a = 55 in)

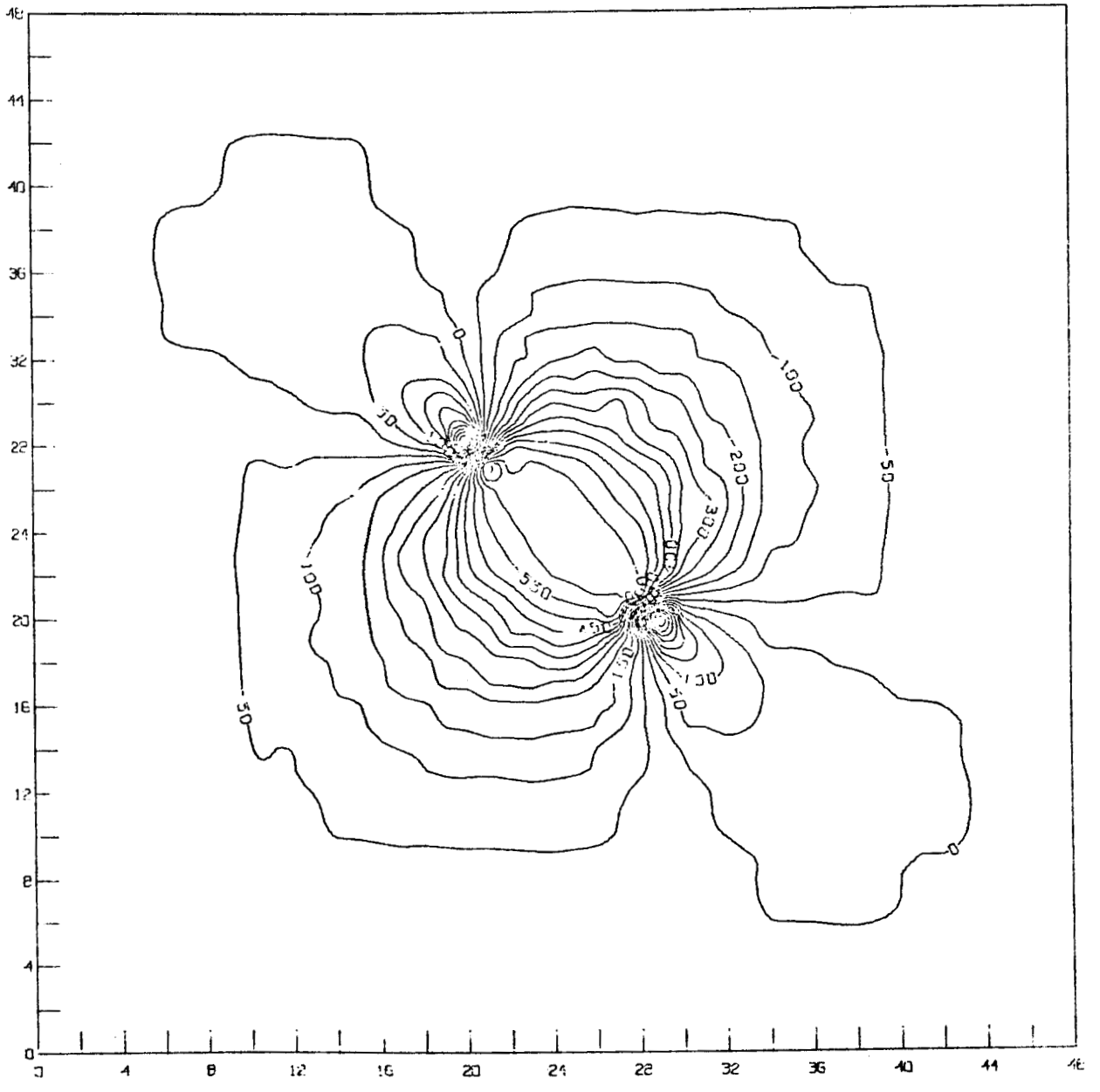

Figure 15. Minimum Normal Stress Contours for Case S_3 and $\beta = 45^{\circ}$ ($p = 625$ psi, $a = 55$ in)

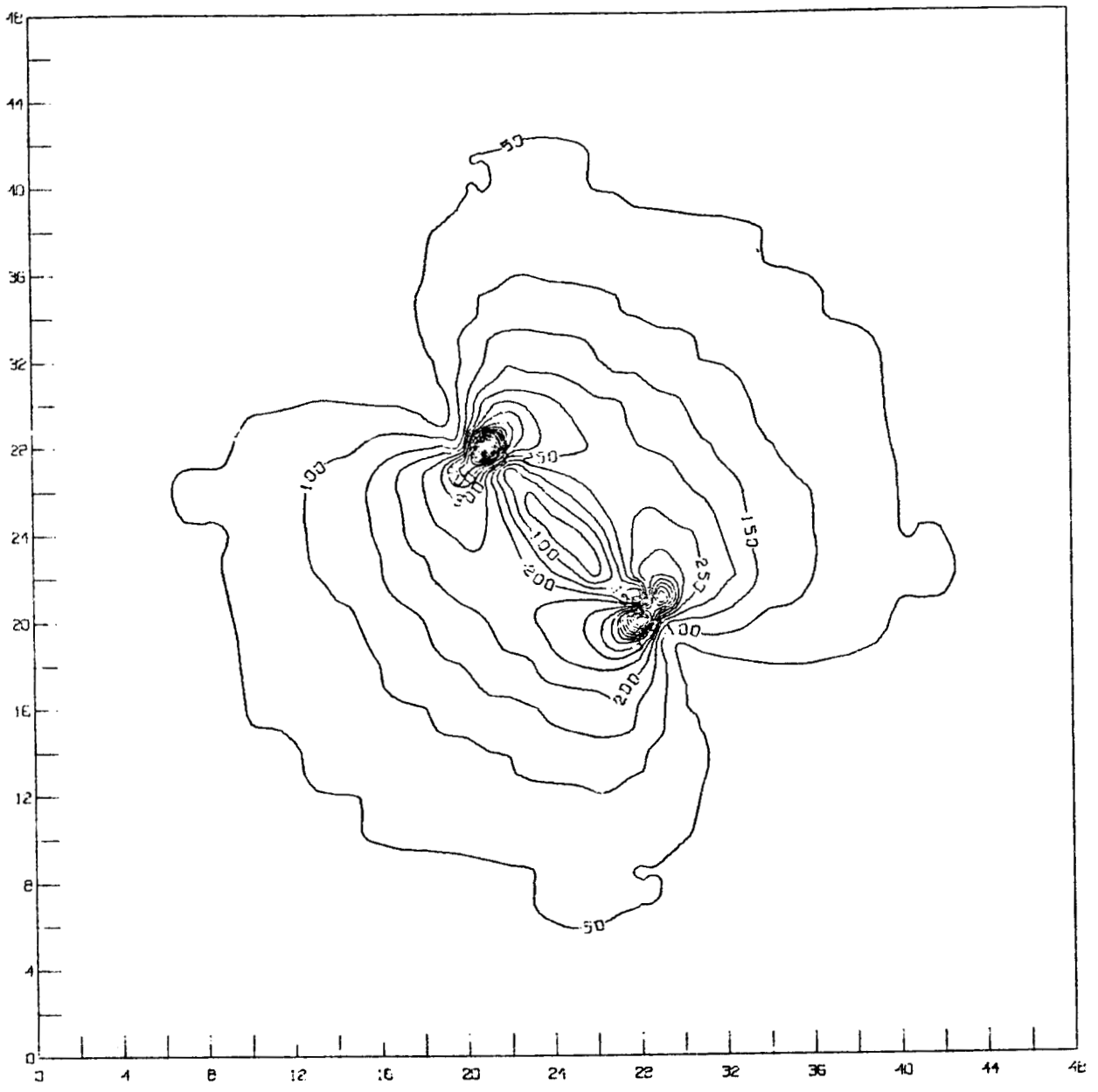

Figure 16. Maximum Shear Stress Contours for Case S_3 and $\beta = 45^o$
($p = 625$ psi, $a = 55$ in)

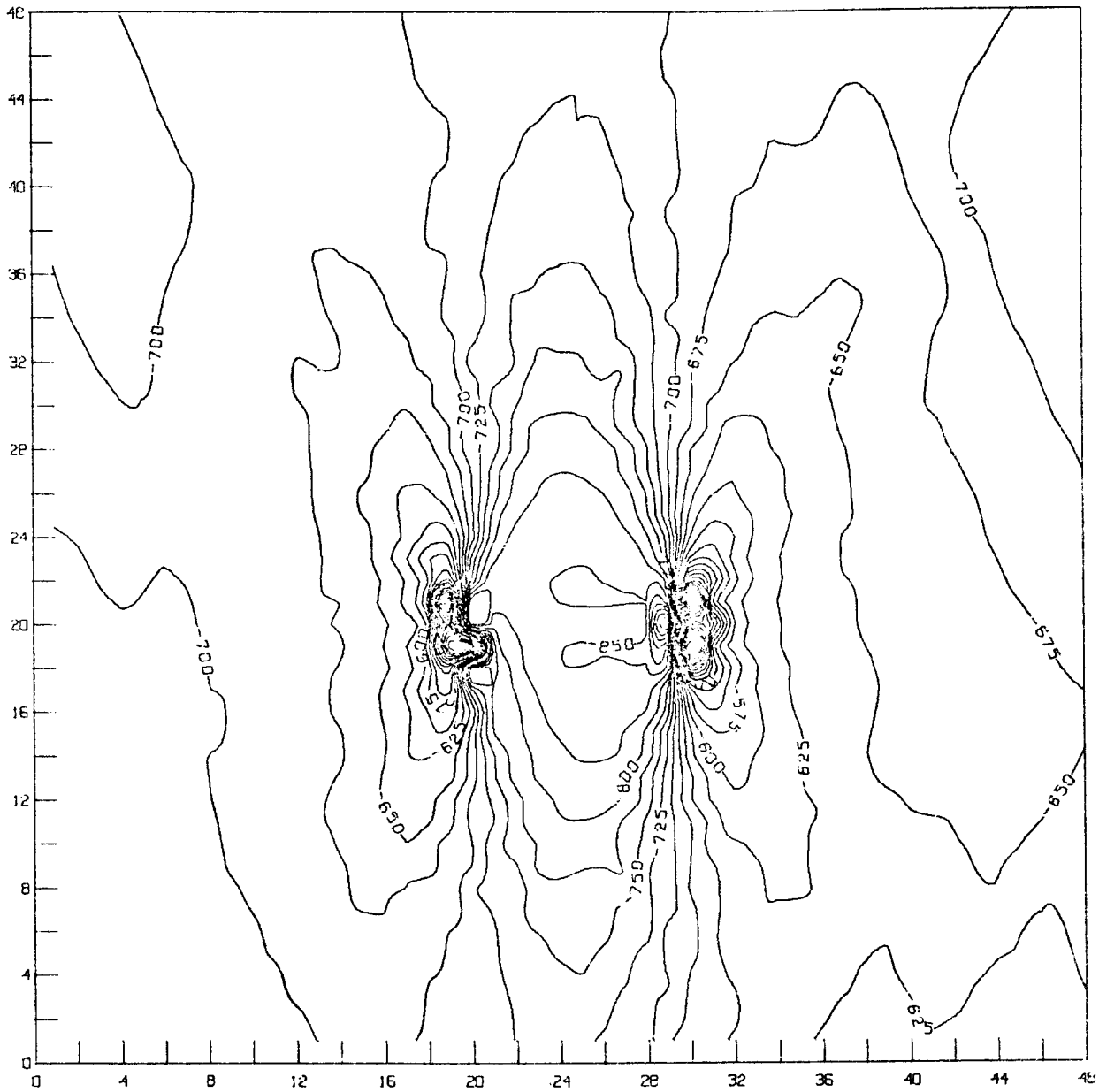

Figure 17. Maximum Normal Stress Contours for Case S_4 and $\beta = 0$
($p = 852$ psi, $a = 55$ in)

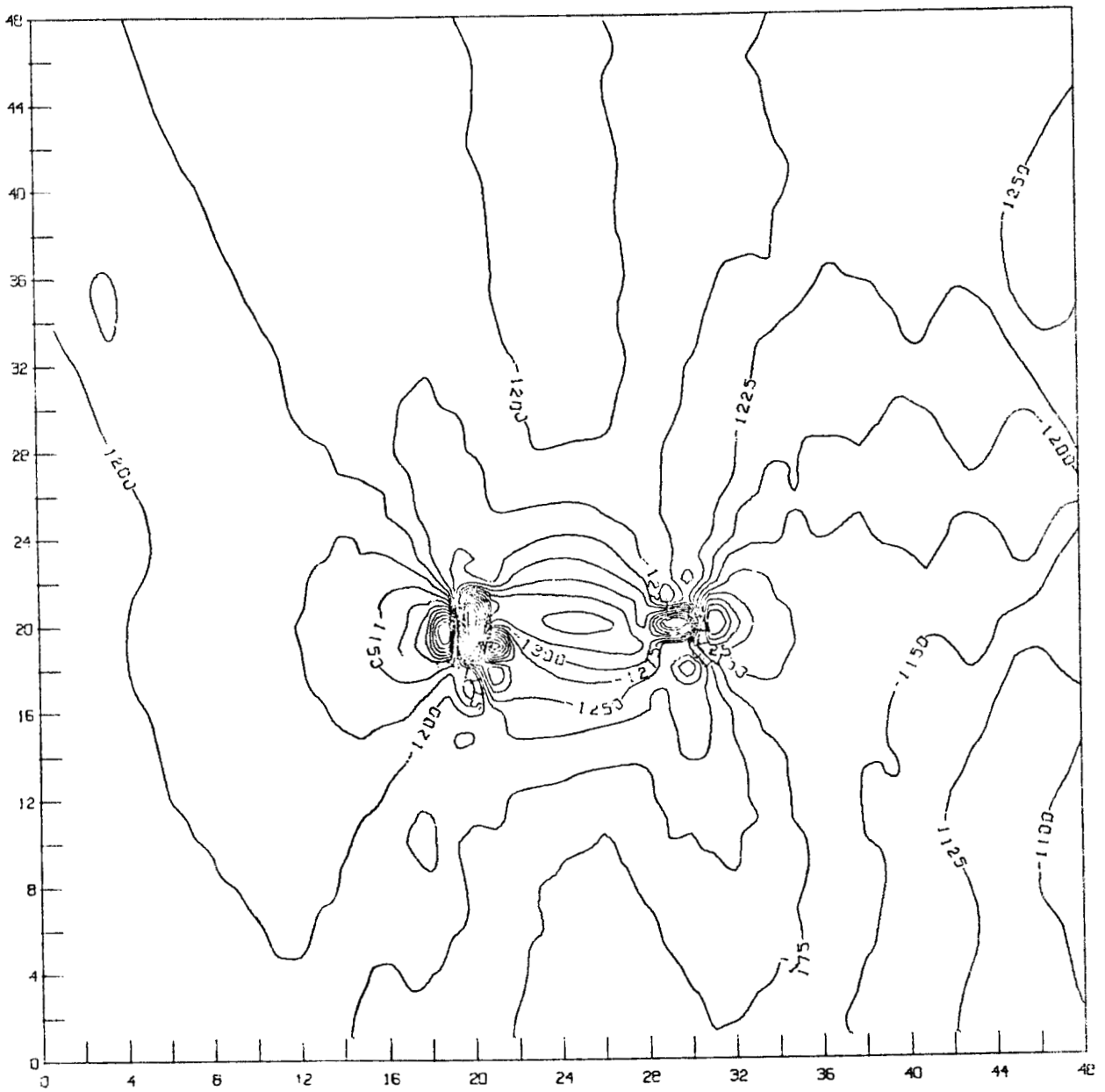

Figure 18. Minimum Normal Stress Contours for Case S_4 and $\beta = 0$
($p = 852$ psi, $a = 55$ in)

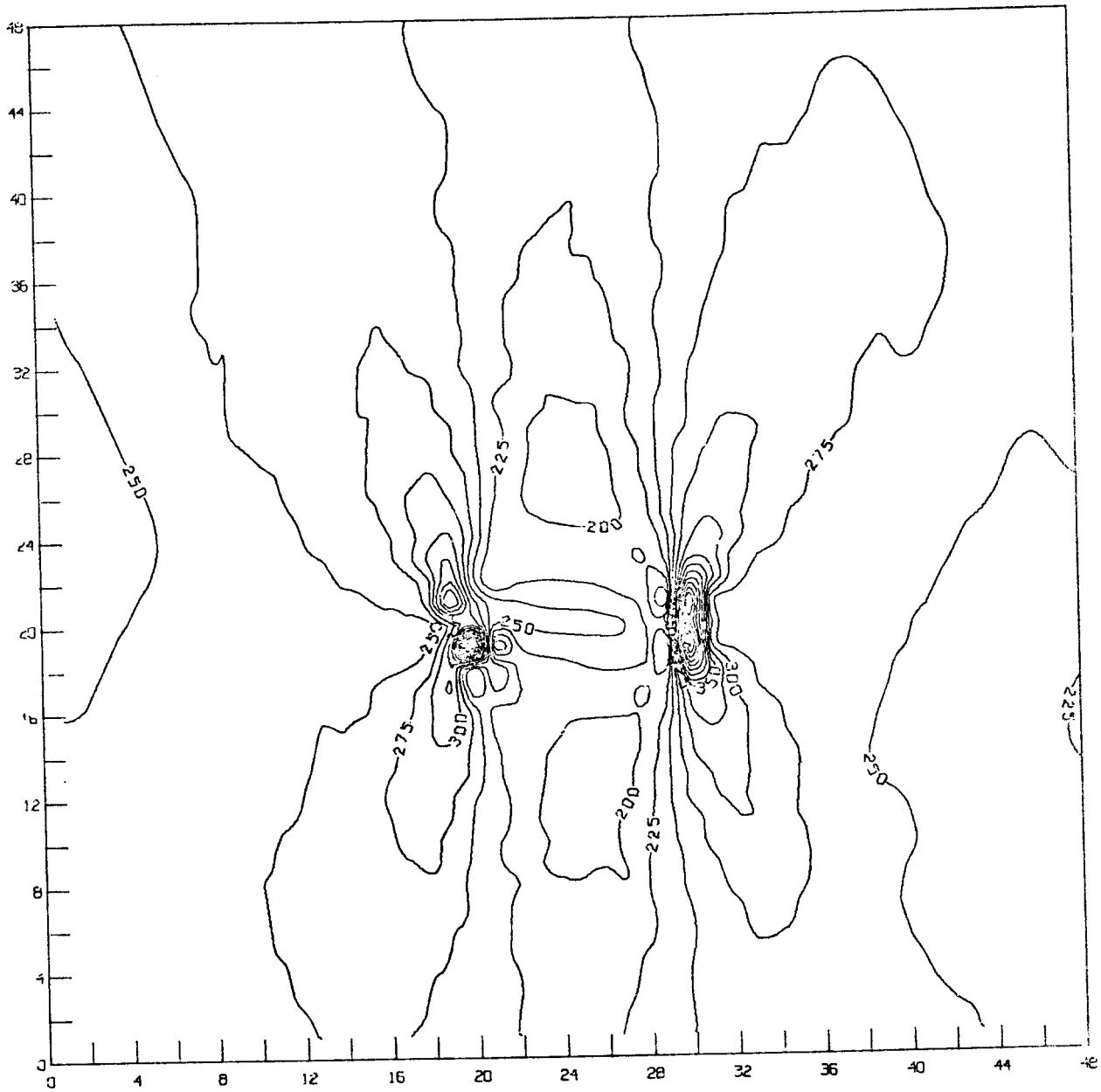

Figure 19. Maximum Shear Stress Contours for Case S_4 and $\beta = 0$
($p = 852$ psi, $a = 55$ in)

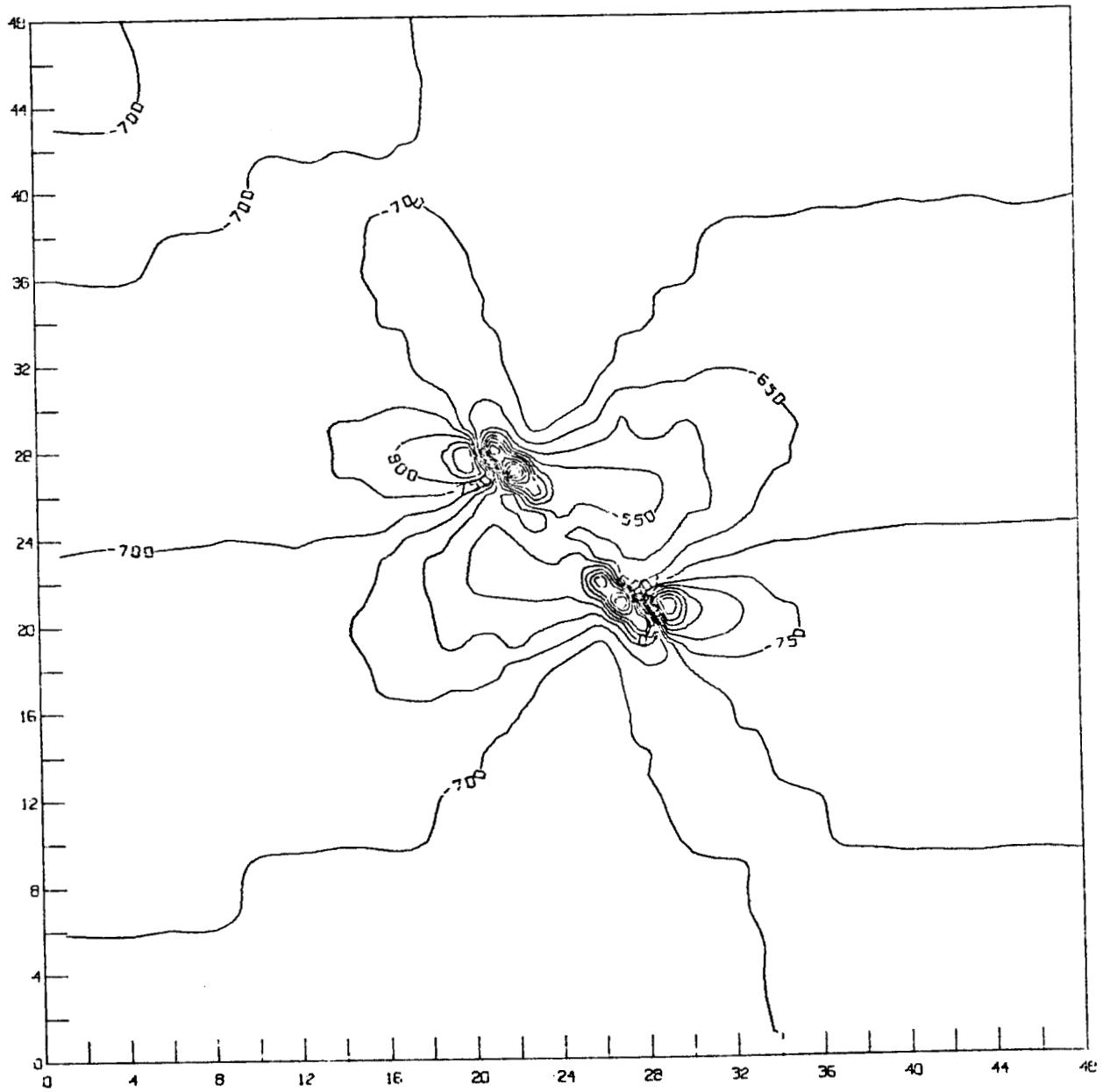

Figure 20. Maximum Normal Stress Contours for Case S_4 and $\beta = 45^o$
(p = 852 psi, a = 55 in)

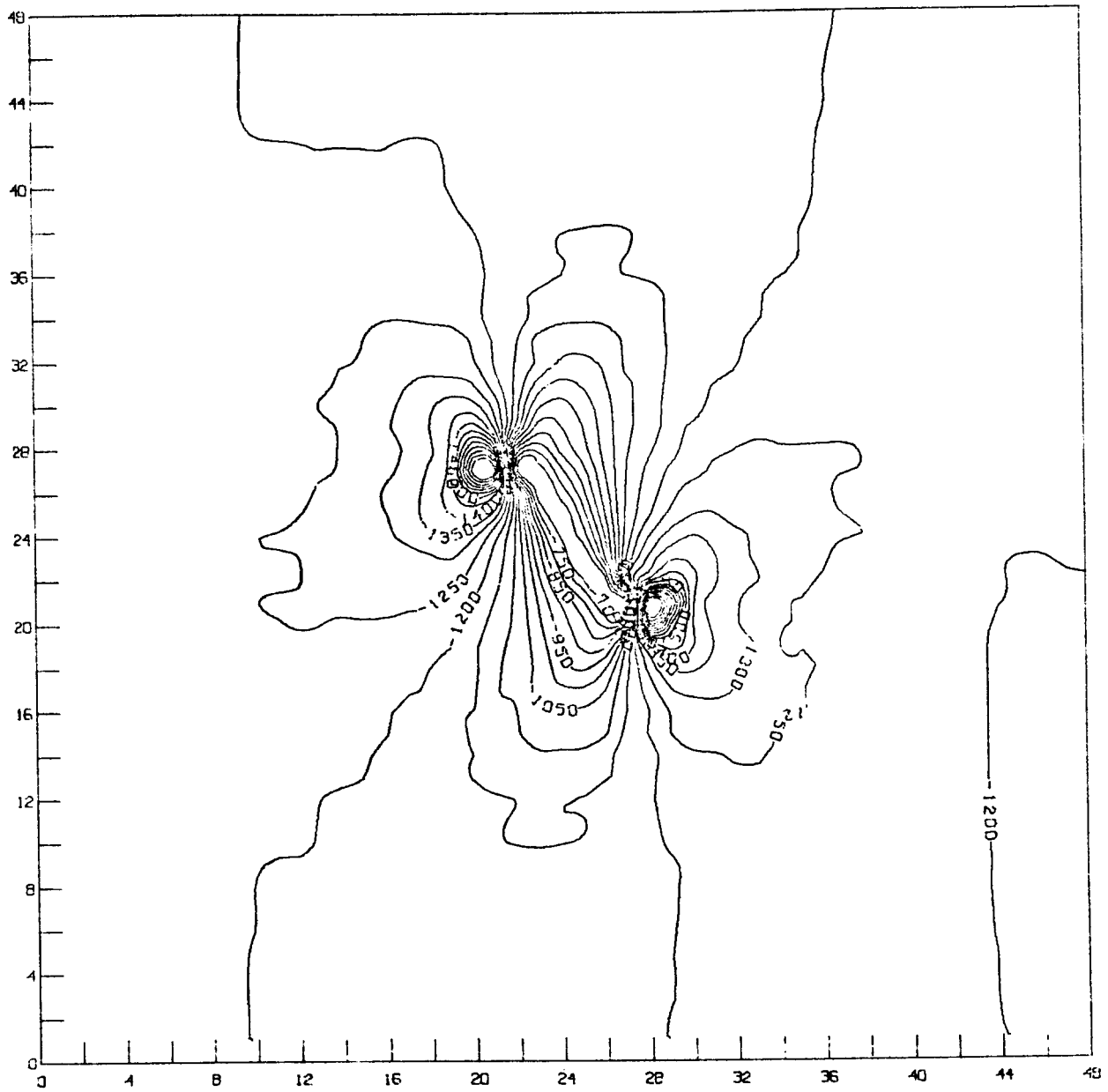

Figure 21. Minimum Normal Stress Contours for Case S_4 and $\beta = 45^{\circ}$
($p = 625$ psi, $a = 55$ in)

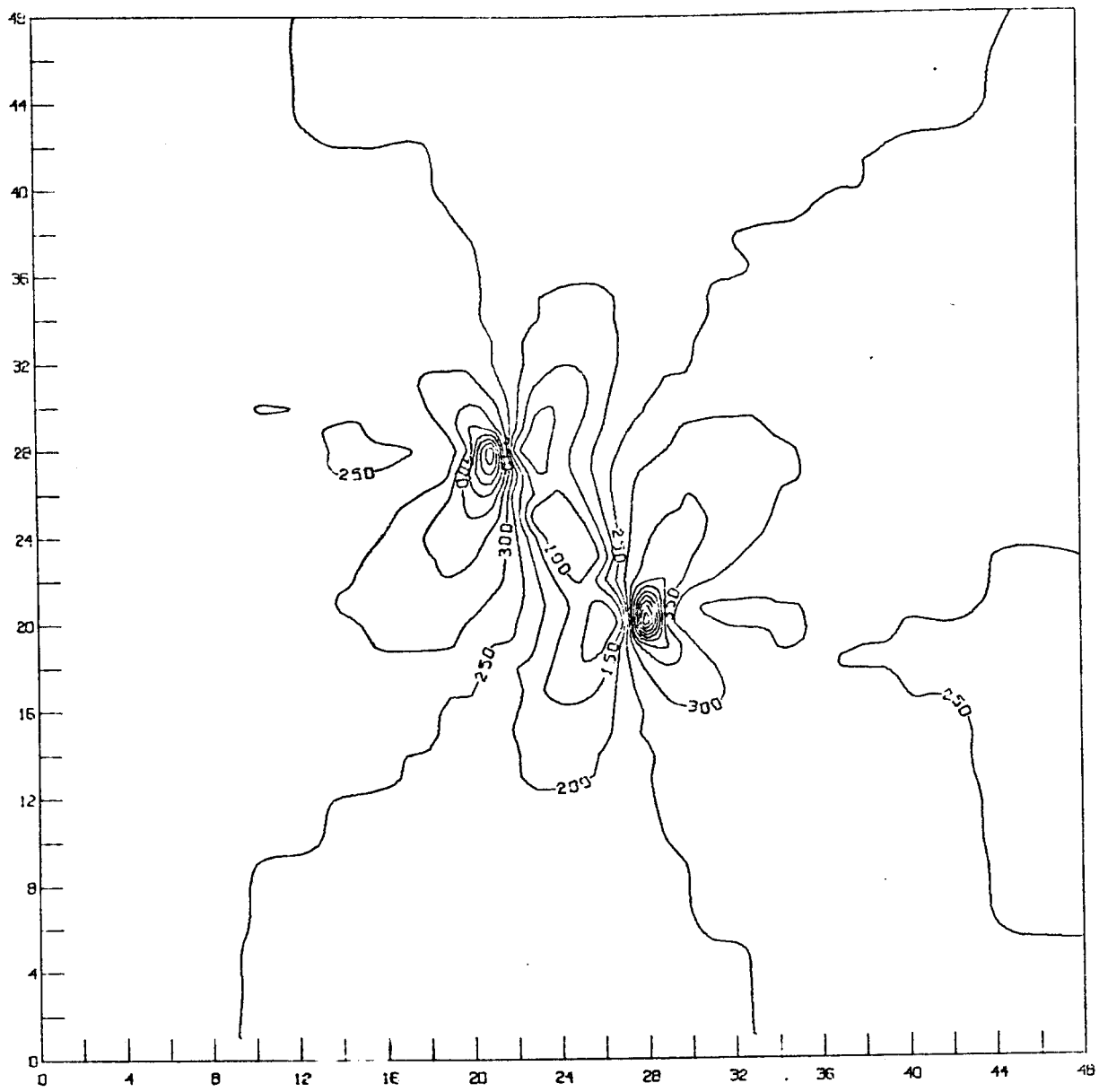

Figure 22. Maximum Shear Stress Contours for Case S_4 and $\beta = 45^o$
($p = 625$ psi, $a = 55$ in)

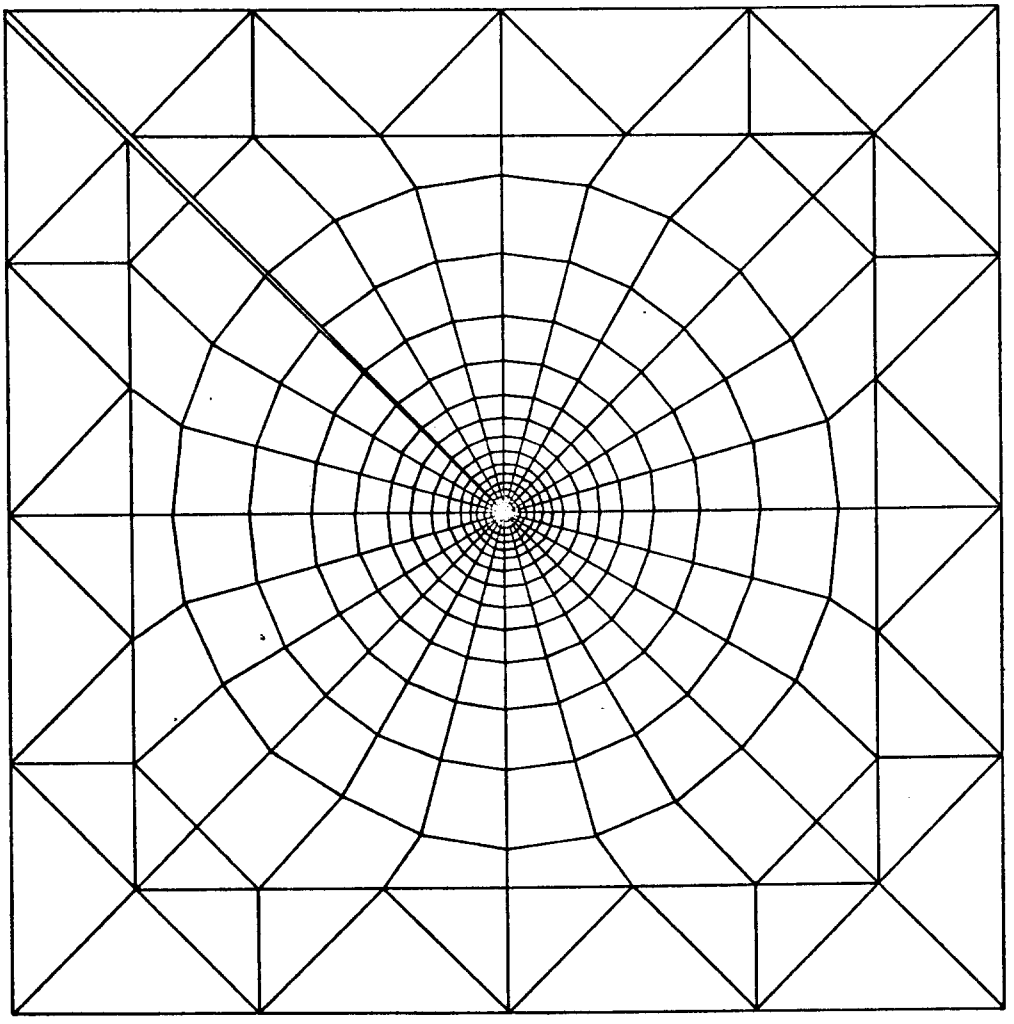

Figure 23. Two Dimensional Crack Tip Element Configuration Corresponding to Figure 10.

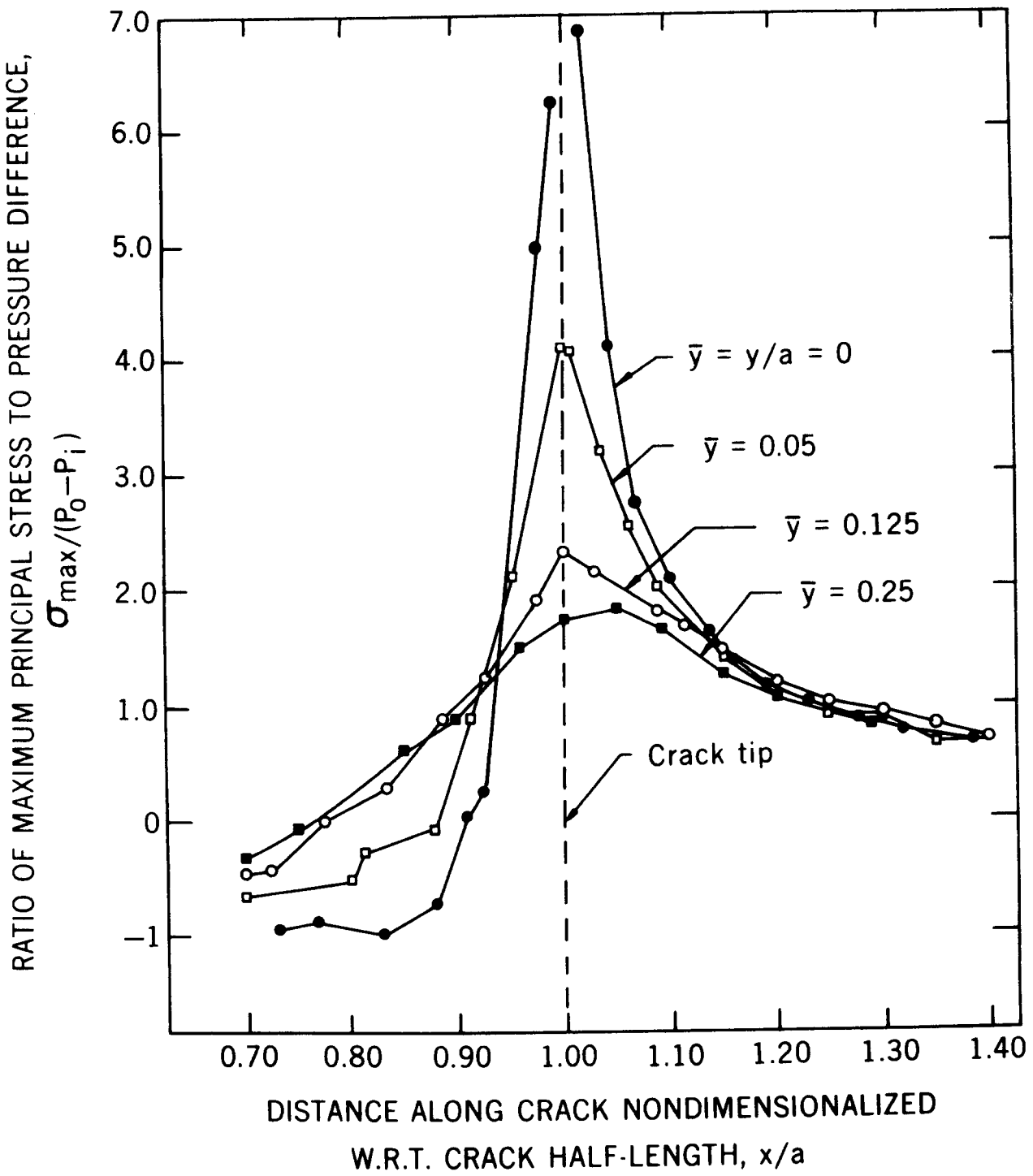

FIGURE 24.MAXIMUM PRINCIPAL STRESS CONCENTRATION FACTORS OF A 2-D MODEL

2.2.2 THREE DIMENSIONAL MODELING

Figure 25 illustrates an octant of the selected three dimensional model with a circular crack which is triangulated. The diameter of the crack in the overburden direction can be scaled by a linear transformation to yield an elliptical cross section crack. The output from the NASTRAN model includes

(i) Six stresses and strains

(ii) Three translational joint displacements

and

(iii) Octahedral shear stresses

A polar plot of the octahedral shear stress concentrations factors, for a vertical circular crack, is shown in Figure 26. The tectonic and overburden stress effects are not included in this plot.

Stress contour plots in any plane for the elliptical crack can be similarly obtained. The stress intensity factor k_1 for the triangulated elliptic crack model agrees well at various locations on the surface of the ellipse with values from equation 13 for $\frac{a}{b} = 2$ (pressurized crack). The effect of tectonic stresses on the model are qualitatively similar to those for the two dimensional case.

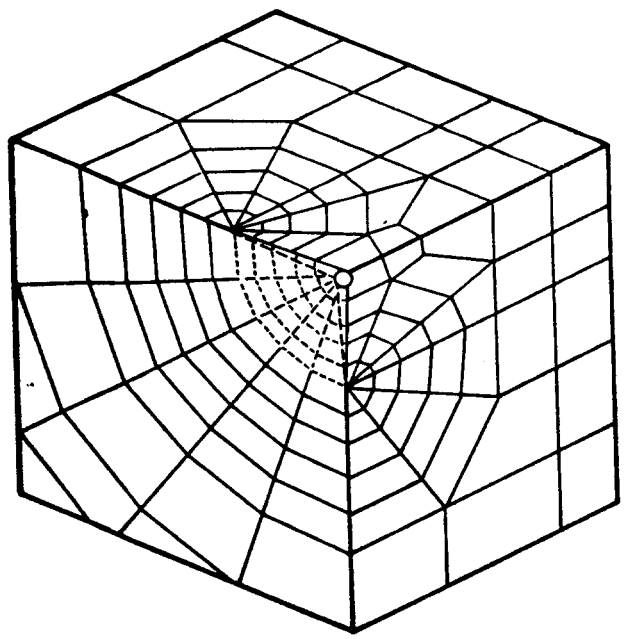

Figure 25. Three Dimensional Finite Element Model with Triangulated Circular Crack. Circular Crack Dimensions can be Linearly Scaled to Yield Elliptic Crack.

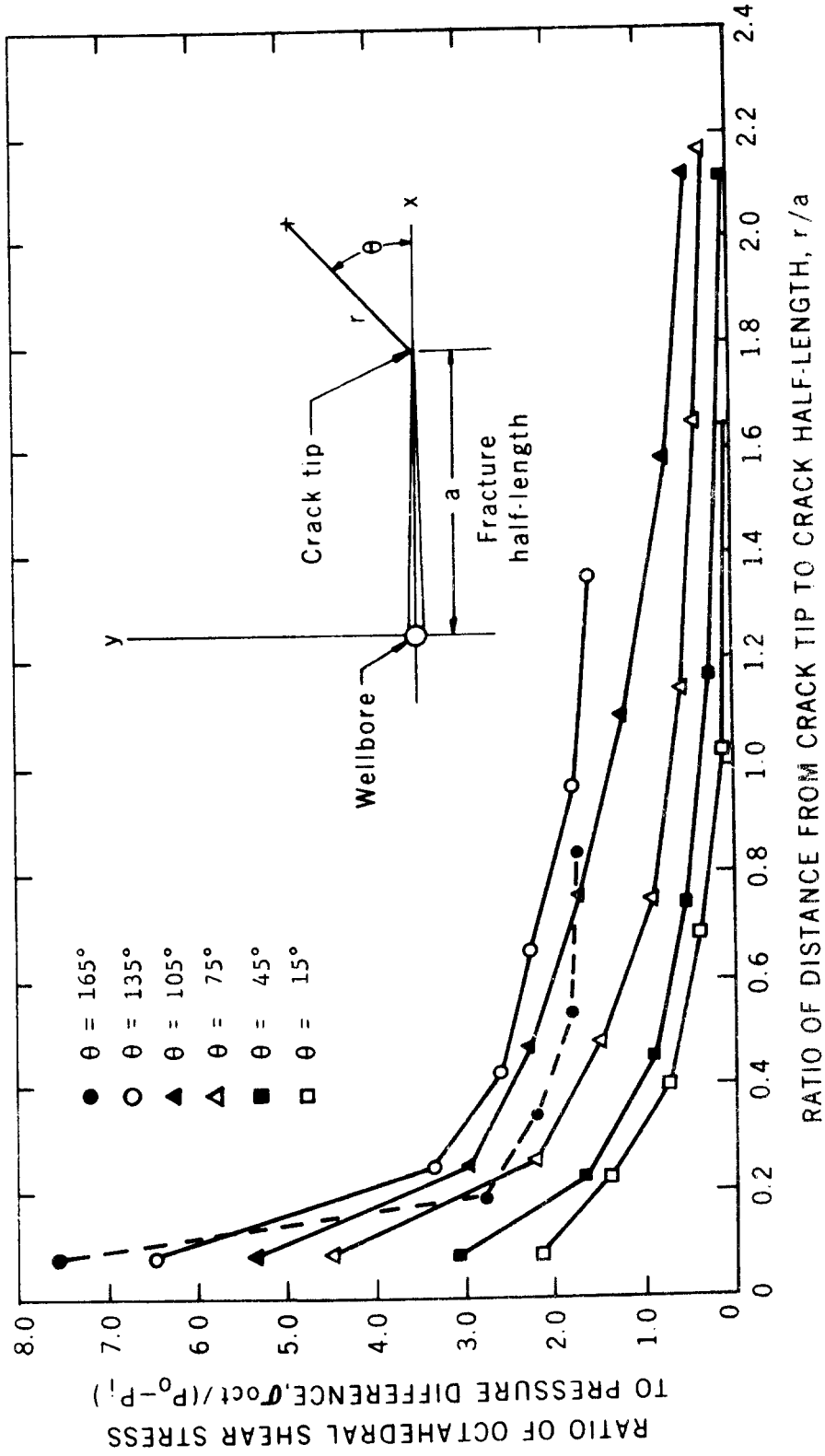

FIGURE 26. POLAR PLOT OF OCTAHEDRAL SHEAR STRESS CONCENTRATION FACTORS OF A 3-D MODEL

2.3 EXACT THEORY AND FINITE ELEMENT COMPARISONS

Classical elasticity theory solutions, applicable for hydraulic fracturing operations, have been given by Shuck and Advani (4). Figure 27 compares these solutions along the significant stress axis (primary direction of induced pressure) with two and three dimensional finite element results. The influence of tectonic and overburden stresses is ignored in these solutions.

Superposition of basic stress situations such as internal pressure and tectonic stresses can be easily accomplished. The superposition concepts are demonstrated in Figures 28.

Detailed comparisons of two dimensional finite element crack tip results for case III (internal pressure only) and case IV (internal pressure and tectonic stresses) with corresponding classical theory values are given in Appendix B (β=0, 45°). The classical theory principle stress values are obtained from the equations

$$\sigma_{xx} = \frac{K_1}{\sqrt{2r}} \cos\frac{\theta}{2}\left(1 - \sin\frac{\theta}{2}\sin\frac{3\theta}{2}\right) - \frac{K_2}{\sqrt{2r}} \sin\frac{\theta}{2}\left(2 + \cos\frac{\theta}{2}\cos\frac{3\theta}{2}\right) + \cdots + (\sigma_1 \cos^2\beta + \sigma_2 \sin^2\beta)$$

$$\sigma_{yy} = \frac{K_1}{\sqrt{2r}} \cos\frac{\theta}{2}\left(1 + \sin\frac{\theta}{2}\sin\frac{3\theta}{2}\right) + \frac{K_2}{\sqrt{2r}} \sin\frac{\theta}{2}\cos\frac{\theta}{2}\cos\frac{3\theta}{2} + \cdots - p \qquad (14)$$

$$\sigma_{xy} = \frac{K_1}{\sqrt{2r}} \cos\frac{\theta}{2}\sin\frac{\theta}{2}\cos\frac{3\theta}{2} + \frac{K_2}{\sqrt{2r}} \cos\frac{\theta}{2}\left(1 - \sin\frac{\theta}{2}\sin\frac{3\theta}{2}\right)$$

where $K_1 = (p + \sigma_1 \sin^2\beta + \sigma_2 \cos^2\beta)\sqrt{a}$

and $K_2 = (\sigma_1 - \sigma_2)\sin\beta\cos\beta\sqrt{a}$

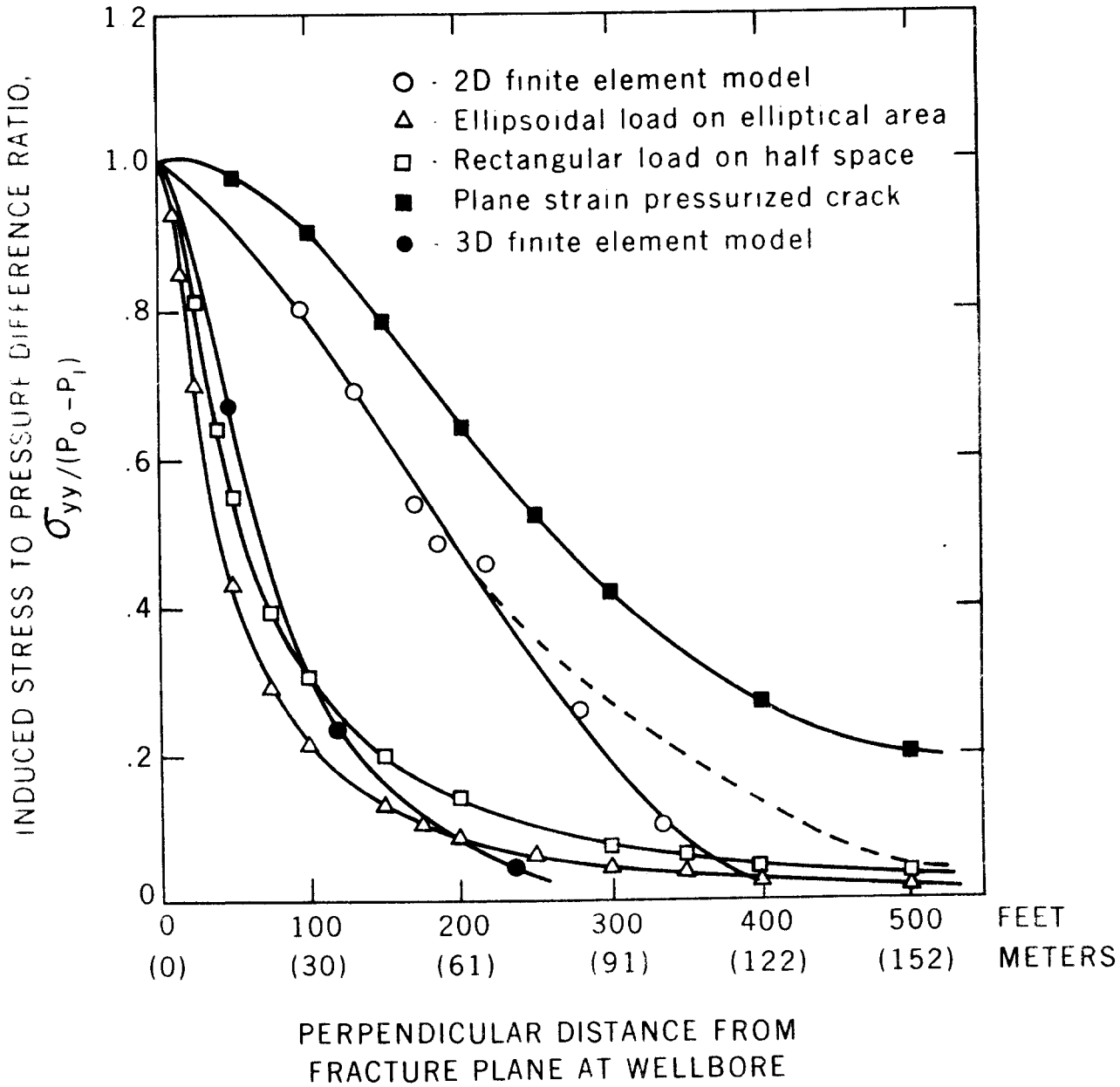

FIGURE 27.COMPARISON OF σ_{yy} FROM F.E.M. AND THEORY OF ELASTICITY

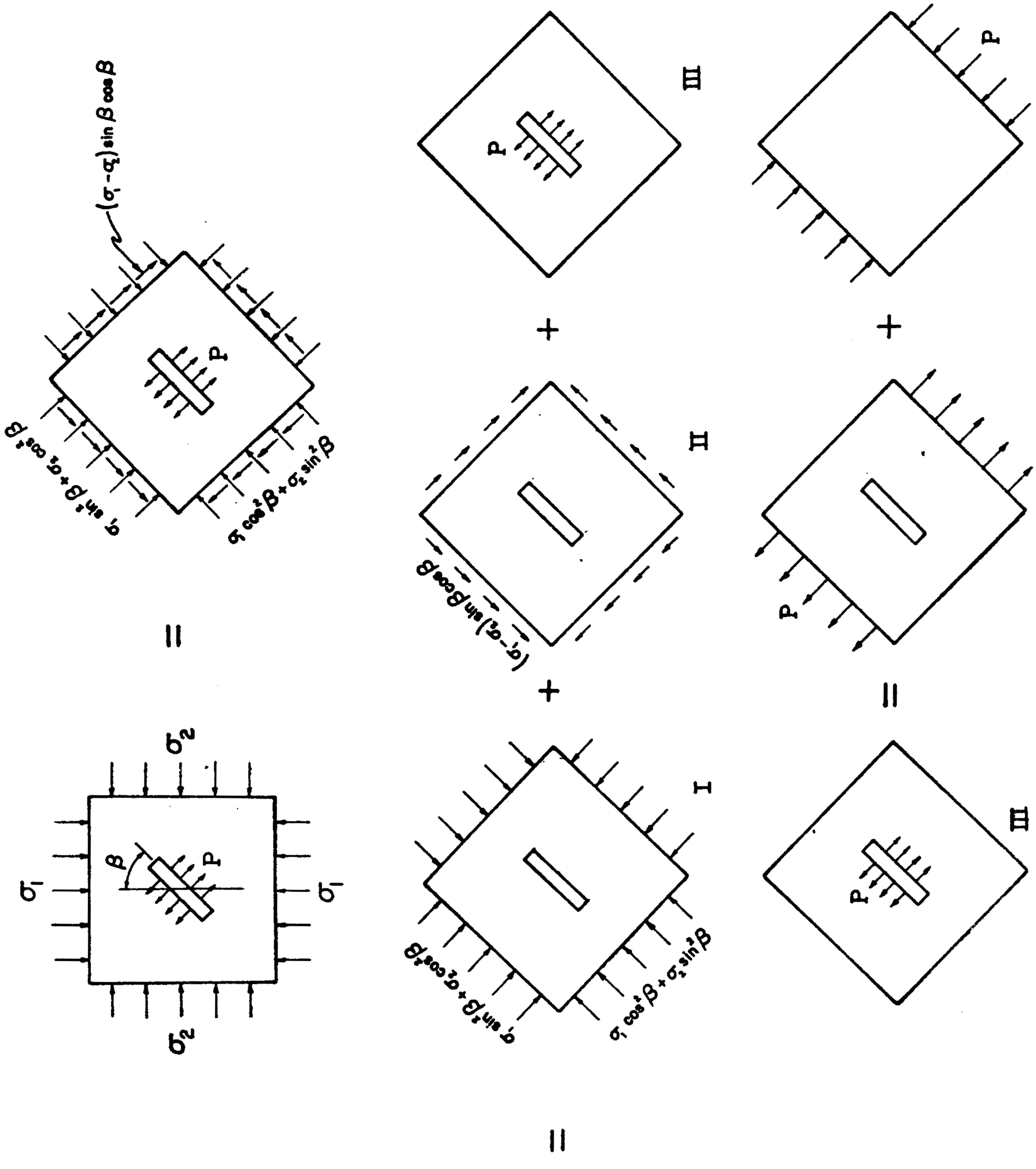

Figure 28. Superposition Concepts Relation to Internal Pressure and Tectonic Stresses.

The x and y coordinate axes in equation (14) are parallel and perpendicular to the crack axis respectively. The crack tip region is defined by $r < \frac{a}{20}$. The principal stress values are compared in Appendix B since the stresses computed by use of NASTRAN are in terms of local element coordinates.

Tables II and III compare crack tip stresses along the crack axis from the 2-D finite element and exact analytical models (Equation 15) for case III (internal pressure only).

Table II
Comparison of 2-D FEM and Exact Analytical Results
for p = 852 psi (Case S_3)
$\beta = 0^o$

	FEM (psi)		Analytical (psi)		$\frac{\sigma_{max}(FEM)}{\sigma_{max}(ANAL)}$	$\frac{\sigma_{min}(FEM)}{\sigma_{min}(ANAL)}$
r/a	σ_{max}	σ_{min}	σ_{max}	σ_{min}		
0.0088	5326.3	4642.1	6502.8	5431.7	0.819	0.856
0.0124	4494.4	3886.1	5474.9	4479.7	0.820	0.867
0.0171	3802.1	3258.6	4643.1	3700.9	0.818	0.880
0.0230	3218.9	2741.9	3992.5	3085.5	0.806	0.888
0.0290	2813.1	2384.7	3547.3	2660.9	0.793	0.896
0.0361	2469.5	2083.0	3174.9	2303.3	0.777	0.904
0.0466	2112.5	1770.0	2789.3	1930.4	0.757	0.916

Table III
Comparison of 2-D FEM and Exact Analytical Results
for p = 625 psi (Case III)

$\beta = 45^{o}$

	FEM (psi)		Analytical (psi)		$\frac{\sigma_{max}\ (FEM)}{\sigma_{max}\ (ANAL)}$	$\frac{\sigma_{min}\ (FEM)}{\sigma_{min}\ (ANAL)}$
r/a	σ_{max}	σ_{min}	σ_{max}	σ_{min}		
0.0088	3907.1	3412.6	4770.6	3984.8	0.819	0.856
0.0124	3297.0	2850.8	4016.5	3286.4	0.820	0.867
0.0171	2789.1	2390.4	3406.3	2715.1	0.818	0.880
0.0230	2361.2	2011.3	2928.9	2263.6	0.806	0.888
0.0290	2063.6	1749.3	2602.4	1952.1	0.793	0.896
0.0361	1811.5	1528.0	2329.2	1689.8	0.777	0.904
0.0466	1549.7	1298.3	2046.2	1416.2	0.757	0.916

Good correlation between the finite element and exact analytical results is observed. The ratio of the stress intensity factors (mode I) i.e., $k_1(FEM)/k_1(ANAL)$ for the computed stresses is relatively constant and falls in the range between 0.80 to 0.90. This small discrepancy can be attributed to the plate F(a/b) factor, i.e., the factor influenced by the plate overall dimension along the crack direction.

The stress intensity factors for the pressurized elliptical crack using the exact solution and finite element model show good correlation. For example, the exact crack tip solution for the σ_z stress is

$$\sigma_{zz} = \frac{k_1}{(2r)^{\frac{1}{2}}} \cos\frac{\theta}{2}\left[1 + \sin\frac{\theta}{2}\sin\frac{3\theta}{2}\right] - p \tag{15a}$$

with

$$k_1 = \frac{p}{E(k)}\left(\frac{b}{a}\right)^{\frac{1}{2}}\left[a^2\sin^2\phi + b^2\cos^2\phi\right]^{\frac{1}{4}} \tag{15b}$$

The finite element values of k_1, obtained from the computed σ_z stresses at $\frac{r}{a} = 0.04$, are compared with corresponding values from equation (15b) in Table 4 for different values of ϕ with $\frac{a}{b} = 2$ (b = 55"). The value of θ (wedge angle) for the crack tip elements varies from 15° to 30°.

Table IV
Comparison of 3-D FEM and Exact Analytical Values of k_1 in terms of Internal Pressure p with $\frac{b}{a} = 2$.

ϕ	4.5^o	14.3^o	26.6^o	44.5^o	72.4^o
k_1 Analytical	4.35p	4.51p	4.87p	5.43p	6.01p
k_1 FEM	4.50p	4.53;	4.65p	4.78p	4.79p

3.0 EXPERIMENTAL RESULTS

The experimental portion of this work dealt primarily with strain gage, crack propagation, and acoustic emission investigations on plate samples with a simulated crack (Figure 29). Preliminary photoelastic experiments conducted by Heavner* indicated that the coatings used were two insensitive for low field strain levels. For geometric stress distribution purposes only, a sheet of CR-39 with a pressurized crack was analyzed using classical photoelasticity. Figure 30 illustrates the isochromatics experienced by the CR-39 sheet at 600 psi.

Experiments on strain gaged Berea sandstone plate samples with internally pressurized cracks were conducted to determine the resulting strain distributions. Figure 31 reveals the computed stresses and orientations from plane stress experiments on two samples. Acoustic emission and crack propagation characteristics were simultaneously monitored. The purpose of these laboratory tests was to obtain qualitative correlations on stress distributions, crack extensions, and to provide additional information on the onset of acoustic emission activity as it related to hydraulic fracturing field experiments. Experiments conducted by MERC have indicated sharp, high frequency bottom hole pressure decreases which are believed to correspond to dynamic fracture extensions. These fracture extensions appear to grow in discrete steps. Measurement of the acoustic signatures of these events along with crack propagation velocity and strain distributions is therefore important for demonstrating the discrete value of fracture extensions. The following subsections detail the strain gage and acoustic emission results.

---

*J. Heavner, "Stress Analysis of Oil Bearing Sandstone," MSME Thesis, West Virginia University, 1975.

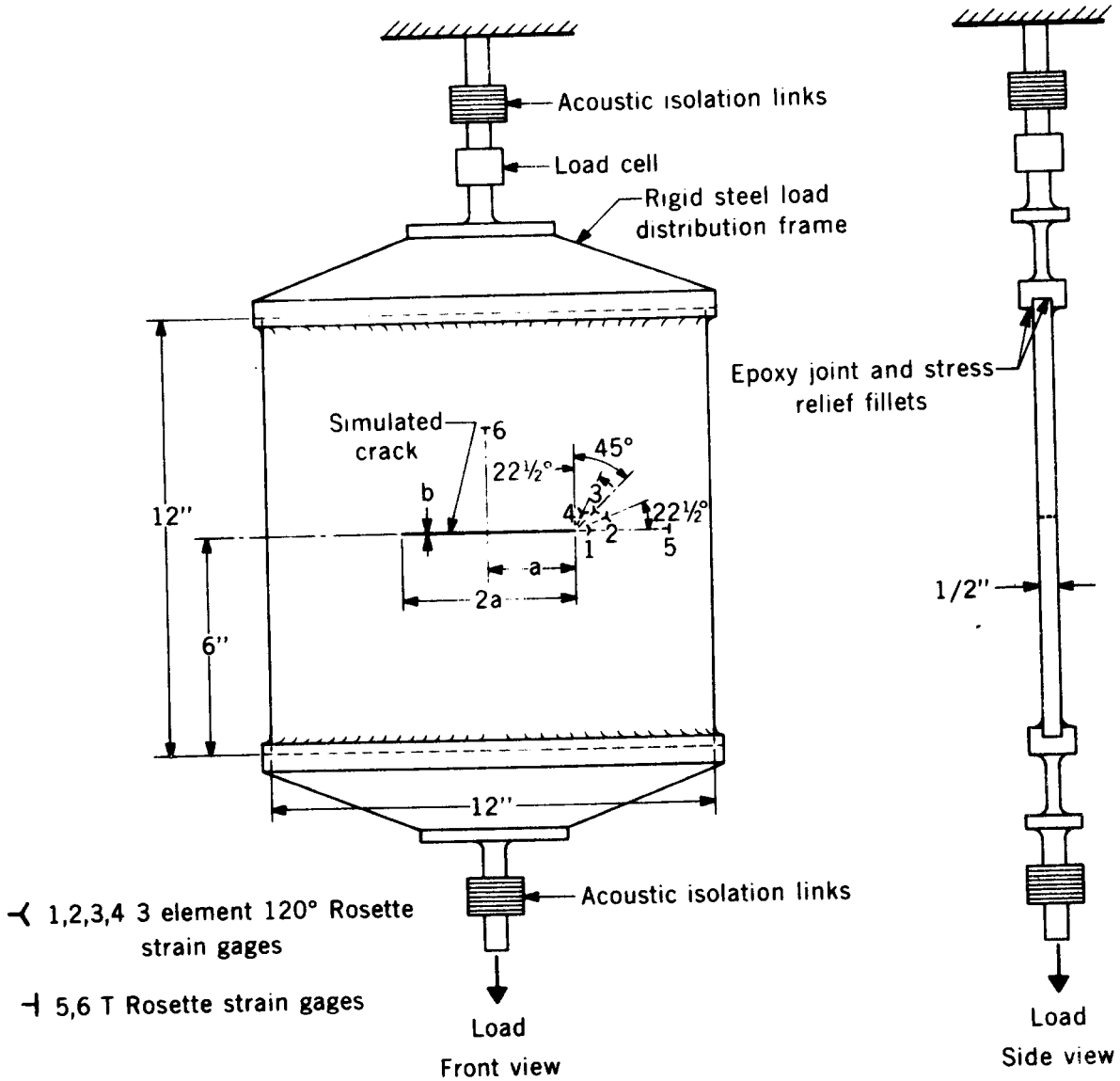

FIGURE 29. Stress Distribution, Acoustic Emission, and Crack Initiation and Propagation Test Apparatus

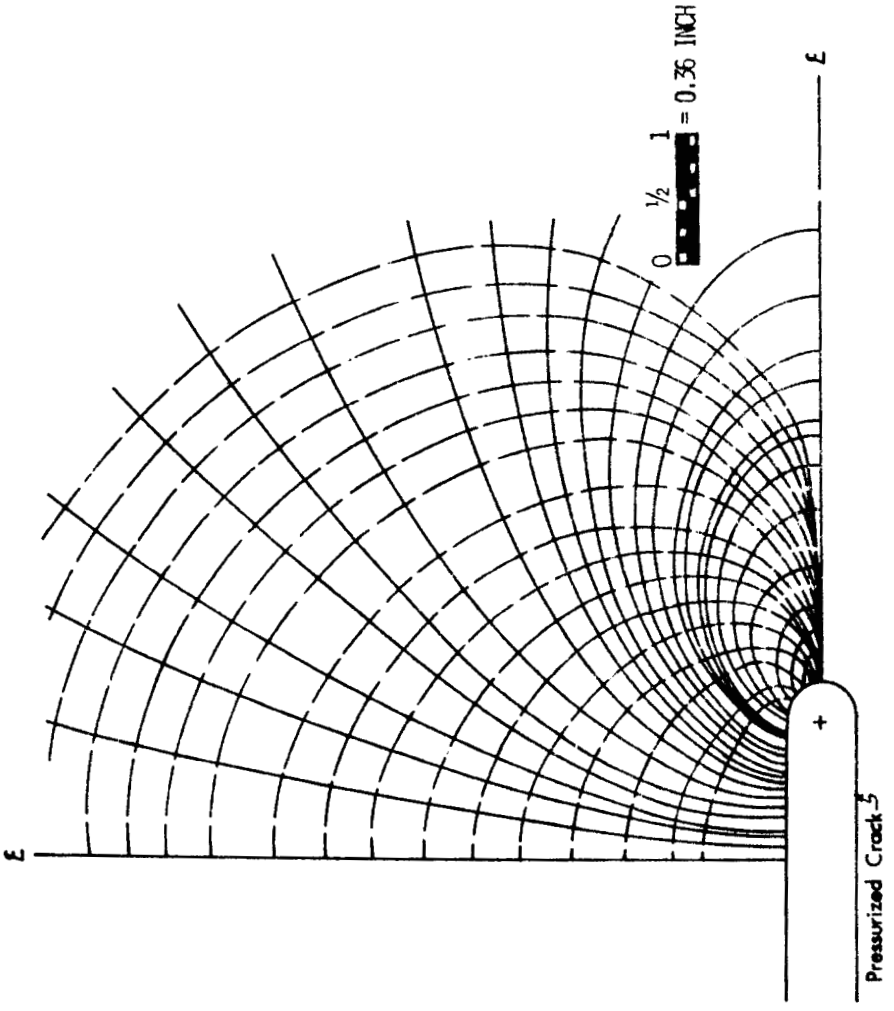

Figure 30. Stress Trajectories Near Crack Tip of Internally Pressurized CR-39 Plate at 600 psi.

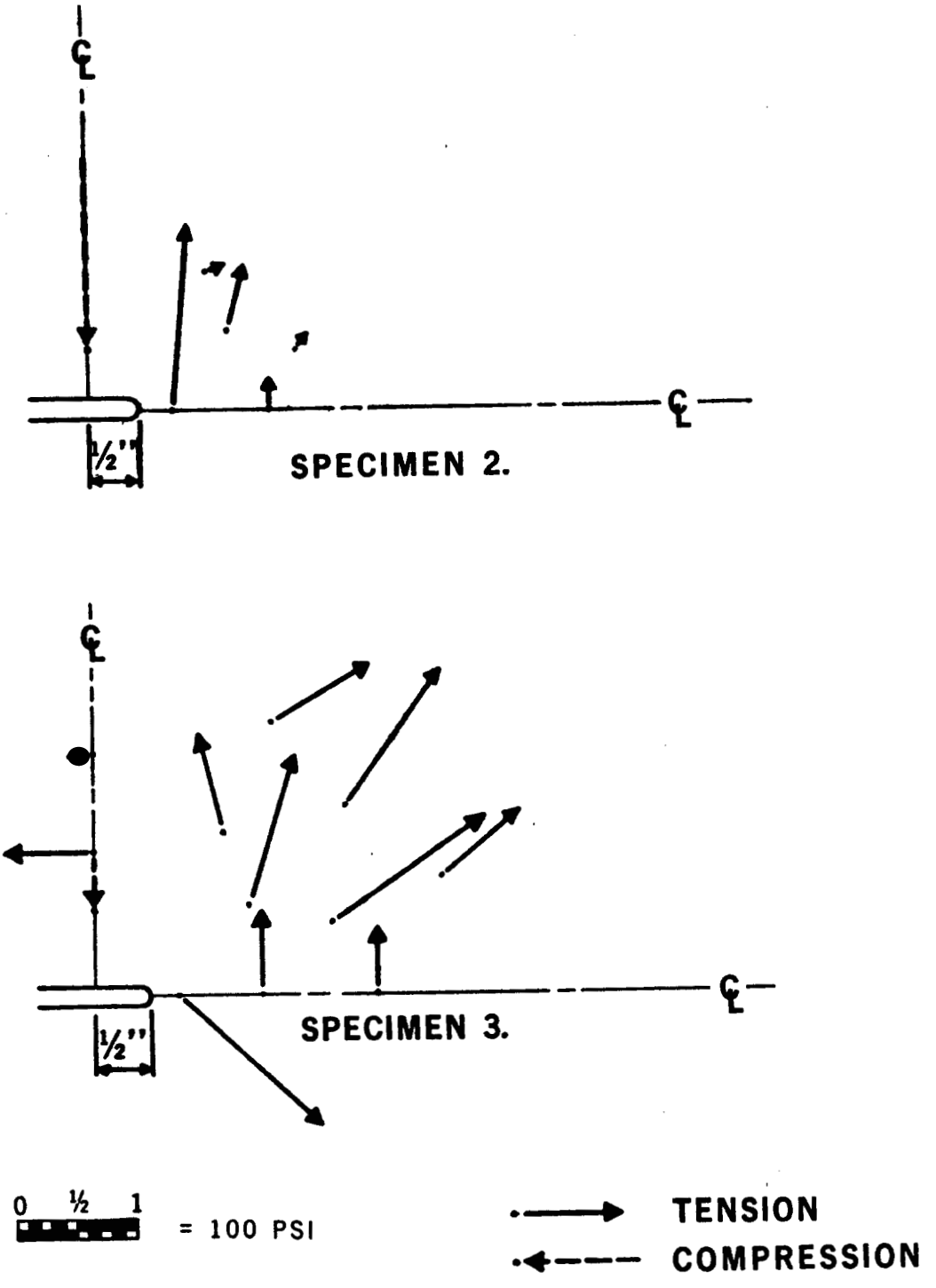

Figure 31. Principal Stress Magnitudes and Orientations for Crack with Internal Pressure p = 800 psi.

3.1 STRAIN GAGE RESULTS

Extensive strain-gage data on Berea Sandstone samples were obtained to determine material and structural properties, verify material linearity/non-linearity, and compare computed model stresses with corresponding experimental values.

Material property determination tests on Berea sandstone cylindrical specimens (3/4" diameter, 1" long) yielded an average Young's modulus $E = 1.56 \times 10^6$ psi and Poisson's Ratio $\nu = 0.22$ in both tension and compression. Linear stress-strain curves were obtained with tensile and compressive specimens fracturing at 327 psi and 6428 psi respectively.

Two types of plane stress experiments were performed to obtain the structural response of plate samples with simulated cracks. The first type of experiment consisted of a square plate with a slit subjected to uniform tensile edge loading, as illustrated in Figure 29. The locations of typical strain measurements are also shown in this figure. This experiment provided base line data for comparison with known solutions of a crack in a uniform tensile field and also served to demonstrate superposition concepts. The far field strain gage data (gage 6) yielded the elastic modulus in tension and Poisson's ratio for Berea sandstone. The second experiment was designed to more closely duplicate reservoir hydraulic fracture conditions. The boundary conditions conformed to the model of an internally pressurized, linear crack, in an "infinite" force plate. As in the first experiment, all variables such as load (or pressure) and strains were sampled simultaneously at a high scan rate while quasi-statically loading (or pressurizing) the plate.

Table IV compares experimental data for a pressurized crack with corresponding finite element model results. The crack length for this test is 1 in. and the gage locations are illustrated in Figure 32. Fracture extension occurred at an internal pressure of 2000 psi. The critical pressure for a 3 inch internal crack in corresponding tests was approximately 900 psi.

Table IV
Experimental and Finite Element Model Comparisons

Crack Internal Pressure psi	Gage	Distance from Crack Tip and Angle	Experiment psi σ_{max}	Experiment psi σ_{min}	Finite Element Model psi σ_{max}	Finite Element Model psi σ_{min}
1200	A	0.16", 0°	879	399	731	491
1600	A	0.16", 0°	2282	793	975	655
1200	B	1.0", 0°	81	-8.3	126	67
1600	B	1.0", 0°	156	27	167	90
1200	C	1.34", 22.5^o	44	-7	59	4
1600	C	1.34", 22.5^o	86	-19	79	5
1200	D	0.91", 45°	165	-50	191	-77
1600	D	0.91", 45°	257	-115	255	-102
1200	E	1.28", 67.5^o	49	-86	119	-63
1600	E	1.28", 67.5^o	76	-136	158	-84

Reasonable correlation between analytical and experimental results is seen above with non-linearity evident in the experimental results. The correspondence between analytical and experimental results, in general, is not good since Berea sandstone is an anisotropic, inhomogeneous, large grain sized, porous material. Opening and closure of micro cracks under stress mades the structural properties non-linear. Microfracturing manifests itself at

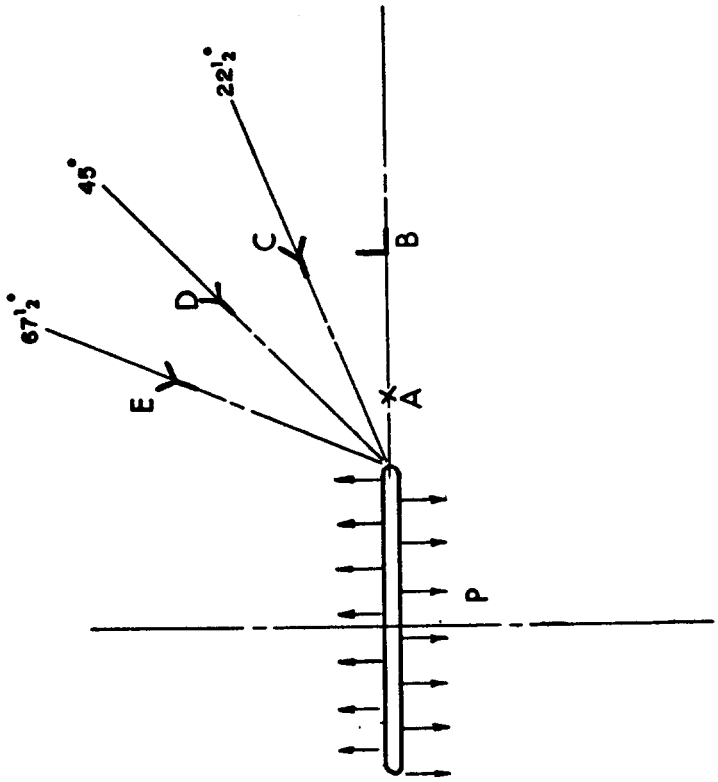

Figure 32. Pressurized Crack with Strain Gage Locations for Data in Table IV.

higher stresses as open pores crush and cracks grow (in planes parallel to the maximum compression). In addition, strain gage experimental techniques may not be accurate since a gage typically envelopes about 8 to 15 grains.

3.2 ACOUSTIC EMISSION RESULTS

Several acoustic emission studies have been reported in literature to locate fractures and orientations and to provide information on failure history. A summary of these techniques can be found in Dunegan and Harris (51), and Knill, Franklin and Malone (52).

Simultaneous acoustic emission (AE), crack propagation and strain gage data is displayed in Figures 33 and 34. Figure 34 is a time expanded version of the data in Figure 33. The acoustic emission sensors were usually mounted close to the four corners of the plate. Traces number 8 in Figure 33 and 7 in Figure 34 are the time codes used in correlating events recorded on different 14 track FM magnetic tape recorders. Trace 1 in Figure 33 is a strain gage plot located at a point 0.91 in. from the crack tip at an inclination of 45° (Gage D in Figure 32). Trace number 2 in Figure 33 illustrates the discrete extensions of one side of a hydraulically induced fracture as measured by a 20 element x 0.40 in. long crack propagation gage. The large fracture extension indicated by acoustic emission channels 3 through 7 on the right side of Figure 33 were not indicated by the crack propagation gage because the fracture had already passed by it. Other acoustic emissions shown in traces 3 through 7 (Figure 33) resulted from fracture extensions from the other half of the crack which was monitored by another crack propagation gage.

Dynamic stress redistribution, typically occurring in field fracturing processes, is illustrated by the strain gage signal in Figure 33. The strain history corresponds to the large transients from the propagating fracture. The acoustic emission from the propagation fractures in the plate has frequencies in the 10K Hz range. It is believed that due to the different sources of acoustic emission associated with reservoir scale fracturing, lower frequency components are generated than those illustrated in Figures 33 and 34. Otherwise, attenuation would be excessive for monitoring the acoustic emission over the required distances associated with field operations.

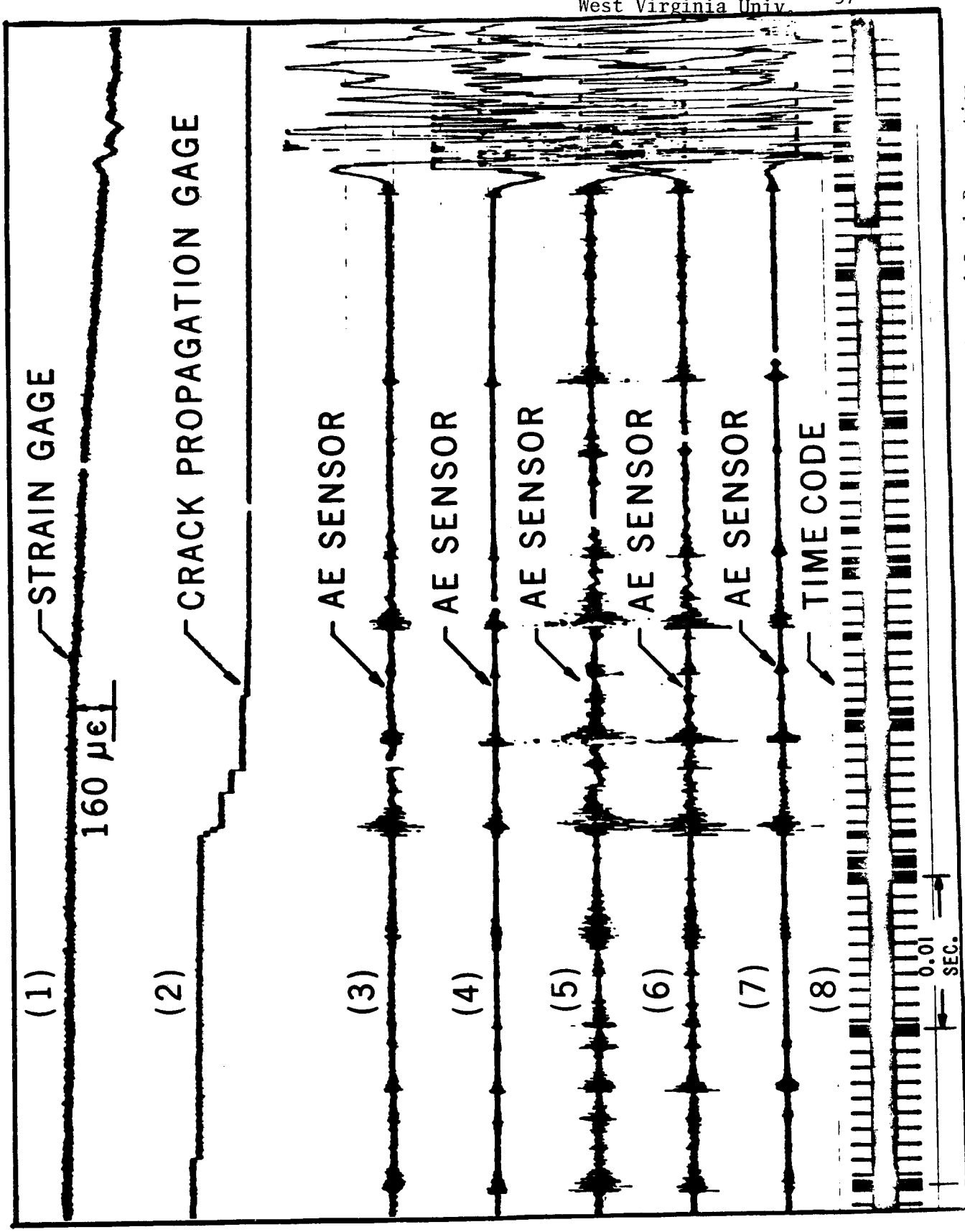

Figure 33. Illustration of Relative Time Relationships Between Acoustic Emission and Crack Propagation.

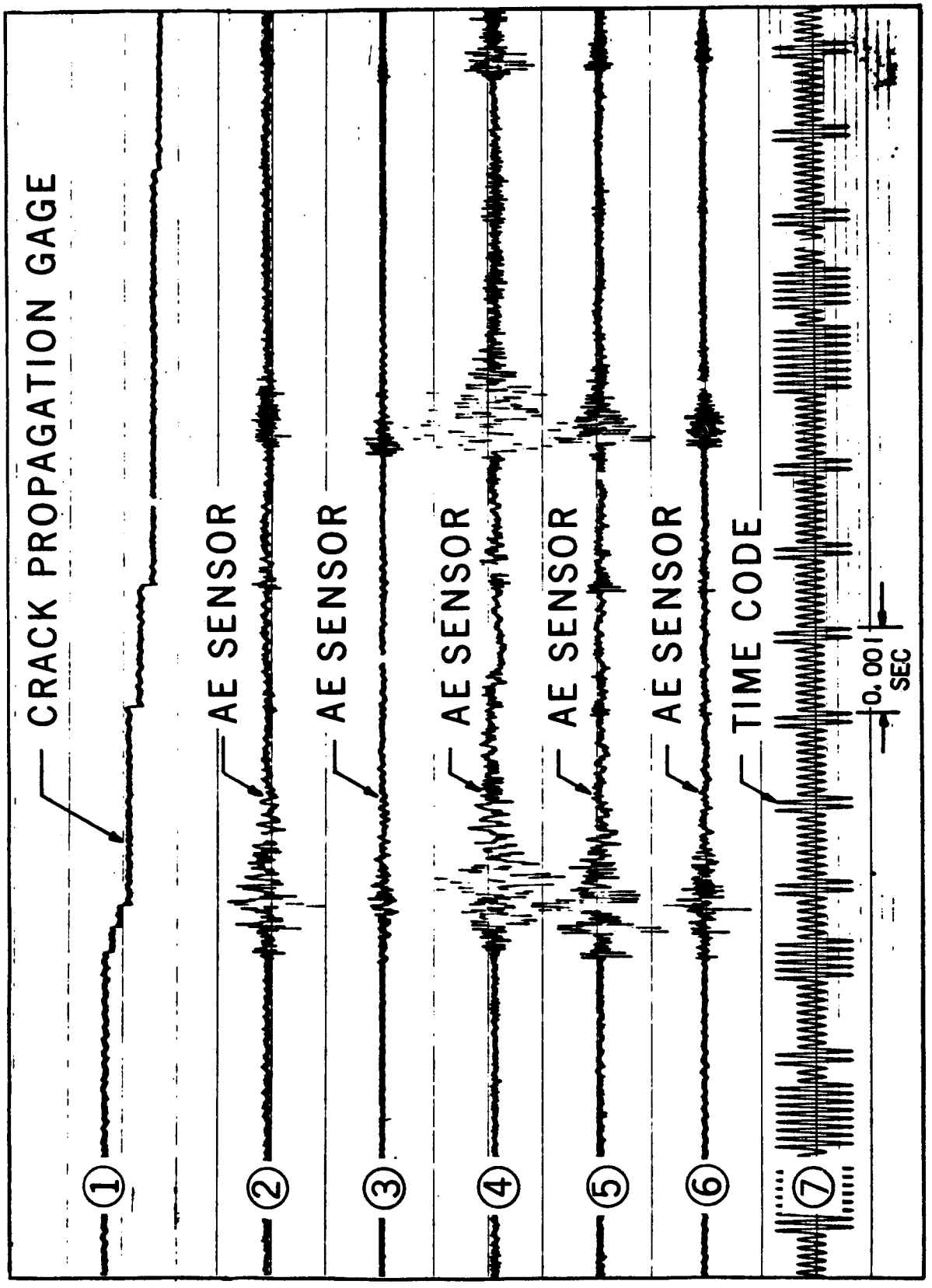

Figure 34. Expanded Time Scale Showing High Frequency Characteristics of Acoustic Emission and Fracture Propagation.

4.0 DISCUSSION OF RESULTS

The two and three dimensional structural models serve as predictive tools for investigating critical pressures in terms of *in situ* stresses, rock mechanical properties, crack geometry, and inclination. In particular, the models simulate the quasi-static stresses resulting from the hydraulic fracturing process and provide interpretive and quantitative information on the following:

(i) fracture initiation, extension, and orientation,

(ii) effects of layering and other variables on fracture propagation and crack geometry,

(iii) directional control of fracture,

and

(iv) laboratory and field experimental correlations.

4.1 FRACTURE INITIATION, EXTENSION, AND ORIENTATION

The condition for fracture initiation around a well bore is (12)

$$P_{critical} = \frac{\sigma_t - 3\sigma_2 + \sigma_1}{2 - \alpha(1-2\nu)/(1-\nu)}$$

where α is related to rock permeabilities and σ_t is the tensile strength of the medium.

For the problem selected here, with fluid flow effects ignored, we have

$$P_{critical} = \sigma_t + 900 \text{ psi}$$

The critical pressures for crack extension as a function of crack length and orientation are given in Figure 7 with a comparison of values in Table I for β=0. Clearly, the penny shaped crack configuration is the optimum shape and would result for a homogeneous and isotropic medium.

The preferred fracture orientations for different crack inclinations (Figure 8) emphasize the directional stability (or instability) of propagating cracks with *in situ* stresses present. Crack propagation orientations

initially inclined to the well bore tend to change direction and eventually align themselves along the major tectonic stress axis. For certain fluid flow rate ranges and material anisotropics and inhomogeneities, the occurence of branched cracks is feasible depending on the energy rate. In this context, Kobyashi (53) has presented dynamic photoelastic data on crack branching and crack arrest in edge cracked tension plates. His results show that the average static strain energy release rate appear to be about five times larger than the average dynamic strain energy rate, thus causing the crack to branch and double the strain energy dissipated at the now two crack tips. In practical situations, the dynamic strain energy is estimated from the total static energy released.

4.2 EFFECTS OF LAYERING AND OTHER VARIABLES

The crack tip and field stresses, obtained from the model, do not appear to be appreciably altered by the multi-layered geometry if the crack configuration is entirely confined in one layer. The influence of the adjacent layer on the crack tip stresses becomes significant if the crack advances to the interface between layers with different material properties. Vertical fractures will be limited by the overlying formation (say shale) by two principal considerations. Firstly, the relative values of S_c and secondly the relative permeabilities and/or porosities can contain the fracture in one layer. These factors can be incorporated in the layered three dimensional finite element model by specifying different S_c (or K_c) across the layers with a suitable fluid pressure profile (computed from Darcy type relations). Additionally, the influence of medium inhomogeneities and anisotropics (such as termination of sandstones, joints, natural faults, etc.) can be simulated.

The consideration of the effects of layering is paramount to the determination of fractured volume since it is a product of fracture height (minor

axis), fracture length (major axis), and crack width. The fracture height can be predicted from the three dimensional finite element model by specifying material properties for the layers (from geological data). Fracture lengths, however, are difficult to estimate but can be determined experimentally (seismic techniques) or indirectly from the fluid flow volume. The crack thickness is obtainable from theoretical considerations using complex variables or potential function methods. For example, Haimison and Fairhurst (12) have obtained the maximum fracture width (W_{max}) in terms of the minor tectonic stress (σ_2) and fluid pressure. They obtain

$$W_{max} = \frac{4(1+\nu)}{3E}(\sigma_2 + p)\left[2(1-\nu) - \alpha(1-2\nu)\right]a$$

For σ_2 = -700 psi, p = 1000 psi, α = 0.8, E = 4.25 x 10^6, ν = 0.22, and a = 2000 in., we have

$$W_{max} = 0.254 \text{ in.}$$

4.3 DIRECTIONAL CONTROL OF FRACTURES

Since fracture initiation and extension is a stability problem, the instantaneous crack direction depends on the prevailing stress conditions and material properties. The crack growth direction can be controlled by suitable superposition of stress fields. Figure 35 illustrates such a possible situation wherein the stresses induced by the pressurized control well influence the well to be fractured. For this case, a net stress exceeding σ_1 (-1200 psi) is necessary to cause the fracture to link up with the control well shown. With 2ℓ = 800, d_2 = 300 ft., d_1 = 0, the two dimensional model results require the pressure in the control well to be at least greater than 1600 psi to alter the crack direction.

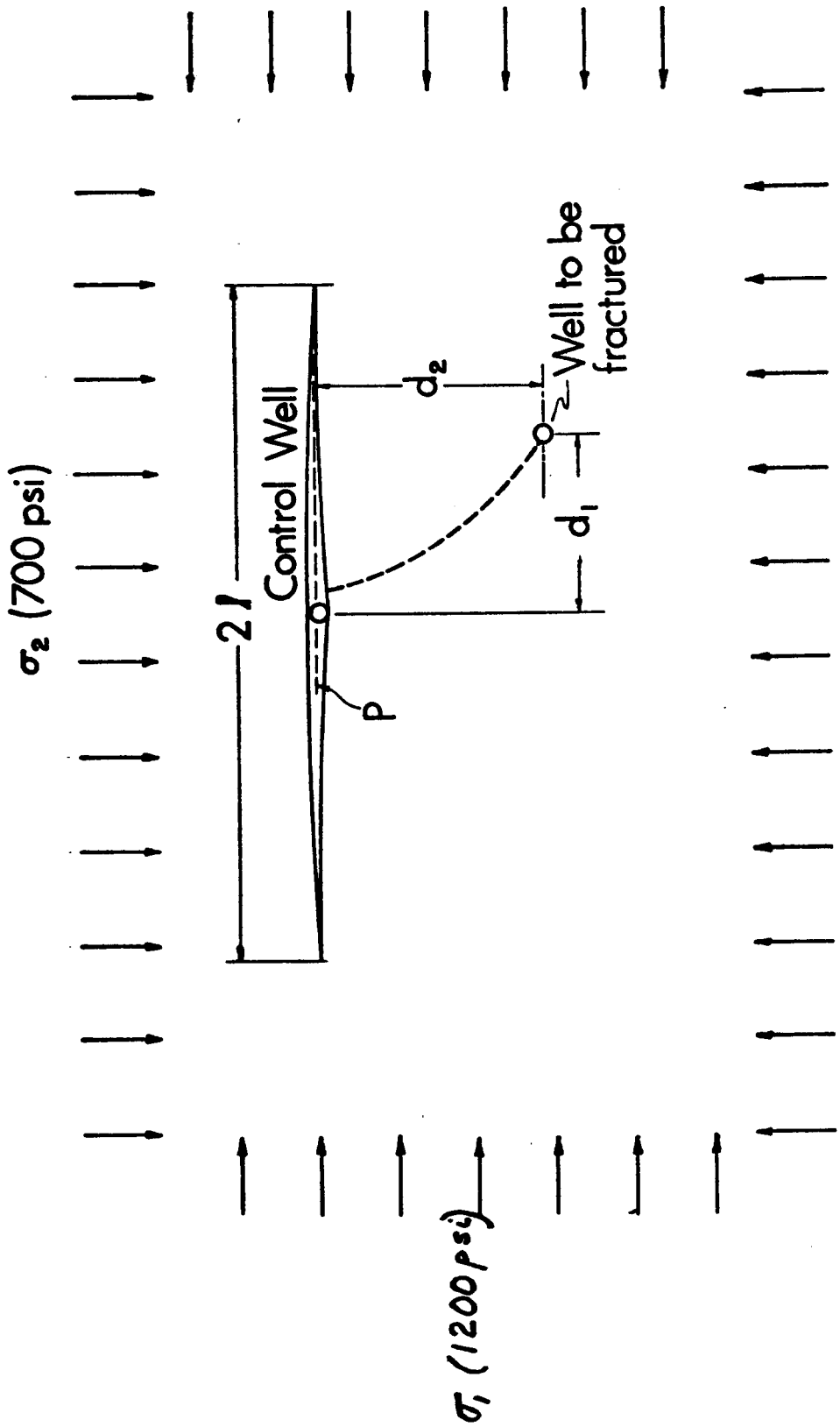

Figure 35. Control Well and Fracture Well Geometry for Directional Control.

4.4 LABORATORY AND FIELD EXPERIMENTAL CORRELATIONS

Laboratory and field experimental correlations are necessary for verification of the theoretical models and giverning fracture mechanisms. Analytical approaches, though hindered by definitions of statistical inhomogenities, anisotropies, and inelasticity of the medium, serve as gross structural predictors, for field fracturing operations. The analytical models at the micro and macro level can, in general, be successfully validated by laboratory experiments which examine local phenomena such as stresses, strains, strain rates, crack propagation velocities, etc. For example, experiments and analyses have demonstrated that crack growth ceases to be stable when the energy release rate reaches a critical value (material property). When crack growth becomes unstable, dynamic elasticity considerations are required. For the case of specimens subjected to fixed end displacements, however, it has been demonstrated that dynamic stress distributions almost coincide with corresponding static values. Techniques such as strain gaging, photoelastic coatings, acoustic emission, and moire are particularly suited for controlled testing of rock samples. In this context, Daniel and Rowlands (54) have recently investigated fracture and wave propagation characteristics in rock media. The measured crack propagation velocities in marble and granite plates (30,000 to 50,000 in/sec) are considerably below the limiting theoretical values. Relatively low values were also obtained for the Berea sandstone samples tested here.

The acoustic emission characteristics coupled with the strain levels provide basic weight on fracture initiation thresholds. Additionally, mapping of the fracture configuration can be achieved.

5.0 CONCLUSIONS AND RECOMMENDATIONS

The reported analytical and experimental investigations describe the stress patterns, fracture initiation thresholds, and fracture inclinations along with the governing influence of mechanical properties, crack geometry and primitive stresses. The studies provide fundamental information on the prediction, control, and optimization of hydraulic fracture within the framework of rock mechanics. The classical and finite element two and three dimensional solutions with the homogeneous elastic, isotropic medium assumptions, serve as initial benchmarks for simulation of the actual field operations. Refinement of finite element crack tips along with incorporation of detailed in situ properties (anisotropies, joints, layers, etc.) in the model will make it an accurate predictive tool.

Additional work should be undertaken in the following areas:

(i) Coupling of fracture mechanics and fluid mechanics models.

(ii) Study of micromechanics of granular material such as couple stress, compression-tension differences, material non-linearity, and dynamic properties.

(iii) Dynamic fracture finite element/finite difference modeling with applications to explosive fracturing.

(iv) Comparative dynamic fracture and wave propagation experiments on sandstone and shale specimens with special emphasis on crack branching and crack arrests.

(v) Linking of multiple cracks and utilization of directional control techniques.

and

(vi) investigation of acoustic emission from an internal propagating fracture in a three dimensional layered medium.

REFERENCES

1. Clark, J. B., "A Hydraulic Process for Increasing the Productivity of Wells," Trans. AIME, V. 186, pp. 1-8, 1949.

2. Anon, "Project Wagon Wheel," Technical Studies Report PNE-WW-1, Ed. El Paso Natural Gas Co., December, 1971.

3. Howard, G. C. and C. R. Fast, "Hydraulic Fracturing," SPE Monograph, V. 2, 1970.

4. Shuck, L. Z. and S. H. Advani, "Induced Stresses in Hydraulic Fracturing Operations," Proceedings, 15th Conference on Rock Mechanics, 1973.

5. Hubbert, M. K. and D. G. Willis, "Mechanics of Hydraulic Fracturing," Trans. AIME, V. 210, pp. 153-168, 1957.

6. In. P. Zhelto and S. A. Khristianovich, "On the Mechanism of Hydraulic Fracture of an Oil Carrying Stratum," 12v. Akad Nauk SSSR OTN No. 5, 1955.

7. Dunlap, I. W., "Fracture Orientation and Rock Stresses in the Springer and Hart Formations," Oklahoma, J. Inst. Petrol., V. 49, No. 477, pp. 289-294, 1963.

8. Dunlap, I. R., "Factors Controlling the Orientation and Direction of Hydraulic Fractures," J. Inst. Petrol., V. 49, No. 477, pp. 282-288, 1963.

9. Fairhurst, C., "Measurement of In Situ Rock Stresses With Particular Reference to Hydraulic Fracturing," Rock Mechanics and Engineering Geology, V. II/3-4, pp. 129-149, 1964.

10. Scheidegger, A. E., "Stresses in the Earth's Crust as Determined from Hydraulic Fracturing Data," Geologic and Bauwesen, V. 29, pp. 45-53, 1962.

11. Kehle, R. O., "The Determination of Tectonic Stresses Through Analysis of Hydraulic Well Fracturing," J. Geophys. Res., V. 69, No. 2, pp. 559-584, 1964.

12. Haimson, B. and C. Fairhurst., "Initiation and Extension of Hydraulic Fractures in Rocks," Soc. Petrol. Engr. Jr., V. 7, No. 3, pp. 310-318, 1967.

13. Haimson, B. and C. Fairhurst, "In-Situ Stress Determination at Great Depth by Means of Hydraulic Fracturing," Proc. 11th Symp. on Rock Mechanics, Berkeley, California, 1969.

14. Haimson, B. and C. Fairhurst, "Hydraulic Fracturing in Porous-Permeable Materials," J. Petrol. Technol., V. 21, No. 7, pp. 811-817, 1969.

15. Daneshy, A. A., "Opening of a Pressurized Fracture in an Elastic Medium," SPE Publication, 1973.

16. Daneshy, Abbas Ali, "True and Apparent Direction of Hydraulic Fractures," Pres. at 46th Ann. Meeting, Soc. Petrol. Eng., AIME, SPE Preprint 3226, 16 pp, 1971.

17. Daneshy, Abbas Ali, "A Study of Inclined Hydraulic Fractures," Soc. Petrol. Engr. Jr., pp. 61-68, 1973, Also SPE Paper 4062.

18. Daneshy, Abbas Ali, James R. Williams, Jr., and Tinsley, John M., "Effect of Treatment Parameters on the Geometry of a Hydraulic Fracture," Soc. of Petr. Engrs., AIME, 1971.

19. McClain, W. C., "Rock Mechanics in the Disposal of Radioactive Wastes by Hydraulic Fracturing," Felsmechanik u. Ingencecergeol, V. 6, pp. 139-161, 1968.

20. Wong, H. Y. and I. W. Farmer, "Hydrofracture Mechanisms in Rock During Pressure Grouting," Rock Mechanics, V. 5, pp. 21-41, 1973.

21. Seth, M. S. and K. E. Gray, "Transient Stresses and Displacement Around a Wellbore Due to Fluid Flow in Transversely Isotropic, Porous Media: I. Infinite Reservoirs," Soc. Petrol. Eng. J., V. 8, No. 1, pp. 63-78, 1968.

22. Seth, M. S. and K. E. Gray, "Transient Stresses and Displacement Around a Wellbore Due to Fluid Flow in Transversely Isotropic, Porous Media: II. Finite Reservoirs," Soc. Petrol. Eng. J., V. 8, No. 1, pp. 79-86, 1968.

23. R. F. Lemon and H. J. Patel, "Effects of Fracture and Reservoir Parameters on Recovery from Low Permeability Gas Reservoirs," SPE Paper No. SPE 5111, 1974.

24. Obert, Leonard and W. I. Duvall, "Rock Mechanics and the Design of Structures in Rock," John Wiley & Sons, 1967.

25. Dreyer, W., "The Science of Rock Mechanics - Part I, The Strength Properties of Rocks," Trans. Tech. Publications, 1972.

26. Jaeger, Charles, "Rock Mechanics and Engineering," Cambridge University Press, 1972.

27. M. M. Protodyakonov, M. I. Koifman, and others, "Mechanical Properties of Rocks," Israel Program for Scientific Translations Ltd., IPST Cat. No. 5104, 1969.

28. "Determination of the In-Situ Modulus of Deformation of Rock," American Society for Testing and Materials Publication 477, 1970.

29. R. N. Schock, H. C. Heard, D. R. Stephens, "Mechanical Properties of Rocks from the Site of the Rio Blanco Gas Stimulation Experiment," Lawrence Livermore Laboratory Report UCRL-51260.

30. R. N. Schock, H. C. Heard, D. R. Stephens, "Comparison of the Mechanical Properties of Graywacke Sandstones from Several Gas Stimulation Sites," Lawrence Livermore Laboratory Report UCRL-51261.

31. R. N. Schock, H. C. Heard, D. R. Stephens, "High-Pressure Mechanical Properties of Rocks from Wagon Wheel No. 1," Pinedale, Wyoming, Lawrence Livermore Laboratory Report UCRL-50963.

32. W. Blake, "Application of the Finite Element Method of Analysis in Solving Boundary Value Problems in Rock Mechanics," Int. J. Rock Mech. Min. Sci. Vol. 3, pp. 169-180, 1966.

33. Y. P. Chugh and H. R. Hardy, "Analytical Study of Pressurized Elliptical Cavities," New Horizons in Rock Mechanics, Proceedings, Fourteenth Symposium on Rock Mechanics, 1972.

34. Barla, G., "Stresses Around a Single Underground Opening Near a Traction Free Surface," Int. J. Rock Mech. and Min. Sc., Vol. 9, pp. 103-126, 1972.

35. Barla, G., "A Method for the Analysis of Stress in Brittle Rock," Int. J. Rock Mech. Min. Sci., Vol. 9, pp. 87-102, 1972.

36. Griffith, A., "The Phenomena of Rupture and Flow in Solids," Phil. Trans. of Royal Soc. of London, Vol. 221, pp. 163-198, 1921.

37. Irwin, R., "Fracture, Handbuch der Physik," Vol. 6, pp. 551-590, 1958.

38. Orowan, E., "Fundamentals of Brittle Behavior of Metals," Fatigue and Fracture of Metals, John Wiley, pp. 139-167, 1952.

39. Sih, G. H., "Handbook of Stress-Intensity Factors for Researchers and Engineers," published by Institute of Fracture and Solid Mechanics, Lehigh University, Pa., 1973.

40. Edited by G. C. Sih, "Mechanics of Fracture 1, Methods of Analysis and Solutions of Crack Problems," Noordhoff International Publishing, Leyden, 1973.

41. Sih, G. and H. Livebowitz, "Mathematical Theories of Brittle Fracture," Fracture ed (H. Libowitz), Vol. 2, pp. 67-190, Academic Press, 1968.

42. H. Tada, P. Paris and G. Irwin, "The Stress Analysis of Cracks Handbook," Del Research Corporation, Allentown, Pennsylvania, 1973.

43. P. D. Hilton and G. C. Sih, "Application of the Finite Element Method to the Calculation of Stress Intensity Factors," Ref.40, pp. 426-483.

44. Wilson, W. K., "Crack Tip Finite Elements for Plane Elasticity," Westinghouse Scientific Paper 71-1E7 - FMPW R-P2, June 7, 1971.

45. Marcal, P., "Three-Dimensional Finite-Element Analysis for Fracture Mechanics," in the Surface Crack: Physical Problems and Computational Solutions, ASME Publication, 1972.

46. Sneddon, I. N., "Crack Problems in the Theory of Elasticity in Developments in Theoretical and Applied Mechanics," Vol. 3, ed. Shaw, Pergamon Press, pp. 73-103, 1967.

47. Kassir, M. B. and G. C. Sih, "Griffith's Theory of Brittle Fracture in Three Dimensions," Int. J. Engineering Science, Vol. 5, pp. 899-918, Pergamon Press, 1967.

48. Paul, B. and L. Mirandy, "An Improved Fracture Criterion for Three-Dimensional Stress States," ASME Paper No. 75-Mat. 11, 75-M.

49. Paul, B. and L. Mirandy, "Stresses at the Surface of a Flat Three Dimensional Cavity," ASME Paper No. 75-Mat. 12.

50. MacNeal, R. N. "NASTRAN Theoretical Manual," NASA CR NA SJ-10049, 1969.

51. Dunegan, H. and D. Harris, "Acoustic Emission Techniques," in Experimental Techniques in Fracture Mechanics, editor, A. Kobayashi, SESA Monograph Series, pp. 38-75, 1973.

52. Knill, J., J. Franklin, and A. Malone, "A Study of Acoustic Emission from Stressed Rock," International J. of Rock Mechanics and Mineral Sciences, Vol. 5, pp. 87-121.

53. Kobayashi, A. S., "Criteria for Crack Branching and Crack Arrest," Technical Report No. 19, Contract N00014-67-A-0103-0400, Department of Mechanical Engineering, U. of Washington, Seattle, 1974.

54. Daniel, I. M. and R. E. Rowlands, "On Wave and Fracture Propagation in Rock Media," Experimental Mechanics, Vol. 15, No. 12, pp. 449-457, 1975.

APPENDIX A

The stress intensity factors, for the inclined crack in Figure A-1, obtained from superposition of the axial and shear loading are [47].

$$K_{I_A} = \frac{\sigma \sin^2\alpha_2 \sqrt{b}}{E(k)} \left\{ \sin^2\theta + \left(\frac{b}{a}\right)^2 \cos^2\theta \right\}^{1/4}$$

$$K_{II_A} = \frac{\sigma \sin\alpha_2 \cos\alpha_2 \sqrt{b}\, k^2}{\left\{ \sin^2\theta + \left(\frac{b}{a}\right)^2 \cos^2\theta \right\}^{1/4}} \left\{ \frac{k'}{C_1} \cos\alpha_1 \cos\theta + \frac{1}{C_2} \sin\alpha_1 \sin\theta \right\}$$

$$K_{III_A} = \frac{\sigma \sin\alpha_2 \cos\alpha_2 \sqrt{b}\,(1-\nu) k^2}{\left\{ \sin^2\theta + \left(\frac{b}{a}\right)^2 \cos^2\theta \right\}^{1/4}} \left\{ \frac{1}{C_1} \cos\alpha_1 \sin\theta - \frac{k'}{C_2} \sin\alpha_1 \cos\theta \right\}$$

where

$$C_1 = (k^2 - \nu)\, E(k) + \nu\, k'^2\, K(k)$$

$$C_2 = (k^2 + \nu k'^2)\, E(k) - \nu\, k'^2\, K(k)$$

$$k^2 = 1 - k'^2, \quad k' = b/a$$

E(k), K(k) are complete elliptic functions of the first and second kind respectively.

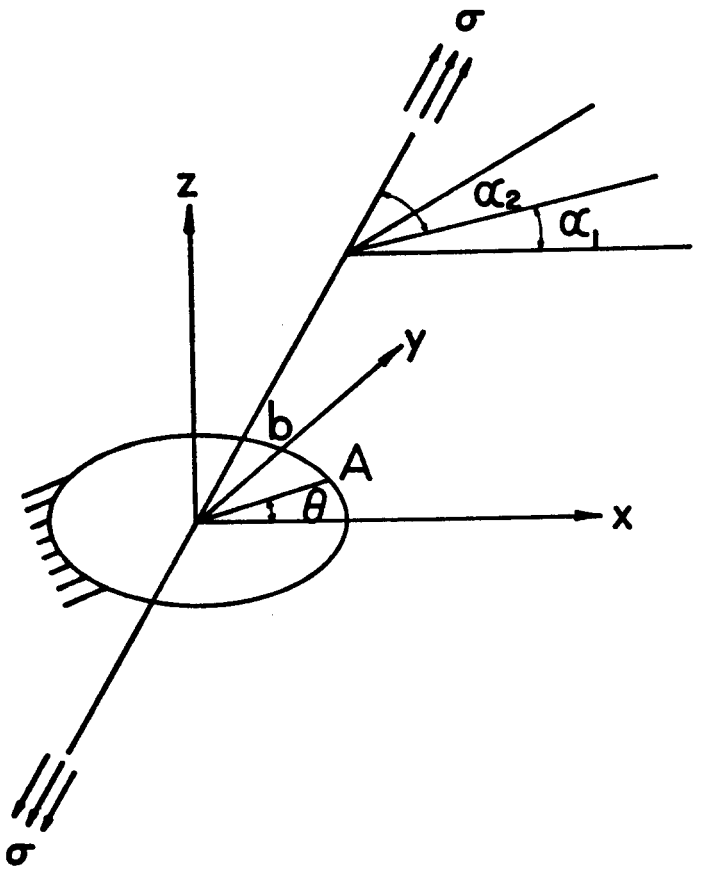

Figure A-1. Elliptic Crack Subjected to Arbitrarily Inclined Shear and Axial Loading.

APPENDIX B

Principal normal and shear stress values in the vicinity of the crack tip, computed from the exact two dimensional theory and finite element model, are presented in the following tables. Results from two cases with a = 55 in. are presented, namely:

(i) internal pressure only (S_3)

($p = 852$ psi, $\beta = 0$; $p = 625$ psi, $\beta = 45^o$)

(ii) internal pressure and tectonic stresses (S_4)

($p = 852$, $\beta = 0$; $p = 625$ psi, $\beta = 45^o$; $\sigma_1 = -1200$ psi, $\sigma_2 = -700$ psi)

The table designations are as follows:

R - distance from crack tip in inches

TH - angle measured from crack axis

SMAX - maximum principal stress (psi)

SMIN - minimum principal stress (psi)

TMAX - maximum shear stress (psi)

Good correlations between exact theory and finite element model results are observed.

R	TH	SMAX	SMIN	TMAX
0.4862	172.5	833.2039	-847.0366	840.1204
0.4862	157.5	2421.7790	-773.8086	1597.7930
0.4862	142.5	3848.8750	-581.8655	2215.3700
0.4862	127.5	5065.4720	-249.9048	2657.6890
0.4862	112.5	6040.3200	226.8318	2906.7440
0.4862	97.5	6759.1600	837.7659	2960.6980
0.4862	82.5	7222.8750	1559.2650	2831.8040
0.4862	67.5	7444.4490	2358.0630	2543.1940
0.4862	52.5	7445.6090	3194.9740	2125.3180
0.4862	37.5	7254.4250	4027.5950	1613.4160
0.4862	22.5	6908.6750	4807.1640	1050.7560
0.4862	7.5	6502.8630	5431.7570	535.5520
0.4862	-7.5	6502.8630	5431.7570	535.5520
0.4862	-22.5	6908.6750	4807.1640	1050.7560
0.4862	-37.5	7254.4250	4027.5950	1613.4160
0.4862	-52.5	7445.6090	3194.9740	2125.3180
0.4862	-67.5	7444.4490	2358.0630	2543.1940
0.4862	-82.5	7222.8750	1559.2650	2831.8040
0.4862	-97.5	6759.1600	837.7659	2960.6980
0.4862	-112.5	6040.3200	226.8318	2906.7440
0.4862	-127.5	5065.4720	-249.9048	2657.6890
0.4862	-142.5	3848.8750	-581.8655	2215.3700
0.4862	-157.5	2421.7790	-773.8086	1597.7930
0.4862	-172.5	833.2039	-847.0366	840.1204

Table B-1. Exact Theory Crack Tip Stresses for Case S_3 and $\beta = 0^o$ (p = 852 psi)

TID 27,649
West Virginia Univ. 73
November 1975

R	TH	SMAX	SMIN	TMAX
0.9400	172.5	598.7598	-847.9580	723.3589
0.9400	157.5	1731.3380	-785.3850	1258.3610
0.9400	142.5	2732.2410	-621.8914	1677.0660
0.9400	127.5	3568.1250	-344.0640	1956.0940
0.9400	112.5	4221.6990	46.3220	2087.6890
0.9400	97.5	4690.1520	534.2319	2077.9610
0.9400	82.5	4982.8590	1093.9190	1944.4710
0.9400	67.5	5118.0620	1692.5550	1712.7540
0.9400	52.5	5119.1360	2294.2140	1412.4610
0.9400	37.5	5012.0500	2862.6120	1074.7190
0.9400	22.5	4829.1910	3357.4730	735.8606
0.9400	7.5	4643.0930	3700.9130	471.0903
0.9400	-7.5	4643.0930	3700.9130	471.0903
0.9400	-22.5	4829.1910	3357.4730	735.8606
0.9400	-37.5	5012.0500	2862.6120	1074.7190
0.9400	-52.5	5119.1360	2294.2140	1412.4610
0.9400	-67.5	5118.0620	1692.5550	1712.7540
0.9400	-82.5	4982.8590	1093.9190	1944.4710
0.9400	-97.5	4690.1520	534.2319	2077.9610
0.9400	-112.5	4221.6990	46.3220	2087.6890
0.9400	-127.5	3568.1250	-344.0640	1956.0940
0.9400	-142.5	2732.2410	-621.8914	1677.0660
0.9400	-157.5	1731.3380	-785.3850	1258.3610
0.9400	-172.5	598.7598	-847.9580	723.3589

Table B-3. Exact Theory Crack Tip Stresses for Case S_3 and $\beta = 0^o$ (p = 852 psi)

R	TH	SMAX	SMIN	TMAX
1.2641	172.5	516.1514	-848.3376	682.2446
1.2641	157.5	1488.5870	-790.1584	1139.3730
1.2641	142.5	2340.1500	-637.6279	1488.8890
1.2641	127.5	3042.5600	-379.6511	1711.1050
1.2641	112.5	3583.1070	-19.9583	1801.5320
1.2641	97.5	3962.8300	425.0176	1768.9060
1.2641	82.5	4194.2300	928.6567	1632.7880
1.2641	67.5	4297.9880	1457.7210	1420.1340
1.2641	52.5	4299.0850	1976.3770	1161.3550
1.2641	37.5	4224.0230	2449.2400	887.3918
1.2641	22.5	4103.3280	2838.9830	632.1729
1.2641	7.5	3992.4540	3085.5450	453.4541
1.2641	-7.5	3992.4540	3085.5450	453.4541
1.2641	-22.5	4103.3280	2838.9830	632.1729
1.2641	-37.5	4224.0230	2449.2400	887.3918
1.2641	-52.5	4299.0850	1976.3770	1161.3550
1.2641	-67.5	4297.9880	1457.7210	1420.1340
1.2641	-82.5	4194.2300	928.6567	1632.7880
1.2641	-97.5	3962.8300	425.0176	1768.9060
1.2641	-112.5	3583.1070	-19.9583	1801.5320
1.2641	-127.5	3042.5600	-379.6511	1711.1050
1.2641	-142.5	2340.1500	-637.6279	1488.8890
1.2641	-157.5	1488.5870	-790.1584	1139.3730
1.2641	-172.5	516.1514	-848.3376	682.2446

Table B-4. Exact Theory Crack Tip Stresses for Case S_3 and $\beta = 0^o$ (p = 852 psi)

r	Tr	SMAX	SMIN	TMAX
1.5947	172.5	459.4258	-848.6199	654.0229
1.5947	157.5	1322.1450	-793.7524	1057.9490
1.5947	142.5	2071.6040	-649.2363	1360.4200
1.5947	127.5	2682.7680	-405.3379	1544.0520
1.5947	112.5	3145.8680	-66.9277	1606.3970
1.5947	97.5	3464.4570	348.7400	1557.8580
1.5947	82.5	3653.2040	814.4202	1419.3920
1.5947	67.5	3734.7520	1296.2860	1219.2330
1.5947	52.5	3735.9100	1757.8820	989.0139
1.5947	37.5	3684.3650	2163.6060	760.3794
1.5947	22.5	3608.7990	2478.7110	565.0439
1.5947	7.5	3547.3350	2660.9800	443.1775
1.5947	-7.5	3547.3350	2660.9800	443.1775
1.5947	-22.5	3608.7990	2478.7110	565.0439
1.5947	-37.5	3684.3650	2163.6060	760.3794
1.5947	-52.5	3735.9100	1757.8820	989.0139
1.5947	-67.5	3734.7520	1296.2860	1219.2330
1.5947	-82.5	3653.2040	814.4202	1419.3920
1.5947	-97.5	3464.4570	348.7400	1557.8580
1.5947	-112.5	3145.8680	-66.9277	1606.3970
1.5947	-127.5	2682.7680	-405.3379	1544.0520
1.5947	-142.5	2071.6040	-649.2363	1360.4200
1.5947	-157.5	1322.1450	-793.7524	1057.9490
1.5947	-172.5	459.4258	-848.6199	654.0229

Table B-5. Exact Theory Crack Tip Stresses for Case S_3 and $\beta = 0^o$(p = 852 psi)

R	TH	SMAX	SMIN	TMAX
1.9837	172.5	411.8242	-848.8718	630.3481
1.9837	157.5	1182.6840	-797.0222	989.8535
1.9837	142.5	1846.8530	-659.6523	1253.2520
1.9837	127.5	2381.8350	-427.9856	1404.9100
1.9837	112.5	2780.1470	-107.6624	1443.9050
1.9837	97.5	3047.2990	283.5215	1381.8890
1.9837	82.5	3199.7600	717.8264	1240.9660
1.9837	67.5	3262.0860	1160.6550	1050.7150
1.9837	52.5	3263.3370	1574.3100	844.5137
1.9837	37.5	3233.0870	1922.1150	655.4856
1.9837	22.5	3197.3790	2172.5930	512.3931
1.9837	7.5	3174.9410	2303.3430	435.7388
1.9837	-7.5	3174.9410	2303.3430	435.7388
1.9837	-22.5	3197.3790	2172.5930	512.3931
1.9837	-37.5	3233.0870	1922.1150	655.4856
1.9837	-52.5	3263.3370	1574.3100	844.5137
1.9837	-67.5	3262.0860	1160.6550	1050.7150
1.9837	-82.5	3199.7600	717.8264	1240.9660
1.9837	-97.5	3047.2990	283.5215	1381.8890
1.9837	-112.5	2780.1470	-107.6624	1443.9050
1.9837	-127.5	2381.8350	-427.9856	1404.9100
1.9837	-142.5	1846.8530	-659.6523	1253.2520
1.9837	-157.5	1182.6840	-797.0222	989.8535
1.9837	-172.5	411.8242	-848.8718	630.3481

Table B-6. Exact Theory Crack Tip Stresses for Case S_3 and $\beta = 0^o$ (p = 852 psi)

R	TH	SMAX	SMIN	TMAX
2.5607	172.5	362.3752	-849.1506	605.7629
2.5607	157.5	1038.0620	-800.7217	919.3923
2.5607	142.5	1614.1460	-671.3225	1142.7340
2.5607	127.5	2070.5410	-452.9438	1261.7420
2.5607	112.5	2401.8890	-151.7778	1276.8330
2.5607	97.5	2615.4950	214.0564	1200.7190
2.5607	82.5	2729.6000	616.3994	1056.6000
2.5607	67.5	2771.0910	1019.5280	875.7817
2.5607	52.5	2772.5180	1383.2820	694.6182
2.5607	37.5	2766.8300	1668.4700	549.1802
2.5607	22.5	2774.7430	1849.5880	462.5774
2.5607	7.5	2789.2380	1930.4290	429.4048
2.5607	-7.5	2789.2380	1930.4290	429.4048
2.5607	-22.5	2774.7430	1849.5880	462.5774
2.5607	-37.5	2766.8300	1668.4700	549.1802
2.5607	-52.5	2772.5180	1383.2820	694.6182
2.5607	-67.5	2771.0910	1019.5280	875.7817
2.5607	-82.5	2729.6000	616.3994	1056.6000
2.5607	-97.5	2615.4950	214.0564	1200.7190
2.5607	-112.5	2401.8890	-151.7778	1276.8330
2.5607	-127.5	2070.5410	-452.9438	1261.7420
2.5607	-142.5	1614.1460	-671.3225	1142.7340
2.5607	-157.5	1038.0620	-800.7217	919.3923
2.5607	-172.5	362.3752	-849.1506	605.7629

Table B-7. Exact Theory Crack Tip Stresses for Case S_3 and $\beta = 0^o$ (p = 852 psi)

ELE. ID	R	TH	SMAX	SMIN	TMAX
2	0.4862	172.5	-50.3521	-1517.5840	733.6167
22	0.4862	157.5	2471.4370	-941.7688	1706.6030
42	0.4862	142.5	4298.6050	-722.1150	2510.3610
62	0.4862	127.5	5559.8240	-431.7776	2995.8010
82	0.4862	112.5	6396.1010	-62.7937	3229.4470
102	0.4862	97.5	6885.9530	440.5259	3222.7140
122	0.4862	82.5	7069.4100	1063.8090	3002.8010
142	0.4862	67.5	7002.0460	1762.4270	2619.8100
162	0.4862	52.5	6748.6600	2510.5800	2119.0410
182	0.4862	37.5	6360.0740	3264.3460	1547.8640
202	0.4862	22.5	5874.4170	3980.7050	946.8577
222	0.4862	7.5	5326.2460	4652.1250	337.0598
242	0.4862	-7.5	5290.0420	4700.4530	294.7966
262	0.4862	-22.5	5844.1710	4035.9810	904.0959
282	0.4862	-37.5	6337.1480	3313.0300	1512.0600
302	0.4862	-52.5	6737.6950	2569.7390	2083.9790
322	0.4862	-67.5	7007.1520	1819.1740	2593.9890
342	0.4862	-82.5	7086.0030	1098.6690	2993.6670
362	0.4862	-97.5	6918.0890	484.2134	3216.9380
382	0.4862	-112.5	6448.2180	-35.8550	3242.0390
402	0.4862	-127.5	5635.4370	-418.4600	3026.9490
422	0.4862	-142.5	4380.0930	-717.8455	2548.9690
442	0.4862	-157.5	2559.0950	-951.4087	1755.2510
462	0.4862	-172.5	32.0876	-1485.1490	758.6189

Table B-8. Finite Element Crack Tip Stresses for Case S_3 and $\beta = 0^o$ (p = 852 psi)

Elt. ID	R	TH	SMAX	SMIN	TMAX
3	0.6807	172.5	-279.4846	-952.9998	336.7576
23	0.6807	157.5	1613.9890	-965.9849	1289.9870
43	0.6807	142.5	3140.8220	-813.6868	1977.2540
63	0.6807	127.5	4284.5740	-561.5256	2423.0510
83	0.6807	112.5	5090.4140	-207.6777	2649.0470
103	0.6807	97.5	5594.6440	236.5159	2679.0650
123	0.6807	82.5	5839.5850	765.4158	2537.0850
143	0.6807	67.5	5860.7070	1355.7100	2252.4980
163	0.6807	52.5	5703.8630	1991.0700	1856.3960
183	0.6807	37.5	5399.8430	2637.6040	1381.1210
203	0.6807	22.5	4989.9330	3278.1350	855.8999
223	0.6807	7.5	4494.3670	3886.1230	304.1233
243	0.6807	-7.5	4460.1950	3923.6930	268.2520
263	0.6807	-22.5	4963.2460	3320.9480	821.1484
283	0.6807	-37.5	5383.5310	2681.6110	1350.9600
303	0.6807	-52.5	5694.4100	2034.9100	1829.7500
323	0.6807	-67.5	5866.6990	1396.7150	2234.9910
343	0.6807	-82.5	5855.2100	801.3738	2526.9180
363	0.6807	-97.5	5624.9020	267.0193	2678.9410
383	0.6807	-112.5	5137.4680	-186.7129	2662.0920
403	0.6807	-127.5	4345.2920	-543.4189	2444.3550
423	0.6807	-142.5	3212.7530	-808.0310	2010.3920
443	0.6807	-157.5	1692.6770	-960.3652	1326.5200
463	0.6807	-172.5	-190.7935	-950.9565	380.0815

Table B-9. Finite Element Crack Tip Stresses for Case S_3 and $\beta = 0^o$ (p = 852 psi)

ELE. ID	R	TH	SMAX	SMIN	TMAX
4	0.9400	172.5	-190.8174	-868.9209	339.0518
24	0.9400	157.5	1131.3640	-886.5134	1008.9380
44	0.9400	142.5	2345.0840	-805.4717	1575.2780
64	0.9400	127.5	3332.8570	-618.7917	1975.8240
84	0.9400	112.5	4069.6860	-333.4006	2201.5420
104	0.9400	97.5	4565.2070	41.6304	2261.7900
124	0.9400	82.5	4839.4880	495.6692	2171.9100
144	0.9400	67.5	4912.5150	1007.4870	1952.5140
164	0.9400	52.5	4819.1560	1562.4230	1628.3670
184	0.9400	37.5	4584.4290	2137.5700	1223.4290
204	0.9400	22.5	4235.7300	2709.3540	763.1882
224	0.9400	7.5	3802.0720	3258.6250	271.7234
244	0.9400	-7.5	3774.9830	3291.2350	241.8746
264	0.9400	-22.5	4214.3120	2746.4720	733.9211
284	0.9400	-37.5	4569.7530	2175.2670	1197.2450
304	0.9400	-52.5	4813.1170	1599.7560	1606.6810
324	0.9400	-67.5	4917.2690	1043.0020	1937.1330
344	0.9400	-82.5	4853.4640	525.3137	2164.0760
364	0.9400	-97.5	4591.5660	68.0688	2261.7500
384	0.9400	-112.5	4109.9450	-312.2913	2211.1180
404	0.9400	-127.5	3383.8120	-605.3625	1994.5860
424	0.9400	-142.5	2405.0620	-798.5669	1601.8140
444	0.9400	-157.5	1199.0100	-885.1355	1042.0720
464	0.9400	-172.5	-120.3030	-867.3220	373.5095

Table B-10. Finite Element Crack Tip Stresses for Case S_3 and $\beta = 0^o$ (p = 852 psi)

ELEM. ID	R	TH	SMAX	SMIN	TMAX
5	1.2641	172.5	-307.1978	-866.2944	279.5483
25	1.2641	157.5	815.7922	-856.1633	835.9778
45	1.2641	142.5	1831.7610	-791.2273	1311.4950
65	1.2641	127.5	2582.0030	-640.5237	1661.2630
85	1.2641	112.5	3338.7290	-404.4319	1871.5800
105	1.2641	97.5	3795.1730	-86.0093	1940.5910
125	1.2641	82.5	4058.4160	306.9812	1875.7180
145	1.2641	67.5	4150.4330	756.1079	1697.1640
165	1.2641	52.5	4085.8390	1243.6330	1421.1030
185	1.2641	37.5	3894.6030	1751.8650	1071.3680
205	1.2641	22.5	3597.2210	2258.2280	669.4971
225	1.2641	7.5	3218.8500	2741.8790	238.4852
245	1.2641	-7.5	3195.7850	2771.1770	212.3042
265	1.2641	-22.5	3578.6380	2289.2280	644.7058
285	1.2641	-37.5	3881.4120	1783.5830	1048.9140
305	1.2641	-52.5	4080.8600	1275.7770	1402.5410
325	1.2641	-67.5	4152.7650	785.6541	1683.5560
345	1.2641	-82.5	4072.4160	332.9670	1869.7240
365	1.2641	-97.5	3818.7320	-62.3772	1940.5540
385	1.2641	-112.5	3372.8430	-387.4131	1880.1270
405	1.2641	-127.5	2727.0070	-629.9800	1678.4930
425	1.2641	-142.5	1883.8230	-783.2341	1333.5290
445	1.2641	-157.5	874.5823	-851.8557	863.2190
465	1.2641	-172.5	-244.8069	-866.0916	310.6423

Table B-11. Finite Element Crack Tip Stresses for Case S_3 and $\beta = 0^o$ (p = 852 psi)

ELE. ID	R	TH	SMAX	SMIN	TMAX
6	1.5947	172.5	-368.2231	-868.3079	250.0424
26	1.5947	157.5	616.5967	-848.3975	732.4971
46	1.5947	142.5	1506.6360	-785.0083	1145.6220
66	1.5947	127.5	2261.4230	-652.8569	1457.1390
86	1.5947	112.5	2853.7700	-445.6523	1649.7100
106	1.5947	97.5	3274.4270	-163.2009	1718.8130
126	1.5947	82.5	3526.9620	185.2285	1670.8660
146	1.5947	67.5	3621.8530	588.4788	1516.6870
166	1.5947	52.5	3577.8750	1029.3000	1274.2880
186	1.5947	37.5	3412.9510	1488.6450	962.1536
206	1.5947	22.5	3150.4220	1946.5000	601.9612
226	1.5947	7.5	2813.1050	2384.6900	214.2074
246	1.5947	-7.5	2790.4300	2409.5300	190.4502
266	1.5947	-22.5	3133.2480	1974.4350	579.4065
286	1.5947	-37.5	3401.1530	1517.2720	941.9402
306	1.5947	-52.5	3571.6790	1057.7270	1256.9770
326	1.5947	-67.5	3624.5190	615.7156	1504.4020
346	1.5947	-82.5	3539.6260	210.0757	1664.7750
366	1.5947	-97.5	3295.7690	-144.0264	1719.8960
386	1.5947	-112.5	2884.0830	-436.4705	1657.2770
406	1.5947	-127.5	2300.3210	-643.2744	1471.7980
426	1.5947	-142.5	1554.0430	-777.9541	1165.9990
446	1.5947	-157.5	668.6614	-845.8528	757.2571
466	1.5947	-172.5	-314.0342	-867.0791	276.5225

Table B-12. Finite Element Crack Tip Stresses for Case S_3 and $\beta = 0^o$ (P = 852 psi)

ELE. ID	R	TH	SMAX	SMIN	TMAX
7	1.9837	172.5	-396.9321	-867.9504	235.5092
27	1.9837	157.5	461.0728	-842.1313	651.6021
47	1.9837	142.5	1246.1560	-781.7651	1013.9590
67	1.9837	127.5	1919.3080	-664.2026	1291.7540
87	1.9837	112.5	2456.4430	-479.3157	1467.8780
107	1.9837	97.5	2844.7580	-227.6091	1536.1830
127	1.9837	82.5	3083.0690	86.2158	1498.4270
147	1.9837	67.5	3179.2660	450.4294	1364.4170
167	1.9837	52.5	3147.8130	850.6824	1148.5650
187	1.9837	37.5	3005.9270	1268.9980	868.4646
207	1.9837	22.5	2773.8030	1686.1220	543.8408
227	1.9837	7.5	2469.4640	2083.0830	193.1903
247	1.9837	-7.5	2450.7730	2105.4790	172.6467
267	1.9837	-22.5	2757.6630	1710.0040	523.8289
287	1.9837	-37.5	2994.9820	1294.4230	850.2800
307	1.9837	-52.5	3142.7720	876.5940	1133.0900
327	1.9837	-67.5	3181.4810	475.8459	1352.8180
347	1.9837	-82.5	3092.2470	108.2839	1491.9810
367	1.9837	-97.5	2863.6070	-209.1160	1536.3620
387	1.9837	-112.5	2484.3570	-465.7717	1475.0640
407	1.9837	-127.5	1955.0470	-654.5706	1304.8090
427	1.9837	-142.5	1288.3890	-776.2534	1032.3220
447	1.9837	-157.5	507.8992	-839.8250	673.8621
467	1.9837	-172.5	-348.3491	-865.6548	258.6528

Table B-13. Finite Element Crack Tip Stresses for Case S_3 and $\beta = 0^o$ (p = 852 psi)

ELE. ID	R	TH	SMAX	SMIN	TMAX
8	2.5607	172.5	-412.3943	-858.4727	223.0391
28	2.5607	157.5	307.8044	-837.0388	572.4216
48	2.5607	142.5	986.2925	-782.6792	884.4858
68	2.5607	127.5	1575.6120	-678.3376	1126.9750
88	2.5607	112.5	2053.0840	-517.0728	1285.0790
108	2.5607	97.5	2403.6350	-294.7605	1349.1970
128	2.5607	82.5	2624.3790	-16.9241	1320.6520
148	2.5607	67.5	2720.0650	308.4224	1205.8220
168	2.5607	52.5	2700.2700	666.9050	1016.6830
188	2.5607	37.5	2580.8130	1042.4070	769.2031
208	2.5607	22.5	2378.9370	1415.3350	481.8003
228	2.5607	7.5	2112.5620	1769.9450	171.3084
248	2.5607	-7.5	2095.9750	1788.8760	153.5490
268	2.5607	-22.5	2366.4830	1436.9680	464.7576
288	2.5607	-37.5	2571.5660	1064.9830	753.2913
308	2.5607	-52.5	2696.2390	690.0330	1003.1040
328	2.5607	-67.5	2721.2210	330.8525	1195.1850
348	2.5607	-82.5	2633.6000	4.0645	1314.7680
368	2.5607	-97.5	2420.6560	-278.8118	1349.7330
388	2.5607	-112.5	2077.5620	-504.1321	1290.8460
408	2.5607	-127.5	1607.7420	-669.7122	1138.7280
428	2.5607	-142.5	1023.9830	-777.2341	900.6091
448	2.5607	-157.5	349.8118	-834.5579	592.1848
468	2.5607	-172.5	-369.0994	-856.5762	243.7383

Table B-14. Finite Element Crack Tip Stresses for Case S_3 and $\beta = 0^o$ (p = 852 psi)

R	TH	SMAX	SMIN	TMAX
0.4862	172.5	611.2524	-621.3589	616.3062
0.4862	157.5	1776.6620	567.6304	1172.1500
0.4862	142.5	2823.6110	426.8313	1625.7210
0.4862	127.5	3716.1380	183.3047	1949.7210
0.4862	112.5	4431.3080	166.4280	2132.4410
0.4862	97.5	4958.6710	614.6111	2172.0310
0.4862	82.5	5298.8710	1143.9120	2077.4790
0.4862	67.5	5461.4290	1729.9170	1865.7560
0.4862	52.5	5462.2730	2343.8890	1559.1920
0.4862	37.5	5322.0110	2954.7200	1183.6460
0.4862	22.5	5068.3510	3526.6370	770.8584
0.4862	7.5	4770.6210	3984.8700	392.8760
0.4862	-7.5	4770.6210	3984.8700	392.8760
0.4862	-22.5	5068.3510	3526.6370	770.8584
0.4862	-37.5	5322.0110	2954.7200	1183.6460
0.4862	-52.5	5462.2730	2343.8890	1559.1920
0.4862	-67.5	5461.4290	1729.9170	1865.7560
0.4862	-82.5	5298.8710	1143.9120	2077.4790
0.4862	-97.5	4958.6710	614.6111	2172.0310
0.4862	-112.5	4431.3080	166.4280	2132.4410
0.4862	-127.5	3716.1380	-183.3047	1949.7210
0.4862	-142.5	2823.6110	-426.8313	1625.7210
0.4862	-157.5	1776.6620	-567.6304	1172.1500
0.4862	-172.5	611.2524	-621.3589	616.3062

Table B-15. Exact Theory Crack Tip Stresses for Case S_3 and $\beta = 45^{\circ}$ (p = 625 psi)

R	TH	SMAX	SMIN	TMAX
0.6807	172.5	516.3901	-621.7131	569.0518
0.6807	157.5	1497.1320	-572.1101	1034.6210
0.6807	142.5	2371.3970	-442.5439	1406.9700
0.6807	127.5	3109.7000	-220.7126	1665.2060
0.6807	112.5	3694.8530	94.1387	1800.3570
0.6807	97.5	4121.0620	492.4138	1814.3240
0.6807	82.5	4392.3550	955.9690	1718.1950
0.6807	67.5	4520.2380	1460.7350	1529.7520
0.6807	52.5	4521.0420	1979.5500	1270.7460
0.6807	37.5	4414.1910	2484.0980	965.0483
0.6807	22.5	4225.0930	2942.1730	641.4614
0.6807	7.5	4016.5040	3286.4130	365.0452
0.6807	-7.5	4016.5040	3286.4130	365.0452
0.6807	-22.5	4225.0930	2942.1730	641.4614
0.6807	-37.5	4414.1910	2484.0980	965.0483
0.6807	-52.5	4521.0420	1979.5500	1270.7460
0.6807	-67.5	4520.2380	1460.7350	1529.7520
0.6807	-82.5	4392.3550	955.9690	1718.1950
0.6807	-97.5	4121.0620	492.4138	1814.3240
0.6807	-112.5	3694.8530	94.1387	1800.3570
0.6807	-127.5	3109.7000	-220.7126	1665.2060
0.6807	-142.5	2371.3970	-442.5439	1406.9700
0.6807	-157.5	1497.1320	-572.1101	1034.6210
0.6807	-172.5	516.3901	-621.7131	569.0518

Table B-16. Exact Theory Crack Tip Stresses for Case S_3 and $\beta = 45^{\circ}$ (p = 625 psi)

R	TH	SMAX	SMIN	TMAX
0.9400	172.5	439.2612	-622.0347	530.6479
0.9400	157.5	1270.1430	-576.1321	923.1379
0.9400	142.5	2004.4290	456.1938	1230.3110
0.9400	127.5	2617.6560	252.3813	1435.0180
0.9400	112.5	3097.1400	34.0044	1531.5680
0.9400	97.5	3440.8160	391.9358	1524.4400
0.9400	82.5	3655.5580	802.5237	1426.5170
0.9400	67.5	3754.7500	1241.6910	1256.5290
0.9400	52.5	3755.5370	1683.0790	1036.2290
0.9400	37.5	3676.9730	2100.0730	788.4497
0.9400	22.5	3542.8110	2463.1250	539.8428
0.9400	7.5	3406.2660	2715.1000	345.5830
0.9400	-7.5	3406.2660	2715.1000	345.5830
0.9400	-22.5	3542.8110	2463.1250	539.8428
0.9400	-37.5	3676.9730	2100.0730	788.4497
0.9400	-52.5	3755.5370	1683.0790	1036.2290
0.9400	-67.5	3754.7500	1241.6910	1256.5290
0.9400	-82.5	3655.5580	802.5237	1426.5170
0.9400	-97.5	3440.8160	391.9358	1524.4400
0.9400	-112.5	3097.1400	34.0044	1531.5680
0.9400	-127.5	2617.6560	252.3813	1435.0180
0.9400	-142.5	2004.4290	-456.1938	1230.3110
0.9400	-157.5	1270.1430	-576.1321	923.1379
0.9400	-172.5	439.2612	-622.0347	530.6479

Table B-17. Exact Theory Crack Tip Stresses for Case S_3 and $\beta = 45^o$ (p = 625 psi)

P	TH	SMAX	SMIN	TMAX
1.2641	172.5	378.6582	-622.3135	500.4858
1.2641	157.5	1092.0560	-579.6335	835.8450
1.2641	142.5	1716.7820	467.7383	1092.2600
1.2641	127.5	2232.0890	-278.4883	1255.2890
1.2641	112.5	2628.6530	14.6196	1321.6360
1.2641	97.5	2907.2340	311.8157	1297.7090
1.2641	82.5	3077.0060	681.2864	1197.8600
1.2641	67.5	3153.1240	1069.4100	1041.8560
1.2641	52.5	3153.9290	1449.9060	852.0120
1.2641	37.5	3098.8560	1796.8150	651.0205
1.2641	22.5	3010.2990	2082.7510	463.7737
1.2641	7.5	2929.9330	2263.6500	332.6443
1.2641	-7.5	2928.9390	2263.6500	332.6443
1.2641	-22.5	3010.2990	2082.7510	463.7737
1.2641	-37.5	3098.8560	1796.8150	651.0205
1.2641	-52.5	3153.9290	1449.9060	852.0120
1.2641	-67.5	3153.1240	1069.4100	1041.8560
1.2641	-82.5	3077.0060	681.2864	1197.8600
1.2641	-97.5	2907.2340	311.8157	1297.7090
1.2641	-112.5	2628.6530	14.6196	1321.6360
1.2641	-127.5	2232.0890	278.4883	1255.2890
1.2641	-142.5	1716.7820	467.7383	1092.2600
1.2641	-157.5	1092.0560	-579.6335	835.8450
1.2641	-172.5	378.6582	-622.3135	500.4858

Table B-18. Exact Theory Crack Tip Stresses for Case S_3 and $\beta = 45^o$ (p = 625 psi)

R	TH	SMAX	SMIN	TMAX
1.5947	172.5	337.0430	-622.5203	479.7817
1.5947	157.5	969.9519	-582.2702	776.1111
1.5947	142.5	1519.7720	-476.2542	998.0134
1.5947	127.5	1968.1380	-297.3323	1132.7350
1.5947	112.5	2307.8850	-49.0764	1178.4810
1.5947	97.5	2541.6170	255.8560	1142.8800
1.5947	82.5	2680.0970	597.4805	1041.3080
1.5947	67.5	2739.9280	950.3805	894.4741
1.5947	52.5	2740.7760	1289.6160	725.5803
1.5947	37.5	2707.9520	1587.2700	557.8411
1.5947	22.5	2647.5000	1818.4520	414.5244
1.5947	7.5	2602.3930	1952.1840	325.1045
1.5947	-7.5	2602.3930	1952.1840	325.1045
1.5947	-22.5	2647.5000	1818.4520	414.5244
1.5947	-37.5	2707.9520	1587.2700	557.8411
1.5947	-52.5	2740.7760	1289.6160	725.5803
1.5947	-67.5	2739.9280	950.3805	894.4741
1.5947	-82.5	2680.0970	597.4805	1041.3080
1.5947	-97.5	2541.6170	255.8560	1142.8800
1.5947	-112.5	2307.8850	-49.0764	1178.4810
1.5947	-127.5	1968.1380	-297.3323	1132.7350
1.5947	-142.5	1519.7720	-476.2542	998.0134
1.5947	-157.5	969.9519	-582.2702	776.1111
1.5947	-172.5	337.0430	-622.5203	479.7817

Table B-19. Exact Theory Crack Tip Stresses for Case S_3 and $\beta = 45^o$ (p = 625 psi)

R	TH	SMAX	SMIN	TMAX
1.9837	172.5	302.1216	-622.7048	462.4133
1.9837	157.5	867.6401	584.6682	726.1543
1.9837	142.5	1354.9900	483.9853	919.3928
1.9837	127.5	1747.3680	313.9463	1030.6570
1.9837	112.5	2039.5850	-78.9595	1059.2720
1.9837	97.5	2235.5820	208.0107	1013.7850
1.9837	82.5	2347.4380	526.6169	910.4109
1.9837	67.5	2393.1690	851.4797	770.9445
1.9837	52.5	2394.0850	1154.9440	619.5708
1.9837	37.5	2371.8850	1410.1080	480.8884
1.9837	22.5	2345.6740	1593.8800	375.8970
1.9837	7.5	2329.1980	1689.8160	319.6909
1.9837	-7.5	2329.1980	1689.8160	319.6909
1.9837	-22.5	2345.6740	1593.8800	375.8970
1.9837	-37.5	2371.8850	1410.1080	480.8884
1.9837	-52.5	2394.0850	1154.9440	619.5708
1.9837	-67.5	2393.1690	851.4797	770.9445
1.9837	-82.5	2347.4380	526.6169	910.4109
1.9837	-97.5	2235.5820	208.0107	1013.7850
1.9837	-112.5	2039.5850	-78.9595	1059.2720
1.9837	-127.5	1747.3680	-313.9463	1030.6570
1.9837	-142.5	1354.9900	483.9853	919.3928
1.9837	-157.5	867.6401	584.6682	726.1543
1.9837	-172.5	302.1216	-622.7048	462.4133

Table B-20. Exact Theory Crack Tip Stresses for Case S_3 and $\beta = 45^o$ (p = 625 psi)

R	TH	SMAX	SMIN	TMAX
2.5607	172.5	265.8447	622.9094	444.3772
2.5607	157.5	761.5425	-587.3821	674.4624
2.5607	142.5	1184.1710	492.4563	838.3140
2.5607	127.5	1518.9970	-332.2559	925.6267
2.5607	112.5	1762.0880	-111.3228	936.7056
2.5607	97.5	1918.8020	157.0505	880.8762
2.5607	82.5	2002.5200	452.2082	775.1563
2.5607	67.5	2032.9640	747.9453	642.5098
2.5607	52.5	2034.0120	1014.8020	509.6050
2.5607	37.5	2029.8290	1224.0300	402.8997
2.5607	22.5	2035.6180	1356.9200	339.3491
2.5607	7.5	2046.2380	1416.2390	314.9998
2.5607	-7.5	2046.2380	1416.2390	314.9998
2.5607	-22.5	2035.6180	1356.9200	339.3491
2.5607	-37.5	2029.8290	1224.0300	402.8997
2.5607	-52.5	2034.0120	1014.8020	509.6050
2.5607	-67.5	2032.9640	747.9453	642.5098
2.5607	-82.5	2002.5200	452.2082	775.1563
2.5607	-97.5	1918.8020	157.0505	880.8762
2.5607	-112.5	1762.0880	111.3228	936.7056
2.5607	-127.5	1518.9970	-332.2559	925.6267
2.5607	-142.5	1184.1710	492.4563	838.3140
2.5607	-157.5	761.5425	-587.3821	674.4624
2.5607	-172.5	265.8447	-622.9094	444.3772

Table B-21. Exact Theory Crack Tip Stresses for Case S_3 and $\beta = 45^o$ ($p = 625$ psi)

ELE. ID	R	TH	SMAX	SMIN	TMAX
2	0.4862	172.5	-36.9238	-1113.2790	538.1777
22	0.4862	157.5	1812.9890	-690.8262	1251.9070
42	0.4862	142.5	3153.2990	-529.7913	1841.5440
62	0.4862	127.5	4078.5160	-316.8367	2197.6770
82	0.4862	112.5	4691.9840	-45.9348	2368.9590
102	0.4862	97.5	5051.3080	323.1934	2364.0590
122	0.4862	82.5	5185.8940	780.4421	2202.7280
142	0.4862	67.5	5136.5190	1292.9670	1921.7770
162	0.4862	52.5	4950.5970	1841.7410	1554.4270
182	0.4862	37.5	4665.5030	2394.6420	1135.4330
202	0.4862	22.5	4309.2960	2920.0930	694.6018
222	0.4862	7.5	3907.1460	3412.6540	247.2466
242	0.4862	-7.5	3880.6600	3448.2290	216.2157
262	0.4862	-22.5	4287.1560	2960.8200	663.1685
282	0.4862	-37.5	4648.7380	2430.4190	1109.1590
302	0.4862	-52.5	4942.5660	1885.1740	1528.6970
322	0.4862	-67.5	5140.1910	1334.5000	1902.8450
342	0.4862	-82.5	5198.0850	806.0056	2196.0410
362	0.4862	-97.5	5074.9720	355.3716	2359.8020
382	0.4862	-112.5	4730.1830	-26.2075	2378.1960
402	0.4862	-127.5	4134.0820	-306.8918	2220.4880
422	0.4862	-142.5	3213.1970	-526.6243	1869.9100
442	0.4862	-157.5	1877.3850	-697.9473	1287.6660
462	0.4862	-172.5	23.7917	-1089.3540	556.5730

Table B-22. Finite Element Crack Tip Stresses for Case S_3 and $\beta = 45^{\circ}$ ($p = 625$ psi)

ELE. ID	R	TH	SMAX	SMIN	TMAX
3	0.6807	172.5	-204.9930	-699.0967	247.0519
23	0.6807	157.5	1184.0200	-708.5867	946.3035
43	0.6807	142.5	2304.0300	-596.8931	1450.4600
63	0.6807	127.5	3143.0410	-411.8784	1777.4590
83	0.6807	112.5	3734.1680	-152.2588	1943.2140
103	0.6807	97.5	4104.0390	173.5803	1965.2290
123	0.6807	82.5	4283.7140	561.5706	1861.0730
143	0.6807	67.5	4299.1950	994.5769	1652.3100
163	0.6807	52.5	4184.1750	1460.5840	1361.7950
183	0.6807	37.5	3961.1140	1934.8770	1013.1170
203	0.6807	22.5	3660.4700	2404.7500	627.8599
223	0.6807	7.5	3297.0000	2850.7890	223.1059
243	0.6807	-7.5	3271.8810	2878.4160	196.7327
263	0.6807	-22.5	3640.9660	2436.3310	602.3179
283	0.6807	-37.5	3949.2530	1967.3230	990.9653
303	0.6807	-52.5	4177.2530	1492.8890	1342.1810
323	0.6807	-67.5	4303.6750	1024.7430	1639.4670
343	0.6807	-82.5	4295.2890	587.9990	1853.6450
363	0.6807	-97.5	4126.2340	195.9485	1965.1430
383	0.6807	-112.5	3768.6350	-136.9443	1952.7900
403	0.6807	-127.5	3187.6810	-398.5808	1793.1320
423	0.6807	-142.5	2356.8610	-592.7046	1474.7820
443	0.6807	-157.5	1241.8350	-704.5120	973.1741
463	0.6807	-172.5	-139.8569	-697.6431	278.8931

Table B-23. Finite Element Crack Tip Stresses for Case S_3 and $\beta = 45^o$ (p = 625 psi)

ELE. ID	R	TH	SMAX	SMIN	TMAX
4	0.9400	172.5	-139.9298	-637.3982	248.7343
24	0.9400	157.5	829.9570	-650.3203	740.1387
44	0.9400	142.5	1720.3040	-590.7859	1155.5450
64	0.9400	127.5	2444.8840	-453.8804	1449.3820
84	0.9400	112.5	2985.3910	-244.4944	1614.9430
104	0.9400	97.5	3348.8810	30.5952	1659.1430
124	0.9400	82.5	3550.0930	363.6687	1593.2110
144	0.9400	67.5	3603.6640	739.1208	1432.2710
164	0.9400	52.5	3535.1990	1146.1700	1194.5130
184	0.9400	37.5	3363.0090	1568.0950	897.4563
204	0.9400	22.5	3107.2180	1987.5190	559.8503
224	0.9400	7.5	2789.1340	2390.4240	199.3550
244	0.9400	-7.5	2769.1950	2414.4370	177.3784
264	0.9400	-22.5	3091.4870	2014.8330	538.3267
284	0.9400	-37.5	3352.2100	1595.7810	878.2146
304	0.9400	-52.5	3530.7280	1173.5640	1178.5820
324	0.9400	-67.5	3607.1560	765.1907	1420.9820
344	0.9400	-82.5	3560.3640	385.3774	1587.4930
364	0.9400	-97.5	3368.2920	49.9807	1659.1560
384	0.9400	-112.5	3015.0130	-229.0417	1622.0280
404	0.9400	-127.5	2482.3020	-444.0593	1463.1790
424	0.9400	-142.5	1764.3870	-585.7358	1175.0620
444	0.9400	-157.5	879.6914	-649.3125	764.5020
464	0.9400	-172.5	-88.1523	-636.2148	274.0313

Table B-24. Finite Element Crack Tip Stresses for Case S_3 and $\beta = 45^o$ (p = 625 psi)

ELEM. ID	R	TH	SMAX	SMIN	TMAX
5	1.2641	172.5	-225.2969	-635.4646	205.0839
25	1.2641	157.5	598.4783	-628.0525	613.2654
45	1.2641	142.5	1343.7470	-580.4033	962.0752
65	1.2641	127.5	1967.4340	-469.8320	1218.6330
85	1.2641	112.5	2449.1800	-296.6321	1372.9060
105	1.2641	97.5	2784.0090	-63.0205	1423.5140
125	1.2641	82.5	2977.1100	225.2339	1375.9370
145	1.2641	67.5	3044.6080	554.7151	1244.9470
165	1.2641	52.5	2997.2570	912.3411	1042.4580
185	1.2641	37.5	2856.9780	1285.1580	785.9094
205	1.2641	22.5	2638.8240	1656.5890	491.1179
225	1.2641	7.5	2361.2620	2011.3570	174.9524
245	1.2641	-7.5	2344.3040	2032.9020	155.7014
265	1.2641	-22.5	2625.1600	1679.3580	472.9011
285	1.2641	-37.5	2847.2680	1308.4470	769.4109
305	1.2641	-52.5	2993.5850	935.9453	1028.8200
325	1.2641	-67.5	3046.3330	576.3967	1234.9680
345	1.2641	-82.5	2987.4080	244.3408	1371.5330
365	1.2641	-97.5	2801.3180	-45.7163	1423.5170
385	1.2641	-112.5	2474.2600	-284.1553	1379.2080
405	1.2641	-127.5	2000.5530	-462.1248	1231.3400
425	1.2641	-142.5	1382.0270	-574.5269	978.2769
445	1.2641	-157.5	641.6499	-624.8687	633.2593
465	1.2641	-172.5	-179.4606	-635.3010	227.9203

Table B-25. Finite Element Crack Tip Stresses for Case S_3 and $\beta = 45^o$ (p = 625 psi)

FLD. ID	R	TB	SMAX	SMIN	TMAX
6	1.5947	172.5	-270.0576	-636.9539	183.4480
26	1.5947	157.5	452.3601	-622.3445	537.3523
46	1.5947	142.5	1105.2460	-575.8394	840.5425
66	1.5947	127.5	1658.9050	-478.8694	1068.8860
86	1.5947	112.5	2093.4330	-326.8599	1210.1450
106	1.5947	97.5	2401.9970	-119.6567	1260.8260
126	1.5947	82.5	2587.2590	135.9280	1225.6660
146	1.5947	67.5	2656.8680	431.7412	1112.5630
166	1.5947	52.5	2624.6020	755.1086	934.7468
186	1.5947	37.5	2503.6450	1092.0530	705.7959
206	1.5947	22.5	2311.0970	1427.9220	441.5879
226	1.5947	7.5	2063.6850	1749.3450	157.1699
246	1.5947	-7.5	2046.9660	1767.6350	139.6650
266	1.5947	-22.5	2298.4280	1448.4610	424.9836
286	1.5947	-37.5	2494.9680	1113.0960	690.9360
306	1.5947	-52.5	2620.0660	775.9875	922.0398
326	1.5947	-67.5	2658.8420	451.7244	1103.5590
346	1.5947	-82.5	2596.5940	154.1787	1221.2080
366	1.5947	-97.5	2417.6910	-105.6099	1261.6500
386	1.5947	-112.5	2115.7530	-315.7498	1215.7510
406	1.5947	-127.5	1687.5230	-471.8562	1079.6890
426	1.5947	-142.5	1140.0200	-570.6836	855.3516
446	1.5947	-157.5	490.5920	-620.4827	555.5374
466	1.5947	-172.5	-230.3114	-636.0361	202.8624

Table B-26. Finite Element Crack Tip Stresses for Case S_3 and $\beta = 45^o$ ($p = 625$ psi)

ELE. ID	R	TH	SMAX	SMIN	TMAX
7	1.9837	172.5	-291.1184	-636.6943	172.7879
27	1.9837	157.5	338.2749	-617.7476	478.0112
47	1.9837	142.5	914.1750	-573.4602	743.8176
67	1.9837	127.5	1407.9510	-487.1938	947.5728
87	1.9837	112.5	1801.9560	-351.5610	1076.7590
107	1.9837	97.5	2086.8000	-166.9058	1126.8530
127	1.9837	82.5	2261.6260	63.3110	1099.1570
147	1.9837	67.5	2332.2040	330.4653	1000.8680
167	1.9837	52.5	2309.1320	624.0715	842.5300
187	1.9837	37.5	2205.0730	930.9263	637.0737
207	1.9837	22.5	2034.7830	1236.8990	398.9419
227	1.9837	7.5	1811.5550	1528.0920	141.7323
247	1.9837	-7.5	1797.8010	1544.6130	126.5944
267	1.9837	-22.5	2022.9120	1254.4750	384.2183
287	1.9837	-37.5	2197.0100	949.6301	623.6902
307	1.9837	-52.5	2305.4330	643.1216	831.1558
327	1.9837	-67.5	2333.8230	349.1328	992.3457
347	1.9837	-82.5	2268.3870	79.4832	1094.4510
367	1.9837	-97.5	2100.6770	-153.3525	1127.0140
387	1.9837	-112.5	1822.5110	-341.6445	1082.0770
407	1.9837	-127.5	1434.2290	-480.1443	957.1873
427	1.9837	-142.5	945.1865	-569.4326	757.3096
447	1.9837	-157.5	372.6443	-616.0466	494.3455
467	1.9837	-172.5	-255.4552	-634.9978	189.7714

Table B-27. Finite Element Crack Tip Stresses for Case S_3 and $\beta = 45^o$ (p = 625 psi)

ELE. ID	R	TH	SMAX	SMIN	TMAX
8	2.5607	172.5	-302.4492	-629.7449	163.6478
28	2.5607	157.5	225.8438	-614.0142	419.9290
48	2.5607	142.5	723.5400	-574.1299	648.8350
68	2.5607	127.5	1155.8330	-497.5781	826.7061
88	2.5607	112.5	1506.0660	-379.2615	942.6643
108	2.5607	97.5	1763.1980	-216.1738	989.6865
128	2.5607	82.5	1925.1380	-12.3594	968.7493
148	2.5607	67.5	1995.3530	226.2976	884.5278
168	2.5607	52.5	1980.8460	489.2571	745.7949
188	2.5607	37.5	1893.2190	764.7021	564.2588
208	2.5607	22.5	1745.1470	1038.2610	353.4431
228	2.5607	7.5	1549.7240	1298.3770	125.6730
248	2.5607	-7.5	1537.5310	1312.3030	112.6135
268	2.5607	-22.5	1735.9580	1054.1590	340.8989
288	2.5607	-37.5	1886.4030	781.2961	552.5535
308	2.5607	-52.5	1977.8850	506.2480	735.8184
328	2.5607	-67.5	1996.2110	242.7532	876.7292
348	2.5607	-82.5	1931.9360	3.0137	964.4609
368	2.5607	-97.5	1775.7420	-204.4739	990.1086
388	2.5607	-112.5	1524.0710	-369.7974	946.9341
408	2.5607	-127.5	1179.4480	-491.2698	835.3596
428	2.5607	-142.5	751.2544	-570.1450	660.6997
448	2.5607	-157.5	256.6924	-612.2041	434.4482
468	2.5607	-172.5	-270.6792	-628.3440	178.8324

Table B-28. Finite Element Crack Tip Stresses for Case S_3 and $\beta = 45^o$ (p = 625 psi)

R	TH	SMAX	SMIN	TMAX
0.4862	172.5	-849.3613	-1053.1260	101.8828
0.4862	157.5	-681.2773	-924.7795	121.7510
0.4862	142.5	-368.7354	-948.5186	289.8916
0.4862	127.5	-67.7065	-973.3164	452.8049
0.4862	112.5	196.1899	-978.2808	587.2354
0.4862	97.5	406.3760	-951.2617	678.8188
0.4862	82.5	551.0334	-884.5010	717.7673
0.4862	67.5	623.6946	-775.1489	699.4219
0.4862	52.5	623.9519	-625.9119	624.9319
0.4862	37.5	558.1702	-445.7119	501.9412
0.4862	22.5	441.8738	-252.0305	346.9521
0.4862	7.5	316.6799	-87.8102	202.2452
0.4862	-7.5	316.6799	-87.8102	202.2452
0.4862	-22.5	441.8738	-252.0305	346.9521
0.4862	-37.5	558.1702	-445.7119	501.9412
0.4862	-52.5	623.9519	-625.9119	624.9319
0.4862	-67.5	623.6946	-775.1489	699.4219
0.4862	-82.5	551.0334	-884.5010	717.7673
0.4862	-97.5	406.3760	-951.2617	678.8188
0.4862	-112.5	196.1899	-978.2808	587.2354
0.4862	-127.5	-67.7065	-973.3164	452.8049
0.4862	-142.5	-368.7354	-948.5186	289.8916
0.4862	-157.5	-681.2773	-924.7795	121.7510
0.4862	-172.5	-849.3613	-1053.1260	101.8828

Table B-29. Exact Theory Crack Tip Stresses for Case S_4 and $\beta = 0$ (p = 852 psi)

R	TH	SMAX	SMIN	TMAX
0.6807	172.5	-849.9805	-1075.6590	112.8395
0.6807	157.5	-732.8784	-942.2332	104.6773
0.6807	142.5	-470.8230	-960.2080	244.6926
0.6807	127.5	-210.1069	-987.4673	388.6802
0.6807	112.5	20.1956	-998.9343	509.5649
0.6807	97.5	204.2651	-982.5303	593.3977
0.6807	82.5	331.1526	-930.7385	630.9456
0.6807	67.5	394.8997	-840.6567	617.7783
0.6807	52.5	395.1401	-714.5522	554.8462
0.6807	37.5	337.8452	-560.5574	449.2014
0.6807	22.5	237.8337	-395.1438	316.4888
0.6807	7.5	134.1255	-258.4524	196.2890
0.6807	-7.5	134.1255	-258.4524	196.2890
0.6807	-22.5	237.8337	-395.1438	316.4888
0.6807	-37.5	337.8452	-560.5574	449.2014
0.6807	-52.5	395.1401	-714.5522	554.8462
0.6807	-67.5	394.8997	-840.6567	617.7783
0.6807	-82.5	331.1526	-930.7385	630.9456
0.6807	-97.5	204.2651	-982.5303	593.3977
0.6807	-112.5	20.1956	-998.9343	509.5649
0.6807	-127.5	-210.1069	-987.4673	388.6802
0.6807	-142.5	-470.8230	-960.2080	244.6926
0.6807	-157.5	-732.8784	-942.2332	104.6773
0.6807	-172.5	-849.9805	-1075.6590	112.8395

Table B-30. Exact Theory Crack Tip Stresses for Case S_4 and $\beta = 0$ (p = 852 psi)

K	TH	SMAX	SMIN	TMAX
0.9400	172.5	-850.4031	-1094.0680	121.8329
0.9400	157.5	-768.1511	-963.1309	97.4899
0.9400	142.5	-550.8372	-972.7402	210.9516
0.9400	127.5	-324.1523	-1000.7620	338.3052
0.9400	112.5	-121.8860	-1016.8070	447.4609
0.9400	97.5	40.4287	-1008.5260	524.4778
0.9400	82.5	152.5088	-968.5576	560.5332
0.9400	67.5	208.8196	-893.9656	551.3926
0.9400	52.5	209.0461	-786.6770	497.8616
0.9400	37.5	158.8494	-654.1921	406.5208
0.9400	22.5	72.4182	-512.1062	292.2622
0.9400	7.5	-13.9893	-397.6316	191.8212
0.9400	-7.5	-13.9893	-397.6316	191.8212
0.9400	-22.5	72.4182	-512.1062	292.2622
0.9400	-37.5	158.8494	-654.1921	406.5208
0.9400	-52.5	209.0461	-786.6770	497.8616
0.9400	-67.5	208.8196	-893.9656	551.3926
0.9400	-82.5	152.5088	-968.5576	560.5332
0.9400	-97.5	40.4287	-1008.5260	524.4778
0.9400	-112.5	-121.8860	-1016.8070	447.4609
0.9400	-127.5	-324.1523	-1000.7620	338.3052
0.9400	-142.5	-550.8372	-972.7402	210.9516
0.9400	-157.5	-768.1511	-963.1309	97.4899
0.9400	-172.5	-850.4031	-1094.0680	121.8329

Table B-31. Exact Theory Crack Tip Stresses for Case S_4 and $\beta = 0$ (p = 852 psi)

R	TH	SMAX	SMIN	TMAX
1.2641	172.5	-850.6951	-1108.5800	128.9428
1.2641	157.5	-790.6230	-984.8118	97.0943
1.2641	142.5	-610.7832	-985.5427	187.3798
1.2641	127.5	-412.1052	-1012.9080	300.4016
1.2641	112.5	-232.5781	-1031.8510	399.6367
1.2641	97.5	-87.8464	-1029.4730	470.8135
1.2641	82.5	12.2695	-998.4722	505.3708
1.2641	67.5	62.5691	-935.8909	499.2300
1.2641	52.5	62.7854	-843.3938	453.0896
1.2641	37.5	18.3311	-727.9795	373.1553
1.2641	22.5	-57.1687	-604.4875	273.6594
1.2641	7.5	-130.1628	-507.2898	188.5636
1.2641	-7.5	-130.1628	-507.2898	188.5636
1.2641	-22.5	-57.1687	-604.4875	273.6594
1.2641	-37.5	18.3311	-727.9795	373.1553
1.2641	-52.5	62.7854	-843.3938	453.0896
1.2641	-67.5	62.5691	-935.8909	499.2300
1.2641	-82.5	12.2695	-998.4722	505.3708
1.2641	-97.5	-87.8464	-1029.4730	470.8135
1.2641	-112.5	-232.5781	-1031.8510	399.6367
1.2641	-127.5	-412.1052	-1012.9080	300.4016
1.2641	-142.5	-610.7832	-985.5427	187.3798
1.2641	-157.5	-790.6230	-984.8118	97.0943
1.2641	-172.5	-850.6951	-1108.5800	128.9428

Table B-32. Exact Theory Crack Tip Stresses for Case S_4 and $\beta = 0$ (p = 852 psi)

R	TH	SMAX	SMIN	TMAX
1.5947	172.5	-850.8784	-1118.5660	133.8440
1.5947	157.5	-803.2952	-1002.4700	99.5878
1.5947	142.5	-649.8403	-996.4587	173.3092
1.5947	127.5	-471.3040	-1022.4700	275.5833
1.5947	112.5	-307.9136	-1042.8880	367.4875
1.5947	97.5	-175.6079	-1044.2180	434.3052
1.5947	82.5	-83.9373	-1019.1510	467.6069
1.5947	67.5	-37.8821	-964.7048	463.4114
1.5947	52.5	-37.6729	-882.3687	422.3479
1.5947	37.5	-78.0757	-778.7886	350.3564
1.5947	22.5	-145.9148	-668.2205	261.1528
1.5947	7.5	-209.8308	-582.7556	186.4624
1.5947	-7.5	-209.8308	-582.7556	186.4624
1.5947	-22.5	-145.9148	-668.2205	261.1528
1.5947	-37.5	-78.0757	-778.7886	350.3564
1.5947	-52.5	-37.6729	-882.3687	422.3479
1.5947	-67.5	-37.8821	-964.7048	463.4114
1.5947	-82.5	-83.9373	-1019.1510	467.6069
1.5947	-97.5	-175.6079	-1044.2180	434.3052
1.5947	-112.5	-307.9136	-1042.8880	367.4875
1.5947	-127.5	-471.3040	-1022.4700	275.5833
1.5947	-142.5	-649.8403	-996.4587	173.3092
1.5947	-157.5	-803.2952	-1002.4700	99.5878
1.5947	-172.5	-850.8784	-1118.5660	133.8440

Table B-33. Exact Theory Crack Tip Stresses for Case S_4 and $\beta = 0$ (p = 852 psi)

R	TH	SMAX	SMIN	TMAX
1.9837	172.5	-851.0225	-1126.9580	137.9678
1.9837	157.5	-812.3125	-1018.9130	103.3006
1.9837	142.5	-680.9055	-1007.3420	163.2186
1.9837	127.5	-519.9846	-1031.5100	255.7627
1.9837	112.5	-370.5728	-1052.7320	341.0801
1.9837	97.5	-248.9856	-1056.8850	403.9502
1.9837	82.5	-164.5923	-1036.6120	436.0103
1.9837	67.5	-122.1917	-988.9036	433.3560
1.9837	52.5	-121.9893	-915.0962	396.5535
1.9837	37.5	-158.9082	-821.5317	331.3118
1.9837	22.5	-220.2104	-721.9185	250.8541
1.9837	7.5	-276.6167	-646.1921	184.7876
1.9837	-7.5	-276.6167	-646.1921	184.7876
1.9837	-22.5	-220.2104	-721.9185	250.8541
1.9837	-37.5	-158.9082	-821.5317	331.3118
1.9837	-52.5	-121.9893	-915.0962	396.5535
1.9837	-67.5	-122.1917	-988.9036	433.3560
1.9837	-82.5	-164.5923	-1036.6120	436.0103
1.9837	-97.5	-248.9856	-1056.8850	403.9502
1.9837	-112.5	-370.5728	-1052.7320	341.0801
1.9837	-127.5	-519.9846	-1031.5100	255.7627
1.9837	-142.5	-680.9055	-1007.3420	163.2186
1.9837	-157.5	-812.3125	-1018.9130	103.3006
1.9837	-172.5	-851.0225	-1126.9580	137.9678

Table B-34. Exact Theory Crack Tip Stresses for Case S_4 and $\beta = 0$ (p = 852 psi)

R	TH	SMAX	SMIN	TMAX
2.5607	172.5	-851.1638	-1135.6870	142.2616
2.5607	157.5	-820.2871	-1037.3960	108.5546
2.5607	142.5	-711.1707	-1020.6690	154.7495
2.5607	127.5	-569.3264	-1042.1470	236.4108
2.5607	112.5	-434.9729	-1063.6750	314.3511
2.5607	97.5	-324.8826	-1070.4050	372.7612
2.5607	82.5	-248.2791	-1054.8850	403.3030
2.5607	67.5	-209.7891	-1014.0630	402.1375
2.5607	52.5	-209.5940	-949.1184	369.7622
2.5607	37.5	-242.7986	-866.0569	311.6292
2.5607	22.5	-297.1963	-777.9395	240.3716
2.5607	7.5	-345.9292	-712.2014	183.1361
2.5607	-7.5	-345.9292	-712.2014	183.1361
2.5607	-22.5	-297.1963	-777.9395	240.3716
2.5607	-37.5	-242.7986	-866.0569	311.6292
2.5607	-52.5	-209.5940	-949.1184	369.7622
2.5607	-67.5	-209.7891	-1014.0630	402.1375
2.5607	-82.5	-248.2791	-1054.8850	403.3030
2.5607	-97.5	-324.8826	-1070.4050	372.7612
2.5607	-112.5	-434.9729	-1063.6750	314.3511
2.5607	-127.5	-569.3264	-1042.1470	236.4108
2.5607	-142.5	-711.1707	-1020.6690	154.7495
2.5607	-157.5	-820.2871	-1037.3960	108.5546
2.5607	-172.5	-851.1638	-1135.6870	142.2616

Table B-35. Exact Theory Crack Tip Stresses for Case S_4 and β = 852 psi)

ELE. ID	R	TH	SMAX	SMIN	TMAX
2	0.4862	172.5	-931.3777	-1434.7470	251.6846
22	0.4862	157.5	-641.9351	-1024.3760	191.2211
42	0.4862	142.5	-119.3154	-1079.8100	480.2471
62	0.4862	127.5	283.5500	-1127.0500	705.3000
82	0.4862	112.5	580.7957	-1142.8310	861.8132
102	0.4862	97.5	779.1062	-1105.2300	942.1687
122	0.4862	82.5	880.6206	-1012.4330	946.5269
142	0.4862	67.5	895.5249	-871.7749	883.6499
162	0.4862	52.5	839.9216	-692.0466	765.9841
182	0.4862	37.5	737.2271	-492.9146	615.0708
202	0.4862	22.5	611.0735	-300.5735	455.8235
222	0.4862	7.5	499.0459	-147.7959	323.4209
242	0.4862	-7.5	468.9565	-101.4565	285.2065
262	0.4862	-22.5	552.1182	-194.5557	373.3369
282	0.4862	-37.5	680.1250	-359.8750	520.0000
302	0.4862	-52.5	800.6890	-541.5640	671.1265
322	0.4862	-67.5	886.4812	-716.8054	801.6433
342	0.4862	-82.5	911.4126	-870.4128	890.9128
362	0.4862	-97.5	858.4038	-975.0913	916.7476
382	0.4862	-112.5	712.9724	-1034.3460	873.6599
402	0.4862	-127.5	469.9370	-1042.5620	756.2495
422	0.4862	-142.5	111.2566	-1016.0070	563.6316
442	0.4862	-157.5	-384.5671	-963.8079	289.6204
462	0.4862	-172.5	-911.8914	-1102.5450	95.3273

Table B-36. Finite Element Crack Tip Stresses for Case S_4 and $\beta = 0$ (p = 852 psi)

ELE. ID	R	TH	SMAX	SMIN	TMAX
3	0.6807	172.5	-874.2559	-1388.7430	257.2441
23	0.6807	157.5	-756.1917	-1082.6210	163.2146
43	0.6807	142.5	-353.5762	-1103.3610	374.8926
63	0.6807	127.5	8.0532	-1145.4900	576.7720
83	0.6807	112.5	290.8435	-1158.7180	724.7810
103	0.6807	97.5	487.1318	-1133.3820	810.2568
123	0.6807	82.5	601.1155	-1061.3640	831.2405
143	0.6807	67.5	636.8496	-948.2871	792.5684
163	0.6807	52.5	606.9053	-799.0342	702.9697
183	0.6807	37.5	525.5217	-629.3967	577.4592
203	0.6807	22.5	416.0542	-455.3042	435.6792
223	0.6807	7.5	312.6931	-314.5681	313.6306
243	0.6807	-7.5	284.3384	-273.6509	278.9946
263	0.6807	-22.5	363.2673	-361.9548	362.6111
283	0.6807	-37.5	478.9109	-513.5359	496.2234
303	0.6807	-52.5	579.1714	-674.9839	627.0776
323	0.6807	-67.5	637.8547	-824.1047	730.9797
343	0.6807	-82.5	636.4297	-943.3672	789.8984
363	0.6807	-97.5	561.9143	-1025.9770	793.9456
383	0.6807	-112.5	406.4165	-1066.7290	736.5728
403	0.6807	-127.5	162.4099	-1066.1670	614.2888
423	0.6807	-142.5	-169.0225	-1033.3530	432.1650
443	0.6807	-157.5	-582.6555	-981.3442	199.3444
463	0.6807	-172.5	-871.4307	-1100.8190	114.6943

Table B-37. Finite Element Crack Tip Stresses for Case S_4 and $\beta = 0$ (p = 852 psi)

ELE. ID	R	TH	SMAX	SMIN	TMAX
4	0.9400	172.5	-851.8169	-1349.5580	248.8705
24	0.9400	157.5	-777.7412	-1129.9460	176.1025
44	0.9400	142.5	-496.0322	-1117.8430	310.9053
64	0.9400	127.5	-189.6616	-1155.9900	483.1646
84	0.9400	112.5	66.9023	-1176.9400	621.9219
104	0.9400	97.5	256.6384	-1163.0750	709.8572
124	0.9400	82.5	374.7190	-1108.4060	741.5627
144	0.9400	67.5	422.8511	-1015.5390	719.1948
164	0.9400	52.5	409.0881	-888.0413	648.5647
184	0.9400	37.5	345.6897	-737.6897	541.6897
204	0.9400	22.5	251.3333	-582.0208	416.6770
224	0.9400	7.5	160.8782	-454.8157	307.8469
244	0.9400	-7.5	137.5017	-419.0017	278.2517
264	0.9400	-22.5	206.7952	-499.8577	353.3264
284	0.9400	-37.5	307.5330	-637.0955	472.3142
304	0.9400	-52.5	389.9182	-781.4963	585.7073
324	0.9400	-67.5	429.5366	-909.9390	669.7378
344	0.9400	-82.5	410.9739	-1009.5350	710.2551
364	0.9400	-97.5	324.4880	-1071.9880	698.2380
384	0.9400	-112.5	166.9744	-1095.4740	631.2244
404	0.9400	-127.5	-62.6848	-1083.2800	510.2976
424	0.9400	-142.5	-353.9348	-1043.6890	344.8777
444	0.9400	-157.5	-674.4080	-1003.9670	164.7793
464	0.9400	-172.5	-845.4731	-1118.1520	136.3392

Table B-38. Finite Element Crack Tip Stresses for Case S_4 and $\beta = 0$ (p = 852 psi)

ELE. ID	R	TH	SMAX	SMIN	TMAX
5	1.2641	172.5	-850.3877	-1361.7370	255.6747
25	1.2641	157.5	-790.6672	-1165.8330	187.5827
45	1.2641	142.5	-578.1077	-1133.2670	277.5798
65	1.2641	127.5	-318.5388	-1164.0510	422.7561
85	1.2641	112.5	-88.6409	-1188.1080	549.7341
105	1.2641	97.5	87.7532	-1183.6900	635.7219
125	1.2641	82.5	200.7200	-1141.9060	671.3137
145	1.2641	67.5	251.9939	-1063.5550	657.7751
165	1.2641	52.5	245.3096	-952.8291	599.0693
185	1.2641	37.5	192.1545	-819.2170	505.6858
205	1.2641	22.5	110.0864	-680.3364	395.2114
225	1.2641	7.5	31.8506	-568.6631	300.2568
245	1.2641	-7.5	12.7500	-538.1875	275.4688
265	1.2641	-22.5	73.2263	-610.2888	341.7576
285	1.2641	-37.5	160.5298	-732.6548	446.5923
305	1.2641	-52.5	230.4937	-861.2358	545.8647
325	1.2641	-67.5	260.1597	-973.4097	616.7847
345	1.2641	-82.5	234.7954	-1056.9190	645.8579
365	1.2641	-97.5	148.0195	-1104.8320	626.4258
385	1.2641	-112.5	-2.8528	-1116.4360	556.7917
405	1.2641	-127.5	-212.6467	-1096.5600	441.9568
425	1.2641	-142.5	-467.3430	-1057.2180	294.9382
445	1.2641	-157.5	-723.7190	-1035.2810	155.7808
465	1.2641	-172.5	-846.2205	-1161.7170	157.7481

Table B-39. Finite Element Crack Tip Stresses for Case S_4 and $\beta = 0$ (p = 852 psi)

ELE. ID	R	TH	SMAX	SMIN	TMAX
6	1.5947	172.5	-849.3833	-1364.1160	257.3667
26	1.5947	157.5	-800.1331	-1188.3030	194.0855
46	1.5947	142.5	-626.2219	-1146.4660	260.1218
66	1.5947	127.5	-398.8315	-1171.1250	386.1470
86	1.5947	112.5	-189.8540	-1195.7700	502.9585
106	1.5947	97.5	-25.6121	-1196.3870	585.3879
126	1.5947	82.5	83.1257	-1163.4370	623.2820
146	1.5947	67.5	133.9702	-1095.1680	614.5698
166	1.5947	52.5	131.8281	-995.9805	563.9043
186	1.5947	37.5	85.1704	-874.7954	479.9829
206	1.5947	22.5	11.5046	-748.7546	380.1296
226	1.5947	7.5	-58.0588	-647.6287	294.7849
246	1.5947	-7.5	-74.4375	-621.5000	273.5313
266	1.5947	-22.5	-20.3660	-686.8215	333.2278
286	1.5947	-37.5	58.1401	-797.9526	428.0464
306	1.5947	-52.5	120.3420	-914.5178	517.4299
326	1.5947	-67.5	143.2417	-1015.0530	579.1479
346	1.5947	-82.5	114.9814	-1087.5430	601.2627
366	1.5947	-97.5	28.5503	-1126.0500	577.3003
386	1.5947	-112.5	-114.5720	-1130.5610	507.9944
406	1.5947	-127.5	-308.4355	-1107.0920	399.3281
426	1.5947	-142.5	-535.7710	-1070.2910	267.2603
446	1.5947	-157.5	-752.2095	-1062.1650	154.9779
466	1.5947	-172.5	-845.6978	-1189.3020	171.8021

Table B-40. Finite Element Crack Tip Stresses for Case S_4 and $\beta = 0$ ($p = 852$ psi)

ELE. ID	P	TH	SMAX	SMIN	TMAX
7	1.9837	172.5	-848.2229	-1362.4020	257.0896
27	1.9837	157.5	-806.9487	-1206.0510	199.5511
47	1.9837	142.5	-662.1663	-1159.2700	248.5525
67	1.9837	127.5	-462.0552	-1178.6520	358.2983
87	1.9837	112.5	-271.6597	-1202.8010	465.5708
107	1.9837	97.5	-118.6787	-1206.8210	544.0713
127	1.9837	82.5	-15.2722	-1180.2110	582.4700
147	1.9837	67.5	35.3027	-1121.0520	578.1777
167	1.9837	52.5	35.7522	-1031.7250	533.7385
187	1.9837	37.5	-5.4438	-921.3062	457.9312
207	1.9837	22.5	-71.4221	-805.7654	367.1716
227	1.9837	7.5	-133.4875	-714.9500	290.7312
247	1.9837	-7.5	-147.3125	-691.6250	272.1563
267	1.9837	-22.5	-98.8594	-750.9531	326.0469
287	1.9837	-37.5	-28.2676	-852.5449	412.1387
307	1.9837	-52.5	26.6389	-959.0452	492.8420
327	1.9837	-67.5	44.9453	-1049.6250	547.2852
347	1.9837	-82.5	14.3315	-1112.8320	563.5815
367	1.9837	-97.5	-69.3792	-1143.4330	537.0271
387	1.9837	-112.5	-205.2021	-1142.6770	468.7373
407	1.9837	-127.5	-384.1938	-1117.5800	366.6929
427	1.9837	-142.5	-588.6636	-1084.1480	247.7426
447	1.9837	-157.5	-771.3093	-1086.2520	157.4718
467	1.9837	-172.5	-844.7131	-1206.4120	180.8492

Table B-41. Finite Element Crack Tip Stresses for Case S_4 and $\beta = 0$ (p = 852 psi)

ELE. ID	R	TH	SMAX	SMIN	TMAX
8	2.5607	172.5	-847.5544	-1356.5080	254.4766
28	2.5607	157.5	-813.3140	-1223.6240	205.1548
48	2.5607	142.5	-695.5649	-1175.2810	239.8588
68	2.5607	127.5	-523.5034	-1188.6140	332.5552
88	2.5607	112.5	-353.3416	-1211.6230	429.1409
108	2.5607	97.5	-213.6631	-1218.4610	502.3994
128	2.5607	82.5	-116.8721	-1198.2600	540.6943
148	2.5607	67.5	-67.6858	-1147.4160	539.8650
168	2.5607	52.5	-64.5891	-1068.3470	501.8796
188	2.5607	37.5	-99.5925	-969.1965	434.8020
208	2.5607	22.5	-157.6865	-865.8760	354.0947
228	2.5607	7.5	-211.7532	-784.6843	286.4656
248	2.5607	-7.5	-223.0615	-765.0010	270.9697
268	2.5607	-22.5	-180.5430	-817.7695	318.6133
288	2.5607	-37.5	-118.4983	-909.0603	395.2810
308	2.5607	-52.5	-70.4626	-1004.8620	467.1995
328	2.5607	-67.5	-57.1997	-1085.1660	513.9839
348	2.5607	-82.5	-88.5244	-1139.1010	525.2881
368	2.5607	-97.5	-169.4285	-1162.2500	496.4114
388	2.5607	-112.5	-296.2202	-1156.8540	430.3169
408	2.5607	-127.5	-458.7761	-1131.2110	336.2180
428	2.5607	-142.5	-637.9766	-1102.3660	232.1953
448	2.5607	-157.5	-787.7507	-1113.3120	162.7805
468	2.5607	-172.5	-844.9924	-1219.8200	187.4136

Table B-42. Finite Element Crack Tip Stresses for Case S_4 and $\beta = 0$ (p = 852 psi)

R	TH	SMAX	SMIN	TMAX
0.4862	172.5	2476.5620	-619.0811	1547.8210
0.4862	157.5	1745.5060	-586.1245	1165.8150
0.4862	142.5	996.7405	-582.2471	789.4939
0.4862	127.5	421.4810	-785.9167	603.6990
0.4862	112.5	221.4460	-1385.5190	803.4827
0.4862	97.5	198.7639	-2169.5100	1184.1370
0.4862	82.5	181.7605	-2952.4080	1567.0840
0.4862	67.5	109.9592	-3660.0500	1885.0040
0.4862	52.5	-44.2751	-4251.4600	2103.5930
0.4862	37.5	-295.0095	-4699.8200	2202.4060
0.4862	22.5	-646.2097	-4989.2070	2171.4990
0.4862	7.5	-1091.5490	-5114.9760	2011.7140
0.4862	-7.5	-1612.5630	-5085.8240	1736.6310
0.4862	-22.5	-2173.2020	-4929.3860	1378.0920
0.4862	-37.5	-2700.2680	-4711.9370	1005.8340
0.4862	-52.5	-3022.4310	-4599.5230	788.5469
0.4862	-67.5	-2929.8260	-4798.4140	934.2947
0.4862	-82.5	-2547.1820	-5182.0580	1317.4380
0.4862	-97.5	-2078.5510	-5546.3860	1733.9190
0.4862	-112.5	-1621.1950	-5795.9250	2087.3660
0.4862	-127.5	-1225.8550	-5883.4920	2328.8180
0.4862	-142.5	-922.4670	-5784.4100	2430.9720
0.4862	-157.5	-725.6577	-5490.9410	2382.6430
0.4862	-172.5	-635.0708	-5011.8390	2188.3860

Table B-43. Exact Theory Crack Tip Stresses for Case S_4 and $\beta = 45^{o}$ (p = 625 psi)

R	TH	SMAX	SMIN	TMAX
0.6807	172.5	1946.1950	-620.2395	1283.2170
0.6807	157.5	1329.7190	-593.7607	961.7400
0.6807	142.5	697.2939	-590.8772	644.0857
0.6807	127.5	209.1299	-761.0234	485.0767
0.6807	112.5	41.1592	-1268.8650	655.0122
0.6807	97.5	21.6370	-1931.1010	976.3694
0.6807	82.5	6.5110	-2592.0110	1299.2610
0.6807	67.5	-53.2947	-3190.9500	1568.8280
0.6807	52.5	-180.4302	-3693.9980	1756.7840
0.6807	37.5	-386.9163	-4078.3490	1845.7160
0.6807	22.5	-676.7815	-4329.8710	1826.5460
0.6807	7.5	-1045.6810	-4443.6440	1698.9820
0.6807	-7.5	-1479.1660	-4425.8550	1473.3440
0.6807	-22.5	-1948.0170	-4298.6130	1175.2990
0.6807	-37.5	-2392.1210	-4116.1830	862.0330
0.6807	-52.5	-2669.8830	-4015.6940	672.9053
0.6807	-67.5	-2599.5600	-4175.8390	788.1411
0.6807	-82.5	-2276.7590	-4499.4840	1111.3640
0.6807	-97.5	-1876.5570	-4811.5390	1467.4900
0.6807	-112.5	-1484.0560	-5028.4060	1772.1760
0.6807	-127.5	-1143.7510	-5108.5930	1982.4220
0.6807	-142.5	-882.0430	-5030.1600	2074.0580
0.6807	-157.5	-712.0242	-4785.8200	2036.8990
0.6807	-172.5	-633.7078	-4382.6640	1874.4790

Table B-44. Exact Theory Crack Tip Stresses for Case S_4 and $\beta = 45^{\circ}$ (p = 625 psi)

R	TH	SMAX	SMIN	TMAX
0.9400	172.5	1514.7980	-621.1924	1067.9950
0.9400	157.5	991.5989	-600.0581	795.8286
0.9400	142.5	453.8821	-598.0583	525.9702
0.9400	127.5	36.4036	-740.7776	388.5906
0.9400	112.5	-105.3987	-1174.0670	534.3342
0.9400	97.5	-122.3994	-1737.2170	807.4092
0.9400	82.5	-136.0383	-2298.8610	1081.4110
0.9400	67.5	-186.0574	-2809.4090	1311.6760
0.9400	52.5	-291.0667	-3240.6620	1474.7970
0.9400	37.5	-461.4570	-3573.0550	1555.7990
0.9400	22.5	-701.3323	-3793.8780	1546.2730
0.9400	7.5	-1007.9900	-3897.9580	1444.9840
0.9400	-7.5	-1370.2430	-3889.4470	1259.6020
0.9400	-22.5	-1764.3990	-3785.9870	1010.7940
0.9400	-37.5	-2140.8960	-3632.1700	745.6370
0.9400	-52.5	-2382.2250	-3541.6880	579.7317
0.9400	-67.5	-2330.0950	-3670.2550	670.0798
0.9400	-82.5	-2056.2120	-3944.8570	944.3223
0.9400	-97.5	-1711.8150	-4214.2420	1251.2140
0.9400	-112.5	-1372.1770	-4404.4210	1516.1230
0.9400	-127.5	-1076.7440	-4478.5070	1700.8820
0.9400	-142.5	-849.0378	-4416.7610	1783.8620
0.9400	-157.5	-700.8870	-4212.3080	1755.7120
0.9400	-172.5	-632.5933	-3870.8910	1619.1480

Table B-45. Exact Theory Crack Tip Stresses for Case S_4 and $\beta = 45^o$ (p = 625 psi)

R	TH	SMAX	SMIN	TMAX
1.2641	172.5	1175.7030	-621.9521	898.8279
1.2641	157.5	725.9099	-605.1038	665.5068
1.2641	142.5	262.7288	-603.8877	433.3083
1.2641	127.5	-99.3672	-724.8667	312.7498
1.2641	112.5	-220.4998	-1099.6520	439.5764
1.2641	97.5	-235.5767	-1584.8570	674.6404
1.2641	82.5	-248.0906	-2068.4250	910.1675
1.2641	67.5	-290.3877	-2509.5220	1109.5670
1.2641	52.5	-377.9167	-2884.4270	1253.2550
1.2641	37.5	-519.8225	-3176.0860	1328.1320
1.2641	22.5	-720.3093	-3372.8760	1326.2830
1.2641	7.5	-977.9739	-3469.4010	1245.7130
1.2641	-7.5	-1284.2060	-3468.2110	1092.0020
1.2641	-22.5	-1619.6220	-3383.4710	881.9246
1.2641	-37.5	-1942.8590	-3252.2540	654.6975
1.2641	-52.5	-2155.2340	-3169.9610	507.3635
1.2641	-67.5	-2117.4410	-3273.6680	578.1135
1.2641	-82.5	-1882.2560	-3509.4740	813.6091
1.2641	-97.5	-1581.8740	-3745.1720	1081.6480
1.2641	-112.5	-1283.9060	-3914.2580	1315.1760
1.2641	-127.5	-1023.8540	-3983.4340	1479.7900
1.2641	-142.5	-822.9736	-3934.7130	1555.8700
1.2641	-157.5	-692.0881	-3761.5400	1534.7260
1.2641	-172.5	-631.7112	-3468.6050	1418.4470

Table B-46. Exact Theory Crack Tip Stresses for Case S_4 and $\beta = 45^{\circ}$ ($p = 625$ psi)

R	TH	SMAX	SMIN	TMAX
1.5947	172.5	942.7742	-622.4824	782.6284
1.5947	157.5	543.4778	-608.6506	576.0642
1.5947	142.5	131.5824	-608.0566	369.8196
1.5947	127.5	-192.6309	-713.9399	260.6545
1.5947	112.5	-299.4753	-1048.6260	374.5754
1.5947	97.5	-313.2839	-1480.2330	583.4749
1.5947	82.5	-325.0640	-1910.1300	792.5332
1.5947	67.5	-362.0300	-2303.5440	970.7573
1.5947	52.5	-437.4807	-2639.8130	1101.1660
1.5947	37.5	-559.7334	-2903.5760	1171.9210
1.5947	22.5	-733.0872	-3083.9290	1175.4210
1.5947	7.5	-957.0525	-3175.3100	1109.1290
1.5947	-7.5	-1224.7800	-3179.1680	977.1938
1.5947	-22.5	-1519.8350	-3107.3010	793.7332
1.5947	-37.5	-1806.4090	-2991.6870	592.6389
1.5947	-52.5	-1998.6510	-2915.2590	458.3040
1.5947	-67.5	-1970.7080	-3001.8890	515.5903
1.5947	-82.5	-1762.2930	-3210.8550	724.2810
1.5947	-97.5	-1492.2670	-3423.2900	965.5115
1.5947	-112.5	-1223.0170	-3577.7950	1177.3880
1.5947	-127.5	-987.3555	-3643.5150	1328.0800
1.5947	-142.5	-804.9753	-3603.6650	1399.3440
1.5947	-157.5	-686.0083	-3451.9210	1382.9560
1.5947	-172.5	-631.1038	-3192.2640	1280.5800

Table B-47. Exact Theory Crack Tip Stresses for Case S_4 and $\beta = 45^o$ (p = 625 psi)

R	TH	SMAX	SMIN	TMAX
1.9837	172.5	747.2573	-622.9368	685.0972
1.9837	157.5	390.4211	-611.7092	501.0652
1.9837	142.5	21.5670	-611.7275	316.6973
1.9837	127.5	-270.9133	-704.7720	216.9292
1.9837	112.5	-365.6729	-1005.8900	320.1086
1.9837	97.5	-378.4749	-1392.4480	506.9868
1.9837	82.5	-389.6770	-1777.2540	693.7886
1.9837	67.5	-422.1436	-2130.6660	854.2617
1.9837	52.5	-487.3882	-2434.5700	973.5913
1.9837	37.5	-593.0635	-2674.4970	1040.9660
1.9837	22.5	-743.5740	-2841.6210	1049.0230
1.9837	7.5	-939.2124	-2928.7220	994.7551
1.9837	-7.5	-1174.6110	-2936.8290	881.1091
1.9837	-22.5	-1435.7740	-2875.7710	719.9985
1.9837	-37.5	-1691.5120	-2773.3190	540.9033
1.9837	-52.5	-1866.6430	-2702.0280	417.6921
1.9837	-67.5	-1846.9440	-2774.3440	463.7004
1.9837	-82.5	-1661.1710	-2960.6130	649.7212
1.9837	-97.5	-1416.7390	-3153.4080	868.3342
1.9837	-112.5	-1171.6800	-3295.5850	1061.9520
1.9837	-127.5	-956.5684	-3358.3300	1200.8800
1.9837	-142.5	-789.7866	-3325.8570	1268.0350
1.9837	-157.5	-680.8752	-3192.0510	1255.5870
1.9837	-172.5	-630.5891	-2960.3000	1164.8550

Table B-48. Exact Theory Crack Tip Stresses for Case S_4 and $\beta = 45^o$ (p = 625 psi)

R	TH	SMAX	SMIN	TMAX
2.5607	172.5	544.0955	-623.4219	583.7588
2.5607	157.5	231.4935	-615.0103	423.2520
2.5607	142.5	-92.2788	-615.8164	261.7688
2.5607	127.5	-352.2568	-695.2507	171.4971
2.5607	112.5	-434.3066	-961.6357	263.6646
2.5607	97.5	-446.1599	-1301.2830	427.5620
2.5607	82.5	-456.8203	-1639.1730	591.1768
2.5607	67.5	-484.5752	-1951.0540	733.2397
2.5607	52.5	-539.1179	-2221.4210	841.1519
2.5607	37.5	-627.4556	-2437.7090	905.1270
2.5607	22.5	-754.1392	-2590.1540	918.0078
2.5607	7.5	-920.2937	-2672.8560	876.2813
2.5607	-7.5	-1122.0860	-2685.3870	781.6504
2.5607	-22.5	-1348.0340	-2635.5660	643.7661
2.5607	-37.5	-1571.6530	-2546.8620	487.6047
2.5607	-52.5	-1728.7220	-2481.1870	376.2327
2.5607	-67.5	-1717.5260	-2538.6960	410.5850
2.5607	-82.5	-1555.5040	-2701.1510	572.8235
2.5607	-97.5	-1337.8300	-2873.3800	767.7747
2.5607	-112.5	-1118.0290	-3002.6270	942.2991
2.5607	-127.5	-924.3770	-3062.1710	1068.8970
2.5607	-142.5	-773.8975	-3037.2780	1131.6900
2.5607	-157.5	-675.5000	-2922.0420	1123.2710
2.5607	-172.5	-630.0498	-2719.2550	1044.6020

Table B-49. Exact Theory Crack Tip Stresses for Case S_4 and $\beta = 45^o$ (p = 625 psi)

ELE. ID	R	TH	SMAX	SMIN	TMAX
2	0.4862	172.5	3181.4430	-598.5681	1890.0060
22	0.4862	157.5	1831.7770	-625.8391	1228.8080
42	0.4862	142.5	896.5242	-680.7747	788.6492
62	0.4862	127.5	438.9626	-1080.4620	759.7126
82	0.4862	112.5	409.7427	-1800.6170	1105.1790
102	0.4862	97.5	461.5117	-2553.6980	1507.6040
122	0.4862	82.5	446.0254	-3196.3990	1821.2120
142	0.4862	67.5	336.7395	-3673.9270	2005.3330
162	0.4862	52.5	107.6733	-3985.2980	2046.4860
182	0.4862	37.5	-224.0510	-4142.9450	1959.4480
202	0.4862	22.5	-610.1584	-4183.8390	1786.8420
222	0.4862	7.5	-1016.0250	-4166.9100	1575.4430
242	0.4862	-7.5	-1393.9570	-4132.0420	1369.0420
262	0.4862	-22.5	-1731.1830	-4100.5030	1184.6590
282	0.4862	-37.5	-2033.6910	-4073.7460	1020.0270
302	0.4862	-52.5	-2289.6150	-4048.4460	879.4148
322	0.4862	-67.5	-2428.7820	-4109.9020	840.5605
342	0.4862	-82.5	-2352.7710	-4349.6640	998.4465
362	0.4862	-97.5	-2064.3560	-4721.9530	1328.7990
382	0.4862	-112.5	-1669.4400	-5134.9330	1732.7460
402	0.4862	-127.5	-1252.8200	-5466.3670	2106.7730
422	0.4862	-142.5	-873.2109	-5614.8510	2370.8200
442	0.4862	-157.5	-572.6401	-5475.6090	2451.4850
462	0.4862	-172.5	-372.9111	-4897.2100	2262.1500

Table B-50. Finite Element Crack Tip Stresses for Case S_4 and $\beta = 45^o$ (p = 625 psi)

ELE. ID	R	TH	SMAX	SMIN	TMAX
3	0.6807	172.5	2394.0610	-584.1860	1489.1240
23	0.6807	157.5	1498.7000	-519.0762	1008.8880
43	0.6807	142.5	740.7178	-566.4678	653.5928
63	0.6807	127.5	333.1094	-900.8594	616.9844
83	0.6807	112.5	245.8325	-1500.2700	873.0513
103	0.6807	97.5	240.4758	-2129.6010	1185.0380
123	0.6807	82.5	209.9895	-2684.2390	1447.1140
143	0.6807	67.5	118.5940	-3123.4060	1621.0000
163	0.6807	52.5	-49.4502	-3439.5500	1695.0500
183	0.6807	37.5	-285.5439	-3634.8940	1674.6750
203	0.6807	22.5	-577.8901	-3728.5470	1575.3290
223	0.6807	7.5	-904.3689	-3742.3810	1419.0060
243	0.6807	-7.5	-1245.1910	-3703.6200	1229.2140
263	0.6807	-22.5	-1582.0790	-3631.7950	1024.8570
283	0.6807	-37.5	-1889.6140	-3554.8220	832.6047
303	0.6807	-52.5	-2116.0270	-3520.5350	702.2546
323	0.6807	-67.5	-2176.2290	-3618.2700	721.0212
343	0.6807	-82.5	-2035.3600	-3864.5140	914.5774
363	0.6807	-97.5	-1768.5950	-4180.0890	1205.7480
383	0.6807	-112.5	-1449.4120	-4475.3350	1512.9620
403	0.6807	-127.5	-1131.7690	-4674.2920	1771.2610
423	0.6807	-142.5	-857.1943	-4717.4920	1930.1480
443	0.6807	-157.5	-664.4229	-4543.0740	1939.3260
463	0.6807	-172.5	-597.8315	-4131.1050	1766.6360

Table B-51. Finite Element Crack Tip Stresses for Case S_4 and $\beta = 45^{\circ}$ (p = 625 psi)

ELE. ID	R	TH	SMAX	SMIN	TMAX
4	0.9400	172.5	1769.4470	-615.1340	1192.2900
24	0.9400	157.5	1169.8300	-564.0173	866.9236
44	0.9400	142.5	582.0020	-576.8145	579.4082
64	0.9400	127.5	214.6401	-808.8901	511.7651
84	0.9400	112.5	113.3755	-1284.4370	698.9067
104	0.9400	97.5	97.0852	-1813.5220	955.3040
124	0.9400	82.5	70.2107	-2298.2100	1184.2100
144	0.9400	67.5	-0.5144	-2699.5480	1349.5170
164	0.9400	52.5	-127.5344	-3006.4660	1439.4660
184	0.9400	37.5	-313.8574	-3215.1430	1450.6430
204	0.9400	22.5	-552.2205	-3329.9670	1388.8730
224	0.9400	7.5	-833.4417	-3365.5580	1266.0580
244	0.9400	-7.5	-1141.7560	-3334.6180	1096.4300
264	0.9400	-22.5	-1458.3600	-3257.7010	899.6711
284	0.9400	-37.5	-1749.1630	-3167.2110	709.0242
304	0.9400	-52.5	-1945.3860	-3131.0510	592.8320
324	0.9400	-67.5	-1958.1550	-3233.5320	637.6892
344	0.9400	-82.5	-1799.0940	-3458.7800	829.8425
364	0.9400	-97.5	-1552.5170	-3712.4190	1079.9500
384	0.9400	-112.5	-1281.8970	-3924.3520	1321.2270
404	0.9400	-127.5	-1027.1010	-4044.8350	1508.8660
424	0.9400	-142.5	-818.1567	-4034.5930	1608.2180
444	0.9400	-157.5	-680.9641	-3872.2850	1595.6600
464	0.9400	-172.5	-627.3755	-3566.8120	1469.7180

Table B-52. Finite Element Crack Tip Stresses for Case S_4 and $\beta = 45^{\circ}$ (p = 625 psi)

ELE. ID	R	TH	SMAX	SMIN	TMAX
5	1.2641	172.5	1395.2450	-625.0574	1010.1500
25	1.2641	157.5	907.4641	-591.4641	749.4641
45	1.2641	142.5	421.6152	-592.8027	507.2090
65	1.2641	127.5	89.9932	-760.1182	425.0557
85	1.2641	112.5	-12.0361	-1148.6500	568.3076
105	1.2641	97.5	-27.4976	-1605.7510	789.1274
125	1.2641	82.5	-47.7930	-2033.5820	992.8945
145	1.2641	67.5	-103.1086	-2397.0160	1146.9540
165	1.2641	52.5	-205.6223	-2678.6890	1236.5330
185	1.2641	37.5	-359.4763	-2876.4600	1258.4910
205	1.2641	22.5	-561.1860	-2990.0630	1214.4380
225	1.2641	7.5	-803.3245	-3028.2380	1112.4570
245	1.2641	-7.5	-1075.9050	-3001.9690	963.0325
265	1.2641	-22.5	-1357.3780	-2929.1840	785.9023
285	1.2641	-37.5	-1616.8060	-2842.0680	612.6304
305	1.2641	-52.5	-1784.3430	-2808.4060	512.0310
325	1.2641	-67.5	-1779.4910	-2904.1330	562.3208
345	1.2641	-82.5	-1626.4950	-3101.8180	737.6616
365	1.2641	-97.5	-1407.0160	-3313.9220	953.4529
385	1.2641	-112.5	-1174.5070	-3480.1170	1152.8040
405	1.2641	-127.5	-962.0586	-3563.5650	1300.7530
425	1.2641	-142.5	-791.9990	-3536.4370	1372.2190
445	1.2641	-157.5	-678.6287	-3385.6210	1353.4960
465	1.2641	-172.5	-623.5540	-3103.4460	1239.9460

Table B-53. Finite Element Crack Tip Stresses for Case S_4 and $\beta = 45^o$ (p = 625 psi)

ELE. ID	R	TH	SMAX	SMIN	TMAX
6	1.5947	172.5	1141.3400	-620.9648	881.1523
26	1.5947	157.5	720.9934	-599.1809	660.0872
46	1.5947	142.5	301.6138	-602.1763	451.8950
66	1.5947	127.5	0.9604	-735.9604	368.4604
86	1.5947	112.5	-99.4224	-1067.9520	484.2651
106	1.5947	97.5	-115.4680	-1473.0930	678.8132
126	1.5947	82.5	-129.9504	-1859.3620	864.7058
146	1.5947	67.5	-174.4963	-2192.5030	1009.0030
166	1.5947	52.5	-260.2671	-2455.8570	1097.7940
186	1.5947	37.5	-392.5056	-2642.9930	1125.2430
206	1.5947	22.5	-568.5791	-2753.6070	1092.5140
226	1.5947	7.5	-784.6023	-2793.2090	1004.3030
246	1.5947	-7.5	-1029.6030	-2769.4580	869.9280
266	1.5947	-22.5	-1286.1550	-2701.0940	707.4702
286	1.5947	-37.5	-1521.5030	-2618.4960	548.4961
306	1.5947	-52.5	-1668.5270	-2585.9720	458.7231
326	1.5947	-67.5	-1654.7250	-2675.7740	510.5251
346	1.5947	-82.5	-1509.9440	-2853.8670	671.9622
366	1.5947	-97.5	-1309.9970	-3038.0020	864.0027
386	1.5947	-112.5	-1104.4790	-3175.7700	1035.6450
406	1.5947	-127.5	-919.5190	-3237.4800	1158.9800
426	1.5947	-142.5	-773.2048	-3203.2320	1215.0130
446	1.5947	-157.5	-674.7119	-3060.4760	1192.8820
466	1.5947	-172.5	-627.2930	-2805.6450	1089.1760

Table B-54. Finite Element Crack Tip Stresses for Case S_4 and $\beta = 45^o$ (p = 625 psi)

ELE. ID	R	TH	SMAX	SMIN	TMAX
7	1.9837	172.5	924.1360	-618.3860	771.2610
27	1.9837	157.5	562.1536	-604.9661	583.5598
47	1.9837	142.5	196.9761	-609.9136	403.4448
67	1.9837	127.5	-74.2397	-720.5728	323.1665
87	1.9637	112.5	-171.7205	-1006.5300	417.4045
107	1.9837	97.5	-186.9187	-1367.2060	590.1438
127	1.9837	82.5	-197.8552	-1717.4570	759.8010
147	1.9837	67.5	-233.3926	-2023.2940	894.9512
167	1.9837	52.5	-305.4414	-2269.4340	981.9961
187	1.9837	37.5	-419.1570	-2447.5930	1014.2180
207	1.9837	22.5	-574.7314	-2555.2690	990.2686
227	1.9837	7.5	-768.2979	-2594.8260	913.2646
247	1.9837	-7.5	-990.6594	-2575.0280	792.1843
267	1.9837	-22.5	-1224.6550	-2510.2810	642.8137
287	1.9837	-37.5	-1439.1040	-2432.3330	496.6140
307	1.9837	-52.5	-1569.3670	-2402.9450	416.7886
327	1.9837	-67.5	-1549.2840	-2485.9030	468.3091
347	1.9837	-82.5	-1411.7460	-2645.1280	616.6912
367	1.9837	-97.5	-1229.4500	-2806.5490	788.5493
387	1.9837	-112.5	-1046.0990	-2921.9000	937.9009
407	1.9837	-127.5	-883.6052	-2966.3950	1041.3950
427	1.9837	-142.5	-756.4221	-2926.2020	1084.8890
447	1.9837	-157.5	-671.0405	-2793.2080	1061.0830
467	1.9837	-172.5	-630.6211	-2567.0030	968.1914

Table B-55. Finite Element Crack Tip Stresses for Case S_4 and $\beta = 45^o$ (p = 625 psi)

ELE. ID	R	TH	SMAX	SMIN	PMAX
8	2.5607	172.5	694.1636	-625.2261	659.6948
28	2.5607	157.5	395.1785	-614.6472	504.9128
48	2.5607	142.5	85.2622	-619.5747	352.4185
68	2.5607	127.5	-153.7634	-708.6741	277.4553
88	2.5607	112.5	-245.0376	-948.7124	351.8374
108	2.5607	97.5	-259.3716	-1262.6900	501.6597
128	2.5607	82.5	-265.7253	-1574.2740	654.2747
148	2.5607	67.5	-292.3618	-1851.5320	779.5854
168	2.5607	52.5	-350.4199	-2077.8300	863.7051
188	2.5607	37.5	-446.1128	-2244.7610	899.3247
208	2.5607	22.5	-580.4800	-2348.3330	883.9263
228	2.5607	7.5	-750.6467	-2389.2910	819.3220
248	2.5607	-7.5	-949.1028	-2373.0840	711.9910
268	2.5607	-22.5	-1159.4580	-2314.5020	577.5225
288	2.5607	-37.5	-1350.7790	-2242.2830	445.7524
308	2.5607	-52.5	-1463.2490	-2215.3440	376.0481
328	2.5607	-67.5	-1437.9660	-2290.1580	426.0964
348	2.5607	-82.5	-1310.5140	-2429.8600	559.6721
368	2.5607	-97.5	-1145.0660	-2567.1200	711.0266
388	2.5607	-112.5	-984.5505	-2658.6590	837.0549
408	2.5607	-127.5	-845.2715	-2687.2910	921.0098
428	2.5607	-142.5	-736.6294	-2642.4960	952.9331
448	2.5607	-157.5	-664.6538	-2521.4700	928.4087
468	2.5607	-172.5	-630.7437	-2328.2560	848.7563

Table B-56. Finite Element Crack Tip Stresses for Case S_4 and $\beta = 45^{\circ}$ (p = 625 psi)